Reliability-Based Life-Cycle Cost Analysis of Engineering Elements and Systems

Reza Lotfalian

Doctor of Philosophy

Department of Mechanical Engineering

McGill University

Montreal, Quebec

August 2017

A Thesis submitted to the Faculty of Graduate Studies and Research in partial fulfillment of the requirements for the degree of Doctor of Philosophy

Dedication

This thesis is dedicated to my family, to Helya, and to my friends, near and far, whose unwavering love and support made it possible to keep a balance between academic and personal aspects of this stage of my life.

Declaration

The contents of this thesis are original. Unless specific reference is given to the work of others, the contents have not been submitted in whole or in part for any other degree at any university. This thesis is my own work and contains nothing which is the outcome of a collaboration with others, unless specified in the text. More specifically, the procedure generated for acquisition cost-performance-reliability analysis, the cost-performance reliability models developed for gears, rolling bearings, electrical insulations, gearboxes and electric motors, as well as the maintenance cost models and the life-cycle cost model developed herein are original contributions to the knowledge.

Reza Lotfalian

August 2017

Acknowledgements

I thank the supervision of Prof. Benoit Boulet, Prof. Peter Radziszewski, Prof. Luc Mongeau, and mentorship of Dr. Sudarshan Martins, who made the PhD experience a pleasant and productive one. Dr. Michael Avedesian's industrial and management viewpoints have been an inspiration throughout this project. Lastly, I gratefully acknowledge the contribution of the Automotive Partnership Canada grant APCPJ418901-11, and the industrial partners of the project: TM4, Linamar and Infolytica.

Abstract

This thesis aims to develop a reliability-based life-cycle cost model for systems of engineering elements. Acquisition cost, maintenance cost, and energy cost are addressed as three major categories of the life-cycle cost. The salvage value and the disposal cost are outside of the scope of this research.

A procedure is proposed for acquisition cost modelling of engineering elements. As a first step, the influence of resizing, material type, manufacturing process, and duty cycle (performance) of the element on its reliability is studied. Next, the correlation of the acquisition cost with the aforementioned parameters is established. Finally, by eliminating the size factor, a relationship is established between the acquisition cost, the performance, the reliability, and the material properties of the element. The proposed procedure is used to develop the cost-performance-reliability (CPR) model of gears, rolling bearings, and electrical insulations. The gear and bearing CPR models accurately predict the catalog prices of original equipment manufacturers for a wide size range. The CPR model of gears and bearings are coupled to develop the system-level gearbox CPR model, which is used in the cost reduction and the reliability allocation of a one-speed gearbox. The electric motor CPR model is established by coupling the component-level CPR models of bearings and insulation.

The failure probability distribution function of an arbitrary element is used as the kernel for developing a maintenance cost model for the element. The time value of money is incorporated to calculate the net present value of the maintenance cost. The model is developed

for a post-failure and two preventive maintenance scenarios. The previous maintenance cost models are generalized by eliminating their embedded assumptions of high reliability and zero inflation rate. This extension improves the accuracy of the maintenance cost models for low-reliability elements in a market where the inflation rate is not negligible. Next, considering a case where the life-cycle cost is the sum of the acquisition cost and maintenance cost, the CPR models of gears and bearings, as well as the developed maintenance cost model are used to explore the design space and reduce the life-cycle cost of gears, bearings, and a one-speed gearbox under different maintenance strategies.

Finally, the CPR and maintenance cost models developed here are used in the reliability and the life-cycle cost analysis of the powertrain of a battery electric step van. The powertrain is composed of a single-speed gearbox, an electric motor, and a battery pack. The design variables are the size of the gears and bearings of the gearbox, and the electric motor's bearing size. The design objective is to reduce the life-cycle cost while meeting specified performance requirements. The results show that setting component-level reliability constraints on individual elements rules out some regions of the design space. By relaxing the component-level reliability constraints, it is possible to find solutions with lower life-cycle cost and higher system-level reliability. This conclusion suggests a design paradigm shift: component-level reliability should be considered as a design variable rather than a design objective.

Abrégé

Cette thèse vise à développer un modèle du coût du cycle de vie des systèmes d'éléments d'ingénierie basé sur la fiabilité. Les coûts d'acquisition, d'entretien et d'énergie sont traités comme trois catégories principales du coût du cycle de vie. La valeur de récupération et le coût d'élimination ne sont pas considérés dans cette recherche.

Une procédure est proposée pour la modélisation du coût d'acquisition d'éléments d'ingénierie. Dans une première étape, nous étudions l'influence de la taille, du type de matériau, du processus de fabrication et du rapport cyclique (performance) de l'élément sur sa fiabilité. Ensuite, une corrélation est établie entre le coût d'acquisition et les paramètres mentionnés ci-haut. Enfin, en éliminant le facteur de la taille, une relation est obtenue entre le coût d'acquisition, la performance, la fiabilité et les propriétés matérielles de l'élément. La procédure proposée est utilisée pour développer le modèle coût-performance-fiabilité (CPF) d'engrenages, de roulements et d'isolation électrique. Les modèles de CPF d'engrenages et de roulements prédisent avec précision les prix des catalogues des fabricants, et ce, pour une vaste gamme. Le modèle CPF des engrenages et des roulements est couplé pour développer le modèle CPF pour la boîte de vitesses, qui est utilisé dans la réduction des coûts et l'estimation de la fiabilité d'une boîte de vitesses. Le modèle CPF du moteur électrique est établi en couplant les modèles CPF des roulements et de l'isolation.

La fonction de distribution de probabilité de défaillance d'un élément arbitraire est utilisée pour développer un modèle du coût d'entretien pour l'élément. La valeur temporelle de

l'argent est incorporée pour calculer la valeur actualisée nette du coût d'entretien. Le modèle est développé pour un scénario d'entretien post-défaillance et deux scénarios d'entretien préventif. Les modèles du coût d'entretien précédents sont généralisés en éliminant les hypothèses intégrées de fiabilité élevée et de taux d'inflation nul. Cette extension améliore la précision des modèles du coût d'entretien pour les éléments à faible fiabilité dans un marché où le taux d'inflation n'est pas négligeable. Ensuite, compte tenu que le coût du cycle de vie est la somme du coût d'acquisition et du coût d'entretien, les modèles d'engrenages et de roulements en CPF, ainsi que le modèle du coût d'entretien, sont utilisés pour analyser et réduire le coût du cycle de vie des engrenages, des roulements et d'une boîte de vitesses sous différentes stratégies d'entretien.

Finalement, en tant qu'étude de cas, les modèles de CPF et du coût d'entretien développés ici sont utilisés dans l'analyse de la fiabilité et le coût du cycle de vie du groupe motopropulseur d'une camionnette électrique. Le groupe motopropulseur est composé d'une boîte de vitesses, d'un moteur électrique et d'une batterie. Les variables de conception sont la taille des engrenages, des roulement de la boîte de vitesses et des roulement du moteur électrique. L'objectif de conception est de réduire le coût du cycle de vie tout en respectant les exigences de performance spécifiées. Les résultats montrent que la sélection des contraintes de fiabilité des éléments individuels exclut certaines régions de l'espace de conception de l'ensemble. Si les contraintes de fiabilité au niveau des composantes sont affaiblies, il est possible de trouver des solutions ayant un coût de cycle de vie plus bas et une plus grande fiabilité au niveau du système. Cette conclusion suggère un changement de paradigme de conception: la fiabilité des composantes devrait être considérée comme une variable de conception plutôt qu'être un objectif de conception.

Acronyms and Nomenclature

Symbol	Description
AC	Acquisition cost
BEV	Battery electric vehicle
BOM	Bill of material
CAD	Canadian Dollar
CPR	Cost-performance-reliability
EC	Energy cost
EV	Electric vehicle
FCV	Fuel cell vehicle
FPDF	Failure probability distribution function
HEV	Hybrid electric vehicle
ICE	Internal combustion engine
ICEV	Internal combustion engine vehicle
LCC	Life-cycle cost
MC	Maintenance cost
NPV	Net present value
OEM	Original equipment manufacturer
OCB	Orange County bus cycle
PFM	Post-failure maintenance
PrM	Preventive maintenance

ROI	Return of investment
rpm	Revolutions per minute
USD	US Dollar
A, B	Quality factors of gears
A_1–A_4	Constants in stress and strength equations
a	Exponent factor for bearing life equation
a_1	Bearing reliability factor
B, D, E, F	Bearing geometry, mm
b	Gear face width
$\mathbf{b}$, $\mathbf{b}^*$	Baseline bearing and scaled bearing
$\bar{C}_F$	Discounted expected failure cost
$\bar{C}_M$, $\bar{\bar{C}}_M$	Discounted expected maintenance cost
C_M^*, C_M^{**}	Normalized discounted expected maintenance cost
$\bar{C}_P$	Discounted expected preventive maintenance cost
C_r	Dynamic load rating of bearings
$\bar{C}_T$	Discounted expected life-cycle cost
c_0	Acquisition cost
$c_1 - c_3$	Constant coefficients
$c_f(t)$	Cost of a failure at instant t
$c_p(t)$	Cost of a preventive maintenance at instant t
$\bar{c}_k$	Discounted maintenance cost of exactly k failures
$\bar{\bar{c}}_k$	Discounted maintenance cost of k-th failure
$\bar{c}_{j,k}$	Discounted cost of k failures in interval j
$\dot{c}_k$	Rate of discounted cost of exactly k failures
$\ddot{c}_k$	Rate of discounted cost of k-th failure
$\dot{c}_{j,k}$	Rate of discounted cost of k failures in interval j
D_{pw}	Diameter of rollers pitch circle

D_w	Diameter of rolling elements
d	Gear pitch diameter or bearing bore diameter
$e(t)$	Discount factor at instant t
f	Failure probability density function of multiple failures
f_C	Bearing geometry, accuracy, and material factor
f_θ	Bearing's temperature factor
$\mathbf{g}$, $\mathbf{g}^*$	Baseline gear and scaled gear
$h(t)$	Hazard function
K_o, K_v, K_S	Overload, dynamic, and size factor of gears
K_B, K_H	Rim thickness and load distributions factors of gears
L_b	Bearing's rating life
L_i	Insulation's characteristic life
L_w	Length of bearing rollers
M	Mass
m	Gear module
m_G	Gear ratio
N	Gear's life
n	Number of preventive maintenances
n_p, n_g	Number of teeth of pinion and gear
P	Equivalent applied load on bearing
$p(t)$	Failure probability density function of one failure
R_b, R_i, R_m	Reliability of bearings, insulation, and motors
$R(t)$	Reliability function
S	Shaft speed
S_F, S_H	Safety factor against bending and pitting
T	Total life cycle
t_p	Block length or element age before preventive maintenance

V	Linear velocity of gear's pitch circle
v_h, v_g	Material removal volume in hobbing and grinding
X	Motor characteristics
Y, Y_J, Y_θ	Tooth form, geometry, and temperature factors
Y_N, Z_N	Bending stress and contact stress cycle factors
Y_Z	Reliability factor
Z	Number of rolling elements of bearings
Z_E, σ_{FP}, σ_{HP}	Mechanical properties
α_0–α_3, β_0–β_4, α_2', β_2'	Factors of gear equations
α_5, β_5, β_h, β_g, β_5', β_5''	Coefficients of cost-mass correlation
α_6, β_6	Coefficients of cost-characteristics correlation
α_θ , $L_{i\theta}$, θ_{max}	Insulation life parameters
γ, $1/\lambda$	Shape parameter and scale parameter of Weibull distributions
γ_1–γ_3	Size scaling factors
δ_f	Downtime of a failure
δ_p	Downtime of a preventive maintenance
θ	Temperature
Λ_1, Λ_2	Factors of stress equations
σ	Bending stress
$\sigma_{all.}$	Allowable bending stress
σ_c	Contact stress
$\sigma_{c,all.}$	Allowable contact stress
ς	Cash flow
ξ	Normalized cost
τ	Torque

Contents

List of Figures

List of Tables

Chapter 1

Introduction

The Model T Ford, introduced in 1908, was the first car manufactured to be accessible by different social classes of the United States. Many stories have been built around the success of the product. Zoologist Nicolas Humphrey starts his article *The Social Function of Intellect* with one such story [1]:

"Henry Ford, it is said, commissioned a survey of the car scrap-yards of America to find out if there were parts of the Model T Ford which never failed. His inspectors came back with reports of almost every kind of failure: axles, brakes, pistons– all were liable to go wrong. But they drew attention to one notable exception, the kingpins of the scrapped cars invariably had years of life left in them. With ruthless logic Ford concluded that the kingpins on the Model T were too good for their job and ordered that in future they should be made to an inferior specification".

Humphrey uses the story to introduce the concept of efficient resources allocation in evolution, which states that natural selection does not over-design a part of an organism; different components of an organism have identical failure rate.

The truth of the story of Ford and kingpins have been questioned [2]. However, even if apocryphal, it raises a question of utmost importance: what is efficient when it comes to resources allocation?

From an engineering design perspective, resources can be design variables such as component sizes, material type, manufacturing process, and system configuration. *Efficient* qualifies the set of design variables which optimizes a specified design objective such as performance/characteristics, overall reliability, and life-cycle cost (LCC).

The interplay between design variables and the performance, reliability, and LCC can be addressed from component-level or system-level viewpoints. In a system of components– having a larger design space compared to the individual components– changing the design variables results in a more complex relation between the system's LCC, performance, and overall reliability. As three important design objectives, it is necessary to have a good understanding of their behavior under a variation of the design variables. Establishing cost-performance-reliability (CPR) models for a component helps engineers understand the cost associated with increasing the reliability and/or performance of that component. In a system of components, the component-level CPR models can be coupled to identify the system-level CPR model, which, in turn, can be used to to optimize each or a combination of design objectives.

The literature on the performance, reliability, and acquisition cost modelling of engineering elements is provided below. Specifically, gears, bearings, electrical insulations, gearboxes, electric motors, and batteries are addressed wherever literature is available, as they are the building blocks of the powertrain of the battery electric step van studies at the end of this thesis. The maintenance cost and energy cost models are reviewed as well.

1.1 Reliability and performance

The reliability, $R(t)$, of an element is defined as the probability that the element operates perfectly up to instant t [3]. The reliability of a component generally depends on its size, material properties, duty cycle, the total number of loading cycles, and environmental conditions. For many engineering elements, the reliability models are well-established and extensively verified by professional associations and are used for decades by engineers/designers.

1.1.1 Gears

The major failure modes of gears are bending and pitting failures. The American Gear Manufacturers Association (AGMA) proposes two equations for the performance and reliability analysis of gears bending failure, and two equations for pitting failure analysis. When the geometry and micro-geometry parameters of the gear, as well as the speed and applied force/torque are given, the bending stress equation gives the *maximum* bending stress on the gear teeth [4, 5]. On the other hand, the bending strength equation relates the maximum *allowable* bending stress to the material property, the number of cycles, the reliability, the safety factor, and the gear temperature [4, 5]. Setting the maximum bending stress equal to the allowable bending stress gives a relation between the torque and reliability of the gear and its geometry, material property, life-cycle, etc. This method, along with numerical methods, is widely used for the gear teeth bending analysis. Similarly, the contact stress equation gives the *maximum* contact stress in terms of the gear geometry and the applied force/torque, whereas the contact strength equation is used for calculating the *allowable* contact stress as a function of the material property of the gear and its mating gear, the safety factor, the gear temperature, the reliability, and the number of cycles [4, 5]. Setting the maximum contact stress equal to the allowable contact stress yields a formula that relates the reliability and torque to the gear geometry, the material property, and

the life-cycle under contact stress. Since bending and pitting are series failure modes, the total reliability of the gear equals the product of reliability against bending and the reliability against pitting.

1.1.2 Bearings

The American Bearings Manufacturers Association (ABMA) proposes the life equation for rolling bearings, which establishes a relationship between the bearing reliability and applied force to its life-cycle, size, material type (as they are implicit in the load carrying capacity), bearing type, and operating condition (temperature, lubrication, alignment, etc.) [6, 7].

1.1.3 Gearbox

The failure of any component in gearbox leads to the gearbox failure. Therefore, the overall reliability equals the product of the reliability of its components. Gear damage, bearing damage, housing failure, faults in the lubrication system, shaft damage, and sealing are among the most important failure modes of gearboxes. The gearbox configuration, design details, and duty cycle can influence the reliability of each component. Sheng [8] reports that 70% of gearbox failures are due to bearing damage, followed by 26% contribution of gear failure. Ribrant [9] results show that 63% of failures are bearing related, while 5% is related to gear damage. The rest of failures are due to oil system and sealing, while no shaft failure is observed [9]. However, bearing failures are responsible for 62% of the downtime, followed by 30% by gears. This suggests that bearing and gear failure are key elements in the reliability analysis of gearboxes.

1.1.4 Electric motors

In different reliability surveys of electric motors, damage to the bearings and winding insulation are reported to be the major failure modes [10–16]. In a reliability survey on 6312 motors for 41,614 motor-years [10], 31% of failures are bearing related and 26% are insulation related. In that article, the failed component is not specified in 21% of the cases. If these unspecified damages are excluded from the analysis, the share of the bearings and insulation failures would be 39% and 33%, respectively. The next dominant failure mode is oil leakage and oil system failure in nearly 9% of the cases. The rest of specified failures correspond to other motor components such as the frame, shaft, cage, wedges, cables, etc. An analysis in [11] indicates the share of 38% for bearings failure and 35% for insulation failure in a pool of 4797 motors. In a reliability survey for the motors in the petroleum and chemical industries [12], by excluding the damages caused by unspecified or by external sources, the failure rate of the bearings and the insulation is 69% and 22%, respectively. A similar result is reported for the offshore induction motors [13]; among the specified internal failures, 69% are bearing related and 21% are insulation related.

In [14, 15], the results of a reliability survey for electric motors is reported. In total, 1141 motors of 75 plants have been studied, where 360 failures have been reported during 5085 unit-years of operation. These articles consider the influence of many factors, including the motor speed, the power, the voltage, the enclosure, and the environment, on the failure rate of the motors. For the motors operating in the nominal power range of 151-373 kW, the average failure rate is 0.0685 per unit-year, whereas this number is 0.0727 for the motors in the range of 374-3730 kW. The failure rate of the second group is only 6.1% higher than the first group in this wide range of power. This implies that for the set of motors studied in [14, 15], the rate of increase of the failure rate is of the order of 1×10^{-6} failures per unit-year-kW. Within a range of 100 kW, the difference in the failure rate of the smallest and the largest motor is in the order of 1×10^{-4} failures per unit-year, which is neglected.

The results of [10–13] suggest that on average 80% of the specified damages corresponds to the bearings or insulation failures. In absence of comprehensive reliability models for the other failure modes of electric motors, it can be assumed that these two major modes are the only damage sources of the product. Failure of a bearing or the insulation results in the motor failure. Therefore, the motor reliability equals the product of the reliability of motor bearings and insulation.

The reliability of bearings are modeled using the method of Section 1.1.2. For insulation, reliability can be modeled as an exponential function of time, where the characteristic time, i.e. mean time between failures (MTBF), is identified by the insulation class and the insulation temperature [17, 18].

1.1.5 Battery pack

The battery reliability is modeled using a Weibull function of the time [19–21]. A Weibull function is characterized by two factors: the shape parameter and the scaling parameter. For batteries, the shape parameter is usually measured experimentally, as demonstrated by Eom et al. [19], Herman et al. [20], and Ran et al. [21]. The scale parameter can be measured experimentally and depends on the battery material and technology, as well as the duty cycle details such as the depth of discharge, the charging and discharging rates, and the operating temperature. Having the shape and scale parameters, the expected life of the battery can be calculated [22]. Alternatively, by knowing the battery expected life from the product datasheet and the Weibull shape parameter, the scale parameter of the Weibull distribution can be calculated from the formula for the mean value of Weibull distributions [22].

1.1.6 Powertrain

The reliability of a system is influenced by its subsystems' reliability as well as the system configuration (series, parallel, standby, etc) [23]. For a powertrain consisting of a gearbox, an electric motor, and a battery pack, where the failure of each subsystem leads to the powertrain failure, the system reliability equals the product of the reliability of the subsystems.

1.2 Cost analysis

Designers of a product may aim to minimize the product's acquisition cost (AC) while targeting specified performance and reliability requirements. In another approach, the target can be to optimize the total cost of ownership or the life-cycle cost (LCC) of the product, which may be composed of the acquisition cost (AC), maintenance cost (MC), energy cost (EC), disposal cost, salvage value, etc.

Generally, a high reliability product has a high AC because of the good quality materials and processes used in its production, whereas its MC is low during its life cycle. On the other hand, it is possible to use low quality materials or manufacturing processes to produce a low reliability, low price product. However, a high MC is expected during its life cycle because its low reliability leads to frequent failures [24]. As schematically illustrated in Fig. 1.1, if the AC-reliability and the MC-reliability correlations of a product are available in the design stage, it is possible to answer an important question: how much must be invested today on the reliability to save on the MC in the future, such that the sum of AC and MC is optimum. In other words, which reliability minimizes the LCC?

In the following sections, the literature on the AC and the MC modelling of products are addressed. Also, the methods for calculating the EC and LCC are discussed.

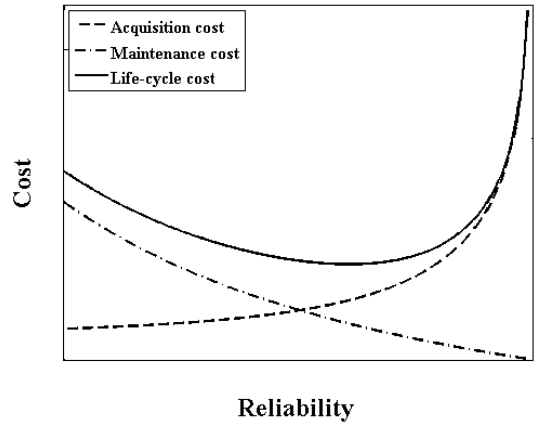

Figure 1.1 Schematic of cost-reliability correlation

1.2.1 Acquisition cost

There are different ways of categorizing the cost of a product. One approach categorizes the AC to direct and indirect costs [25]. Material, labor, and tooling expenses are identified in the direct cost. Indirect cost includes expenses such as engineering, R&D, general and administrative, which do not correspond to a specific product, yet are necessary for production. The indirect cost is generally applied as a lumped overhead factor on the direct costs to give the total cost associated with the manufacture, sale, and support of the product. The result is the AC of the product for the manufacturer. Adding the overhead for the factory profit margin on the latter gives the price or the AC for the customer [25].

At an early design stage, it may not be feasible to accurately estimate the acqusition cost of a product. Instead, the design team members may use their intuition to predict cost of each category. Otherwise, an available database on costing of analogous products may be used by the designers to predict the cost of the new product [26]. A third option is to use some rules of thumb to estimate the manufacturing and indirect costs in terms of the material cost. As an example, the 1-3-9 rule states that in a high volume in-house production, the manufacturing cost

is around three times the material cost, and the selling price is roughly nine times the material cost. These multipliers, however, highly depend on the industry and the product [27].

As the design process progresses and more details of the product are available, parametric cost estimation may be used [26]. In this approach a mathematical relation is established between the acquisition cost of the product and its mass M or its engineering characteristics X. The material cost models often consider a linear relation between the AC of a product and its mass ($C_0 = \alpha_5 + \beta_5 M$), whereas cost-performance models linearly correlate the AC to X ($C_0 = \alpha_6 + \beta_6 X$) [25, 28]. In these relations, β_5 and β_6 are variable cost which include the marginal cost of increasing the mass or improve the characteristics of the product. The variable cost is influenced by the material type, manufacturing and post-manufacturing processes, labor, etc. The parameters α_5 and α_6 are the fixed cost which are composed of the rent, administration, depreciation, etc. Depending on the level of accuracy required for identifying the fixed and variable costs, the past data may be analyzed using high-low method or the least square regression method, among other methods broadly used in accounting cost estimation [25, 26, 28].

These linear models are used from either the manufacturer's or the customer's point of view. The reason is that the acquisition cost of a product for a costumer is equal to its acquisition cost for the manufacturer times the profit margin factor. Some examples of the linear models are presented in [29] for electric motors, in [29, 30] for batteries, in [31] for the internal combustion engines and the power electronics, and in [32, 33] for gears. Empirical linear cost-performance or cost-mass models are common in component-level and system-level AC modelling of electric vehicles [29, 34–37].

The cost-mass correlations are easy to establish. However, they fail to answer the following question: what is the interplay between the acquisition cost of a product and its performance and/or reliability? In the AC-performance models, the effect of reliability is not taken into account. This question is of utmost importance when engineers target a specific performance and reliability and shall meet cost considerations. To answer this question, a model

must indicate how costly it is to increase the reliability of a product at different performance levels.

Some cost-reliability models are proposed in [24, 38]. These models have three features in common: (a) cost is monotonically increasing with reliability, (b) it is a convex function, and (c) it trends to infinity as the reliability tends to unity. Aside from these three mathematical features, no analytical or experimental validation is provided for these models. These models are used in reliability allocation and acquisition cost optimization of series systems [38], redundant systems [39], and series/parallel systems [40, 41].

The models proposed in [24, 38] show significantly different behaviors as the reliability approaches unity. To find the accurate cost model of a specific product, it is important to assess the failure mechanisms of the product and study how costly it is to increase the product's reliability under a specific performance (or duty cycle) by changing the size, the material type, the manufacture process, etc. The resulting cost-performance-reliability (CPR) model will provide a strong tool in cost optimization and reliability allocation problems. This problem has not been addressed in the literature.

1.2.2 Maintenance cost

The maintenance cost analysis is founded on its reliability function, $R(t)$. The failure probability distribution function (FPDF) is derived from the reliability. The FPDF is next used to determine the failure frequency, which could be translated to the maintenance cost of the element [42, 43]. Another important consideration is the type of maintenance practice; Is it a complete repair, a partial repair (where the repaired part could not be considered as new), or a replacement? Furthermore, the maintenance strategy plays a role [42, 43]; is the maintenance conducted after a failure occurs, or is there a preventive maintenance schedule?

The answers to these questions depend on the type of the element, the role it plays in the system, the downtime of a preventive maintenance activity versus that of a post-failure maintenance, and the cost of a preventive maintenance versus the cost of a of a failure [42, 43]. It is challenging to establish a model that answers all of the aforementioned questions. Instead, most of the present models focus on a specific maintenance type or strategy. A review of the literature is presented here.

Under a post-failure maintenance (PFM) strategy, the component is either repaired or replaced by a new one upon failure. This process is repeated as necessary until the end of the project life target, T [43]. To avoid unscheduled failures which are inherent in PFM strategies, a preventive maintenance (PrM) strategy may be adopted. Two such strategies are discussed.

The first preventive maintenance strategy, denoted by PrM1, is called a block replacement policy, where a periodic preventive maintenance is scheduled at intervals t_p. However, any failure within a block will force a maintenance event to occur. The second preventive strategy, PrM2, is an age replacement policy. Here, a preventive maintenance is conducted after a part operates for a period/cycle t_p. This implies that a maintenance shall be conducted if either a failure occurs or the part reaches the age t_p [42].

Note that each block of the PrM1 may be considered as a PFM strategy. If a PFM model is developed, it may be easily generalized to develop the PrM1 model. If $t_p = T$, no preventive maintenance is conducted throughout the life of the project and, therefore, the PrM1 strategy reduces to PFM; PFM is a special case of PrM1. Therefore, the rest of this section only addresses the PrM1 and PrM2 models.

The PrM1 strategy approach provides a formalism for calculating the expected maintenance cost of a block per block length. In this strategy [42, 43], the expected maintenance cost of a block is $c_p + H(t_p)c_f$, where t_p is the block length, c_p is the cost of a preventive maintenance, c_f is the cost of a failure, and $H(t)$ is the expected number of failures up to instant t. Function

$H(t)$ is determined by the failure probability, which itself depends on the reliability of the part. The derivation of $H(t)$ is addressed in details in [42, 43] (or see Section 5.2.1 here). In this approach, t_p is determined such that the rate of the expected maintenance cost $\left(c_p + H(t_p)c_f\right)/t_p$ is minimized.

For the PrM2 strategy [42, 43], the expected cost per unit time is defined as the ratio of the expected cost of a cycle to the expected cycle length (see Eqn. (5.51) here). Again, t_p is determined such that the rate of the expected maintenance cost is minimized. The PrM1 and PrM2 models assume no inflation rate. Another underlying assumption of the PrM2 model is that the project has an infinite horizon [43, 44].

These models have been extensively used in the literature for maintenance schedule optimization. Lin et al. [45] use the PrM2 strategy for a system with maintainable and nonmaintainable failure modes to minimize the rate of the expected maintenance cost. Grall et al. [46] introduce a condition-based inspection/preventive maintenance model, which extends the PrM2 model of Blischke et al [42] and Jardine et al. [43] by considering the inspection cost. Lhorente et. al. [47] use the PrM2 model to minimize the cash flow rate of the maintenance of armatures. Zequeira and Berenguer [48], and Bartholomew-Biggs et. al. [49] modify the PrM1 model by adding a term to account for imperfect maintenances, where the maintained component is not in the as new condition. Lim et. al. [50] modify the PrM2 model of [42, 43] to consider the effect of imperfect maintenance, where after the maintenance event the reliability of the component is less than unity. In [51] the downtime of failures and preventive maintenances are introduced in the denominator of the PrM2 model (see Eqn. (5.51) here) to increase the accuracy of the model. Tabriz et. al. [52] introduce stochastic shocks to the reliability function and use the PrM2 model for determining the best maintenance strategy for single as well as parallel units.

Although the cost models in [46–52] slightly differ from those of [42, 43], they all assume that the inflation rate is zero. This assumption may be justified if t_p is not long, if the inflation rate is negligible, or if the purpose of the cost analysis is just a comparative study

between different options. However, having a model where the inflation rate is introduced has the advantage of accurately calculating the net present value (NPV) of the project. The other point to mention is the implication of the term $c_f\big(1-R(t_p)\big)$ in the PrM2 model $\big($see Section 5.2.3$\big)$. The term $1-R(t_p)$ is the probability that the part fails to operate up to t_p, with no maintenance event after the failure. Therefore, $c_f\big(1-R(t_p)\big)$ represents the maintenance cost of one failure, neglecting the possibility of failure of the replaced component. Consequently, the numerator of the PrM2 model $\big($see Section 5.2.3$\big)$ gives a lower bound for the expected maintenance cost of an operating cycle by ignoring the maintenance cost associated with having two or more failures.

The aforementioned assumptions should be dropped to develop reliability-based PFM and PrM models which take into account the time value of money, consider any possible number of failures, and introduce the downtime of failures and preventive maintenances.

1.2.3 Energy cost

Having the power and the efficiency of a system identified, energy consumption per cycle of the system can be calculated. For short run projects, it is possible to assume that the energy source price is fixed. For long run projects, it is important to consider price fluctuations of the energy source. Annual Energy Outlooks of the Department of Energy provide projections on the oil and electricity prices under different market conditions [53].

1.3 Powertrain

As the methods and models developed in this thesis are used in the reliability and LCC analysis of the powertrain of an electric step van, the literature of this topic is specifically addressed in more detail here.

Cost is one of the major factors in market adoption of a new product/technology such as electric vehicles (EV). EVs benefit from a lower energy consumption compared to the internal combustion engine vehicles (ICEV), as the efficiency of electric motors is generally much higher than internal combustion engines (ICE). When decelerating, instead of dissipating the kinetic energy in the brakes, it can be stored in batteries through regenerative breaking. This further enhances the efficiency of the system. One drawback of EVs is their high acquisition cost, mainly due to components such as the electric motor and the battery pack.

Purchasing an EV with a high AC may be justified by its lower energy cost when compared to ICEV options. To identify the potential economic advantage of EVs over ICEVs, a comprehensive LCC analysis is necessary, where different cost categories such as the AC, the MC, the EC, the salvage value of the product, and government incentives (if applicable) are taken into account.

EVs appear in different concepts/designs/configurations such as hybrid electric vehicles (HEV), fuel cell vehicles (FCV), and battery electric vehicles (BEV). HEVs couple an electric motor and a battery pack to the ICE of conventional vehicles. The motor and the engine provide the power, each operating at its optimum efficiency point to reduce the energy consumption. Compared to HEVs, BEVs exclude the combustion engine in favor of lowering the number of components, increasing efficiency, and decreasing the EC. FCVs replace the battery pack with a fuel cell as the energy storage unit. In general, fuel cells are more expensive, heavier, and less efficient than Li-ion batteries, and they require more infrastructure for diffusing into the market [54, 55]. Therefore, the market is more inclined toward HEVs and BEVs.

To get the same performance as HEVs, a BEV deploys a larger electric motor and battery pack, which results in a high AC. Battery cost is a major expense in the AC and LCC of electric vehicles [34, 55–57]. In a scenario where the future gasoline price increases and battery cost declines, HEVs and BEVs can economically compete with ICEVs [58, 59]. Also, when the

battery cost is a large portion of LCC, the life-cycle cost is very sensitive to the variation of the battery cost in the market [60]. This sensitivity decreases as the battery prices decline.

From 2007 to 2014, BEV manufacturers expecienced an 8% average annual reduction in the battery cost, reaching 300 USD/kWh in 2014 [61]. In late 2015, GM announced that the cost of Li-ion batteries for the company was 145 USD/kWh, and will continue to drop to 100 USD/kWh by 2021 [62]. Tesla projects the same figure of 100 USD/kWh by 2020 [63].

Empirical cost-performance or cost-mass models are common in component-level and system-level AC modelling of electric vehicles [29, 34–37]. A more detailed AC analysis first identifies the direct manufacturing cost, including material, labor, and tooling costs. Next, an overhead factor is applied to the direct manufacturing cost to account for the indirect manufacturing costs such as general and administrative, engineering, and sales expenses. Lastly, the profit margin is applied to determine the price of the product [25]. If applicable, tax rates should be included on the price to get the AC of the product.

In the maintenance cost analysis, one method is to express the MC of the product as a fraction of its AC. Seixas et al. [64] assume that the annual MC is 1% of the capital cost of BEVs. In another approach, the MC of electric vehicles is estimated using empirical data [65, 66]. A comparison of FedEx HEV and diesel delivery trucks shows that the maintenance cost of the HEV options is 0.128 USD/km, whereas the figure is 0.139 USD/km for diesel options [67]. The difference is not significant, especially noting that the HEV fleet is newer than the diesel fleet; the average mileage of the diesel options is 73,924 km versus the average mileage of 24,001 km for the HEVs [67].

The aforementioned methods for estimating MC are easy to implement, but have two drawbacks. Firstly, they highly depend on drive cycle and operations condition of the vehicle. Therefore, they can not be reliably used for other drive cycles. Second, they provide the average over a fleet and, therefore, do not reflect the design details of individual vehicles. A more precise

approach to the MC analysis is developing a model which reflects the impact of design details of a product on its maintenance cost. Examples of such a model are presented in [42, 43].

Compared to ICEVs, higher tank-to-wheel efficiency of EVs result in a lower energy consumption. However, a more accurate comparision must incorporate the total well-to-wheel consumption of both options. Depending on the electricity source, the well-to-wheel impact of EVs may or may not have an advantage over ICEVs [68, 69]. Another key consideration is the range and the driving cycle of the vehicle. For a small range, in spite of their high efficiency, the energy savings of EVs is not sufficient to pay off their high AC [70]. Frequent stops must be involved in the drive cycle to leverage the advantage of regenerative braking and reduce energy consumption when compared to ICEVs.

To address the aforementioned issues, it is important to develop a model which takes into account the influence of the design details of powertrain of electric vehicles in their LCC. In designing the powertrain, the variables are the element sizes/types. The requirements are commonly top speed, gradability, acceleration time, emissions, reliability, etc. The objective function may be economic indicators such as efficiency, acquisition cost, or life-cycle cost of the product. Simpson studied the battery sizing of plug-in HEVs on the cost and fuel consumption of the system [37]. In a work by Fan [71], the objective function was efficiency of a BEV, while the dynamics of the system is outside of the scope of that research. Morozov et al [72] selected the gear ratio of the transmission to optimize the energy consumption of a BEV delivery truck.

Study of the literature shows that a framework is required for studying the influence of the design variables on the powertrain reliability on one side, and on the economic indicators of the system on the other. The framework must include component-level CPR models, as well as maintenance cost and energy cost models to equip designers for the LCC analysis of the product.

Throughout the thesis, the SI system of units has been used unless otherwise specified. The case studies herein are gedanken experiments.

1.4 Thesis objectives and outline

The goal of the present research is to develop a reliability-based life-cycle cost model for engineering elements and systems. A part of the motivation is to build a tool to be used by engineers/designers in the LCC and reliability optimization of engineering systems, although the focus of this study is not the optimization procedure itself. Whenever optimization is used in the case studies of this thesis, it refers to finding the best solution(s) among the options available in the design space of the case study.

The goal of this research will be achieved by meeting the following objectives:

1. Generating a procedure for establishing a relation between the acquisition cost of a product and its reliability and performance.
2. Developing the CPR model of gears.
3. Deriving the CPR model of rolling bearings.
4. Building the CPR model for gearboxes by combining the CPR models of sub-systems.
5. Establishing the CPR model of electrical insulations.
6. Developing the CPR model of electric motors by combining the CPR models of sub-systems.
7. Establishing reliability-based cost models for a post-failure strategy and two preventive maintenance strategies.
8. Conducting the LCC analysis for a system of components for reliability and cost improvement of the system using the CPR models of its components as well as the maintenance cost models.

The LCC in this research is composed of the AC, the MC, and the EC, while other cost categories, such as disposal cost and salvage value are outside of the scope of this thesis. Each of these objectives will be addressed in separate chapters, specifically:

- In Chapter 2, Objective 1 is addressed. Next, Objective 2 is conducted using the proposed procedure for CPR modelling. The accuracy of the gears model is validated using the price catalog of an original equipment manufacturers (OEM).
- In Chapter 3, the CPR modelling procedure is used to meet Objective 3. The bearing model is validated using the price catalog of an OEM. Next, Objective 4 is tackled by coupling the gear and bearing models. In a case study, the influence of the gear and bearing size on the gearbox reliability and acquisition cost is shown.
- Objective 5 is focused on in the first part of Chapter 4. Next, by coupling the bearing and electrical insulation models, Objective 6 is dealt with. A numerical example is included to study the interplay between the cost and reliability of an electric motor on one side and its bearing size and insulation class on the other.
- Chapter 5 is devoted to Objective 7. Cost models are developed for a post-failure and also two preventive maintenance strategies. The models extend the previous work in literature to low-reliability situations and non-zero inflation rates. As a case study, the bearing size and gear size of a conceptual gearbox are determined to reduce the sum of the acquisition and maintenance costs of the gearbox.
- In Chapter 6, Objective 8 is met by addressing the LCC of the powertrain of a battery electric step van. The best designs are indicated to improve the reliability and reduce the LCC of the product while ensuring that the specified performance requirements are met.
- Chapter 7 summarizes the major findings of the research. It also proposes three main applications where this research can be used for or extended to.

1.5 Contribution to the knowledge

The followings are the original contributions of the present research to the literature:

1. A novel procedure is proposed for modelling the cost-performance-reliability (CPR) behavior of engineering elements and systems.
2. The CPR models of gears, rolling bearings, and electrical insulations are developed using the proposed procedure.
3. The CPR model of gearboxes is built by coupling the CPR models of gears and bearings.
4. The CPR model of electric motors is established using the CPR model of bearings and electrical insulations.
5. Maintenance cost models are derived for a post-failure and two preventive maintenance strategies. These models extend the models in the literature to the cases where the inflation rate is not negligible or the end-of-cycle reliability of the component is not close to unity.
6. The LCC model of the powertrain of single-speed battery electric truck is built using the developed CPR and maintenance cost models in order to enable engineers/designers to evaluate the LCC of the powertrain.

Chapter 2

Acquisition Cost-Performance-Reliability Modelling of Gears

From project economics perspective, it is interesting to quantify the cost of quality of a product. This includes the investment required to improve the material quality, endurance, size, or type of the product. The first objective of this chapter is to generate a procedure for cost-performance-reliability (CPR) modelling of engineering elements. The second objective is to use the proposed procedure for establishing the CPR model of spur and helical gears.

2.1 Model formulation

The reliability, $R(t)$, of a component is the probability that the component operates properly up to instant t [3]. Two decisions may be made to improve the reliability and/or the performance of a mechanical part. The first one is increasing the size of the component. This method is appropriate wherever the fatigue resistance of the part is improved by size enhancement. The second method is using higher quality materials or manufacturing processes. Each of these

decisions result in a higher acquisition cost. In the following section, a systematic approach is introduced for modelling the influence of these two decisions on the performance, reliability and the acquisition cost of engineering elements.

2.1.1 Cost-performance-reliability modelling procedure

The following procedure can be used in CPR modelling of engineering elements:

1. A baseline element with a specified material type and geometry is considered. A failure analysis is conducted to find the relation between the reliability of the element and its size, material properties, and performance.

2. The size of the baseline element is changed by scaling factors to reach a set of arbitrary scaled elements. The sizes of the scaled elements are then substituted in the reliability relation to study how the reliability is influenced by the scaling factor at a specified performance and material properties. The result is the reliability-performance-size scaling relation.

3. A simple relation is postulated between the acquisition cost of the element and its size, which is then translated into the cost-size scaling relation [25, 28].

4. The scaling factor is eliminated from the relations established in steps 2 and 3 to develop the acquisition cost-performance-reliability (CPR) model of the element. In this relation, the material properties is also included as a parameter which can be tuned for other types of materials.

In this procedure, the scaling factor is a continuous design variable whereas the material type is a discrete one. Mathematically speaking, the outcome of this analysis for each material

type is a surface in the cost-performance-reliability (CPR) space. The CPR surface of the part will be shifted by switching from one material to another.

2.1.2 CPR modelling of gears

In the rest of this chapter, the procedure introduced in Section 2.1.1 is used for CPR modelling of gears. As a well accepted and broadly used method, AGMA stress and strength equations of gears [4] are used to relate the performance and reliability to other design parameters, including the mechanical properties, life, safety factor, environment factors, etc. The gear performance is the applied torque. It is assumed that a cooling system controls the gear's temperature and there is no considerable variation in the mechanical properties of the gears as a result of temperature variation. The SI system of units has been used unless otherwise specified.

Size, performance and reliability

The dominant failure mechanisms of gears are the bending stress failure and the surface pitting failure [4]. The former is caused by the fatigue of the teeth undergoing cycling bending loads whereas the latter is a result of the contact stress fatigue. In both cases, size scaling of the gear affects its fatigue life and, consequently, its reliability. This effect is studied in this section.

For a spur or helical gear, denoted by $\mathbf{g}$, with the module m, the pitch diameter d, and the face width b that undergoes a throughput torque τ, the AGMA stress equation for the maximum bending stress is [4]

$$\sigma = \frac{2A_1 K_s K_v \tau}{bdmY_J}, \tag{2.1}$$

where

$$A_1 = K_o K_H K_B. \tag{2.2}$$

The overload factor K_o depends on the smoothness of operation of the power source and the driven machine to add the influence of externally applied loads to the nominal torque. This is a fixed number when the driving machine and the general features of the driven system are not changed [4]. The nonuniform distribution of load accross line of contact is accounted for in the load distribution factor K_H, which is dependent to factors such as the gear enclosure, teeth geometry, and gear mounting on the shaft. The Rim-thickness factor K_B adjusts the stress if the rim thickness is not sufficient to support the tooth root [4]. The gears studied here have sufficient rim thickness and, therefore, $K_B = 1$. This way, on the right-hand side of Eqn. (2.2), only K_H is influenced by resizing. As shown in Tab. 2.4, the influence of size on K_H is not significant. Therefore, in CPR modelling, it is assumed that A_1 is unchanged under size scaling.

The dynamic factor K_v is given by

$$K_v = \Big(1 + \frac{\sqrt{200V}}{A}\Big)^B, \tag{2.3}$$

where V is the pitch circle velocity in m/s, $B = 0.25(12 - Q_v)^{2/3}$, and $A = 50 + 56(1 - B)$. The AGMA quality number Q_v is determined by the surface finishing accuracy [4]. The formulation derivation here is simplified if K_v is a power-law of V. Therefore, the following alternative relation is proposed

$$K_v = \alpha_0 V^{\beta_0} \; ; \;\; \beta_0 = 0.045(12 - Q_v)^{0.71} \; , \;\; \alpha_0 = 1 + 0.0024(12 - Q_v)^{2.13}. \tag{2.4}$$

The maximum difference between Eqn. (2.3) and Eqn. (2.4) is 1% when $V \geq 3$ m/s, which is the velocity range addressed in this chapter.

The size factor K_s is given by [4]

$$K_s = 1.19\big(bm\sqrt{Y}\big)^{0.054}. \tag{2.5}$$

Table 2.1 Parameters of the approximated relation for geometry factor

Gear ratio	0.75	1.00	1.25	1.33
α_1'	0.375	0.411	0.439	0.446
β_1'	0.246	0.232	0.222	0.219
α_1	0.164	0.170	0.175	0.178
β_1	0.181	0.180	0.277	0.175

The tooth form factor Y is dependent to the gear parameters listed in [73]. Following the method introduced in AGMA 908-B89 [73], Y is calculated assuming no addendum modification, pressure angle of 14.5 °, zero helix angle, gear thinning of 0.024 *mm* for backlash, cutting tool pitch diameter of 5 *m*, and tool tip radius of 0.25 *mm*. With this parameters, within less than 1% error, Y can be approximated by

$$Y = \alpha_1' n_g^{\beta_1'}, \tag{2.6}$$

where n_g is the teeth number, and Tab. 2.1 gives the value of α_1' and β_1'.

The bending stress geometry factor Y_J depends on n_g and the gear ratio [4]. For gears with the aforementioned parameters, Y_J can be approximated with

$$Y_J = \alpha_1 n_g^{\beta_1}, \tag{2.7}$$

where α_1 and β_1 are given in Tab. 2.1. The maximum difference between Eqn. (2.7) and the result of AGMA 908-B89 is less than 2%.

The allowable bending stress of the spur and helical gears is given by the AGMA strength equation [4]

$$\sigma_{all.} = \frac{A_2 \sigma_{FP} Y_N}{Y_{Z1}}. \tag{2.8}$$

where

$$A_2 = \frac{1}{S_F Y_\theta}. \tag{2.9}$$

If the oil temperatures is below 120 $^\circ C$ [4], which it is considered here, the temperature factor $Y_\theta = 1.0$. The safety factor S_F remains unchanged under size scaling as it is often a design requirement. Therefore, A_2 is constant under size scaling. The allowable bending stress is denoted by σ_{FP} and depends on the gear material and post manufacturing processes such as heat treatment. The stress cycle factor Y_N is given by

$$Y_N = \alpha_2 N^{-\beta_2}, \tag{2.10}$$

where N is the gear's life in cycles. The constants α_2 and β_2 depend on the hardness of the gear teeth and are presented in [4]. The reliability factor Y_{Zi} is defined by

$$Y_{Zi} = \alpha_3 - \beta_3 \mathrm{Ln}(1 - R_i), \;\; i = 1; \text{ against bending }, i = 2; \text{ against pitting} \tag{2.11}$$

in which R_i is the gear's end of cycle reliability against the failure mechanisms. The constants α_3 and β_3 are [4]

$$(\alpha_3, \beta_3) = \begin{cases} (0.658, 0.0759)\,; & 0.5 < R_i < 0.99 \\ \\ (0.500, 0.109)\,; & 0.99 \leq R_i \leq 0.9999 \end{cases} \tag{2.12}$$

Setting the maximum bending stress in Eqn. (2.1) equal to the allowable stress in Eqn. (2.8) yields an equation with two factors Λ_1 and Λ_2

$$\Lambda_2 = \frac{A_2}{2A_1}\Lambda_1, \tag{2.13}$$

where

$$\Lambda_2 = \frac{\tau Y_{Z1}}{Y_N}, \tag{2.14}$$

contains the performance, the reliability, and the life factor of the gear **g**, whereas

$$\Lambda_1 = \frac{bdY_J m\sigma_{FP}}{K_v}, \tag{2.15}$$

is composed of the geometry and the mechanical property. Equation (2.13) implies that the ratio

$$\frac{\Lambda_2}{\Lambda_1} = \frac{K_v \tau Y_{Z1}}{bdY_N Y_J m\sigma_{FP}} = \frac{A_2}{2A_1}, \tag{2.16}$$

is invariant under any change in the size and mechanical properties of a gear. Therefore, for any other gear $\mathbf{g}^*$, it is possible to write

$$\frac{\Lambda_2^*}{\Lambda_1^*} = \frac{\Lambda_2}{\Lambda_1}, \tag{2.17}$$

where the parameters with a superscript asterisk correspond to $\mathbf{g}^*$. Rearrangement of Eqn. (2.17) yields

$$\frac{\tau^*}{\tau}\frac{Y_{Z1}^*}{Y_{Z1}}\frac{Y_N}{Y_N^*} = \frac{b^*}{b}\frac{d^*}{d}\frac{Y_J^*}{Y_J}\frac{K_v}{K_v^*}\frac{m^*}{m}\frac{\sigma_{FP}^*}{\sigma_{FP}}. \tag{2.18}$$

Now consider that the gear $\mathbf{g}^*$ may be geometrically mapped on the gear **g** by

$$d^* = \gamma_1 d \ , \ b^* = \gamma_2 b \ , \ m^* = \gamma_3 m, \tag{2.19}$$

where γ_1, γ_2, and γ_3 are the radial, axial, and module scaling factors, respectively. The first scaling relation in Eqn. (2.19) along with Eqn. (2.4) imply

$$K_v^* = \gamma_1^{\beta_0} K_v. \tag{2.20}$$

The first and third relations in Eqn. (2.19) imply

$$n^* = \frac{\gamma_1}{\gamma_3} n, \tag{2.21}$$

which along with Eqn. (2.5)-(2.7) yields

$$K_s^* = \gamma_1^{0.027\beta_1'}\gamma_2^{0.054}\gamma_3^{0.054-0.027\beta_1'}K_s\ ,\ \ Y_J^* = \gamma_1^{\beta_1}\gamma_3^{-\beta_1}Y_J. \tag{2.22}$$

Since $0.027\beta_1' << 1$, the terms $\gamma_1^{0.027\beta_1'}$ and $\gamma_3^{-0.027\beta_1'}$ can be approximated by unity, as justified in Section 2.2.1. With this approximation, Eqn. (2.18)-(2.22) give

$$\frac{\tau^*}{\tau}\frac{Y_{Z1}^*}{Y_{Z1}} = \gamma_1^{\beta_1-\beta_0+1}\gamma_2^{0.946}\gamma_3^{0.946-\beta_1}\frac{\sigma_{FP}^*}{\sigma_{FP}}\frac{Y_N^*}{Y_N}, \tag{2.23}$$

which is the performance-reliability-material (PRM) model against bending failure under a constant torque. If the applied torque is cycle-dependent, $\tau(N)$, Eqn. (2.23) is generalized to

$$\frac{Y_{Z1}^*}{Y_{Z1}} = \gamma_1^{\beta_1-\beta_0+1}\gamma_2^{0.946}\gamma_3^{0.946-\beta_1}\frac{\sigma_{FP}^*}{\sigma_{FP}}\frac{\int_0^{N^*}\frac{dY_N^*}{\tau^*(N)}}{\int_0^{N}\frac{dY_N}{\tau(N)}}, \tag{2.24}$$

where Y_{Z_1} is the bending reliability factor after N cycles, and dY_N is the differential form of the stress cycle factor of Eqn. (2.10). If

$$N^* = N,\ \ \tau^*(N) = \tau^* f(N),\ \ \tau(N) = \tau f(N), \tag{2.25}$$

where $f(N)$ is an arbitrary function, the general PRM model Eqn (2.24) simplifies to

$$\frac{\tau^*}{\tau}\frac{Y_{Z1}^*}{Y_{Z1}} = \gamma_1^{\beta_1-\beta_0+1}\gamma_2^{0.946}\gamma_3^{0.946-\beta_1}\frac{\sigma_{FP}^*}{\sigma_{FP}}, \tag{2.26}$$

The meaning of condition (b) above is that the only difference between $\tau^*(N)$ and $\tau(N)$ is the amplitude. This condition is practical when among two gearboxes, one undergoes a heavier torque while the general pattern or loading cycle is not altered. In the rest of this chapter, conditions (a) and (b) are considered in model derivation. Note that by setting $N^* = N$, Eqn. (2.23) is also reduced to Eqn. (2.26).

If the gears have identical material properties, Eqn. (2.26) is reduced to

$$\frac{\tau^*}{\tau}\frac{Y^*_{Z1}}{Y_{Z1}} = \gamma_1^{\beta_1-\beta_0+1}\gamma_2^{0.946}\gamma_3^{0.946-\beta_1}. \tag{2.27}$$

which is the performance-reliability-size (PRS) model of spur and helical gears against bending failure.

AGMA proposes the following stress equation for calculating the contact stress of spur and helical gears [4]

$$\sigma_c = Z_E\sqrt{\frac{2A_3K_vK_s\tau}{dd_wb}}, \tag{2.28}$$

with

$$A_3 = \frac{K_oK_HZ_R}{Z_I}. \tag{2.29}$$

The elastic coefficient Z_E depends on the material type of the gear and its mating gear, and d_w is the pitch diameter of the pinion [4]. Z_R is a place holder for the residual stress and plastic effects on the teeth surface. Until more information is available for such effects, it is set equal to unity [4]. The geometry factor for pitting resistance is denoted by Z_I. For spur gears, it depends on the gear ratio and the pressure angle, implying that it is fixed under the size scaling of Eqn. (2.19). For helical gears with 20° normal pressure angle, 25° helix angle, normal module of 4 *mm*, gear ratio of 1.67, and the range of pinion teeth from 24 to 48, a size-independent Z_I assumption leads to a maximum error of 2.1%. This example shows that Z_I is weakly influenced by resizing. In the rest of this analysis, it is assumed that Z_I is size-independent for helical gears as well. This way, under a size scaling, A_3 can be treated as a constant.

The AGMA allowable contact stress equation of spur and helical gears is

$$\sigma_{c,all.} = \frac{A_4\sigma_{HP}Z_N}{Y_{Z2}}, \tag{2.30}$$

where

$$A_4 = \frac{Z_W}{S_H Y_\theta}. \tag{2.31}$$

The safety factor against pitting S_H is often pre-determined by the design requirements and, thus, is not size-dependent. The hardness ratio Z_W depends on the gear ratio and the ratio of the hardness of the pinion and the gear [4]. For the gear ratio of 2.0, if the hardness ratio changes from 1.2 to 1.7, Z_W varies from 1.003 to 1.007. For the gear ratio of 3.0 and the same range of hardness ratio, Z_W changes from 1.004 to 1.013. For the purpose of the present formulation, this effect is negligible and Z_W is considered as a constant under Eqn. (2.19). Therefore, A_4 is considered size-independent. σ_{HP} is the allowable contact stress, and Z_N is the stress life cycle factor given by

$$Z_N = \alpha_2' N^{-\beta_2'}, \tag{2.32}$$

in which the constants α_2' and β_2' depend on the working condition of the gear and are presented in [4]. Y_{Z2} is the reliability factor against surface pitting failure given by Eqn. (2.11). A similar arguments that resulted Eqn. (2.23) from Eqn. (2.1) and Eqn. (2.8) yield

$$\frac{\tau^*}{\tau}\left(\frac{Y_{Z2}^*}{Y_{Z2}}\right)^2 = \gamma_1^{2-\beta_0}\gamma_2^{0.946}\gamma_3^{-0.054}\left(\frac{\sigma_{HP}^*}{\sigma_{HP}}\right)^2\left(\frac{Z_E}{Z_E^*}\right)^2, \tag{2.33}$$

which is the PRM model for the gears against pitting failure. For the gears of the same material type, Eqn. (2.33) is simplified to

$$\frac{\tau^*}{\tau}\left(\frac{Y_{Z2}^*}{Y_{Z2}}\right)^2 = \gamma_1^{2-\beta_0}\gamma_2^{0.946}\gamma_3^{-0.054}. \tag{2.34}$$

Equations (2.27) and (2.34) establish the interplay between the performance, reliability, and size scaling of spur and helical gears against bending and pitting failures, respectively.

Size and cost

The gear AC can be written as [32]

$$C_0 = \alpha_5 + \beta_5 M + \beta_h v_h + \beta_g v_g, \tag{2.35}$$

where M is the gear's bill of material mass. The marginal cost of increasing the gear mass β_5 depends on the material and manufacturing process. The last two terms consider the gear teeth formation using hobbing/shaping and grinding, where v_h is the material removal volume in the hobbing/shaping, and v_g is the volume removed of the tooth grinding [32]. Parameters β_h and β_g are the marginal cost per volume of hobbing/shaping and grinding, respectively [32]. If the gear teeth are formed using casting, there is no hobbing/shaping cost because $v_h = 0$.

The mass M is scaled with $d_a^2(b + b_h)$, in which d_a denotes addendum and b_h is the project of the gear hub. Assuming that b_h and b have equal scaling factor and assuming that d_a can be approximated by d, the mass becomes proportional to $d^2 b$. The removal volume of hobbing/shaping v_h is scaled with dbm, and v_g is scaled with $db\delta$, in which δ is the grinding thickness [32]. If δ is proportional to the teeth size, it is scaled with m. Therefore, v_g can be written in terms of dbm. This way, the last two terms on the right-hand side of Eqn. (2.35) reduce to one term, which gives

$$C_0 = \alpha_5 + \beta_5' d^2 b + \beta_5'' dbm. \tag{2.36}$$

In Eqn. (2.35) and (2.36), fixed costs and indirect production costs, including administration, marketing, depreciation, and R&D and engineering expenses are accounted for by α_5 [28]. For a specified heat treatment method and hardness target, the heat treatment expense is weakly influenced by the gear size, as devised by a specialist [75]. Therefore, its cost is also reflected in α_5. The factors β_5' and β_5'' implicitly consider the variable cost of the material type, material property, and gear geometry/micro-geometry.

The geometry and AC of at least three gears are required to find the three unknowns α_5, β_5', and β_5'' of Eqn. (2.36). Here, it is proposed that the size-cost model is established using five data points. The baseline gear is the first data point. Two other data points are gears with module and face width identical to the baseline; one with a smaller and one with a larger pitch diameter. The final two gears are with the pitch diameter of the baseline; one with a smaller and one with a larger module compared to the baseline. This method is used in Section 2.2.

Equations (2.19) and (2.36), along with the definition of normalized cost as

$$\xi = \frac{C_0^* - \alpha_5}{C_0 - \alpha_5}, \tag{2.37}$$

yield

$$\xi = \begin{cases} \dfrac{\gamma_1^2 + \beta_4 \gamma_1}{1 + \beta_4} \; ; & \gamma_2 = \gamma_3 = 1 \\ \gamma_2 \; ; & \gamma_1 = \gamma_3 = 1 \\ \gamma_3 \; ; & \gamma_1 = \gamma_2 = 1 \end{cases} ; \quad \beta_4 = \frac{\beta_5'' m}{\beta_5' d}. \tag{2.38}$$

In Eqn. (2.38), the first line is a radial scaling. The second line addresses axial scaling when radial scaling is not allowed due to space limitations. The last line of Eqn. (2.38) is used when neither radial nor axial scaling is possible because of space constraints. In that situation, the design is tweaked by scaling the module. When the third line is used, the second term on the right-hand of Eqn. (2.36) is constant. In this case, α_5 is replaced by $\alpha_5 + \beta_5' d^2 b$ in Eqn. (2.37).

Cost-performance-reliability relation

In designing against bending failure, Eqn. (2.27) and Eqn. (2.38) may be used to eliminate the size scaling factors and derive the CPR model of bending failure

$$\frac{\tau^*}{\tau}\frac{Y^*_{Z1}}{Y_{Z1}}=\begin{cases}\left(\sqrt{\frac{\beta_4^2}{4}+(1+\beta_4)\xi}-\frac{\beta_4}{2}\right)^{\beta_1-\beta_0+1}\ ;\ \gamma_2=\gamma_3=1\\ \xi^{0.946}\ ;\ \gamma_1=\gamma_3=1\\ \xi^{0.946-\beta_1}\ ;\ \gamma_1=\gamma_2=1\end{cases}. \tag{2.39}$$

By eliminating the scaling factors from Eqn. (2.34) and Eqn. (2.38), the CPR model of pitting failure is achieved

$$\frac{\tau^*}{\tau}(\frac{Y^*_{Z2}}{Y_{Z2}})^2=\begin{cases}\left(\sqrt{\frac{\beta_4^2}{4}+(1+\beta_4)\xi}-\frac{\beta_4}{2}\right)^{2-\beta_0}\ ;\ \gamma_2=\gamma_3=1\\ \xi^{0.946}\ ;\ \gamma_1=\gamma_3=1\\ \xi^{-0.054}\ ;\ \gamma_1=\gamma_2=1\end{cases}. \tag{2.40}$$

The product of the reliability of each failure mode gives the total reliability [4]

$$Y^*_Z=\alpha_3-\beta_3\mathrm{Ln}(1-R^*)\ ;\ R^*=R^*_1R^*_2, \tag{2.41}$$

Substitution of Eqn. (2.11) into Eqn. (2.41) gives

$$1-R^*=\exp\big(\frac{\alpha_3-Y^*_{Z1}}{\beta_3}\big)+\exp\big(\frac{\alpha_3-Y^*_{Z2}}{\beta_3}\big)-\exp\big(\frac{\alpha_3-Y^*_{Z1}}{\beta_3}+\frac{\alpha_3-Y^*_{Z2}}{\beta_3}\big). \tag{2.42}$$

Substitution of Y_{Zi}^{*} from Eqn. (2.39) and (2.40) into Eqn. (2.42) gives the overall CPR model. The CPR model of radial size scaling is

$$\begin{aligned}
&1-R^{*}= \\
&\exp\Big(\frac{\alpha_3-Y_{Z1}\frac{\tau}{\tau^{*}}\big(\sqrt{\frac{\beta_4^2}{4}+(1+\beta_4)\xi}-\frac{\beta_4}{2}\big)^{\beta_1-\beta_0+1}}{\beta_3}\Big)+ \\
&\exp\Big(\frac{\alpha_3-Y_{Z2}\sqrt{\frac{\tau}{\tau^{*}}}\big(\sqrt{\frac{\beta_4^2}{4}+(1+\beta_4)\xi}-\frac{\beta_4}{2}\big)^{1-\frac{\beta_0}{2}}}{\beta_3}\Big)- \\
&\exp\Big(\frac{\alpha_3-Y_{Z1}\frac{\tau}{\tau^{*}}\big(\sqrt{\frac{\beta_4^2}{4}+(1+\beta_4)\xi}-\frac{\beta_4}{2}\big)^{\beta_1-\beta_0+1}}{\beta_3}+ \\
&\qquad\frac{\alpha_3-Y_{Z2}\sqrt{\frac{\tau}{\tau^{*}}}\big(\sqrt{\frac{\beta_4^2}{4}+(1+\beta_4)\xi}-\frac{\beta_4}{2}\big)^{1-\frac{\beta_0}{2}}}{\beta_3}\Big).
\end{aligned} \tag{2.43}$$

For axial scaling, substitution of Eqn. (2.39), (2.40) into (2.42) results

$$\begin{aligned}
1-R^{*}=&\exp\Big(\frac{\alpha_3-Y_{Z1}\frac{\tau}{\tau^{*}}\xi^{0.946}}{\beta_3}\Big) \\
&+\exp\Big(\frac{\alpha_3-Y_{Z2}\sqrt{\frac{\tau}{\tau^{*}}}\xi^{0.473}}{\beta_3}\Big) \\
&-\exp\Big(\frac{\alpha_3-Y_{Z1}\frac{\tau}{\tau^{*}}\xi^{0.946}}{\beta_3}+\frac{\alpha_3-Y_{Z2}\sqrt{\frac{\tau}{\tau^{*}}}\xi^{0.473}}{\beta_3}\Big).
\end{aligned} \tag{2.44}$$

For module scaling, the CPR model becomes

$$\begin{aligned}
1-R^{*}=&\exp\Big(\frac{\alpha_3-Y_{Z1}\frac{\tau}{\tau^{*}}\xi^{0.946-\beta_1}}{\beta_3}\Big) \\
&+\exp\Big(\frac{\alpha_3-Y_{Z2}\sqrt{\frac{\tau}{\tau^{*}}}\xi^{-0.027}}{\beta_3}\Big) \\
&-\exp\Big(\frac{\alpha_3-Y_{Z1}\frac{\tau}{\tau^{*}}\xi^{0.946-\beta_1}}{\beta_3}+\frac{\alpha_3-Y_{Z2}\sqrt{\frac{\tau}{\tau^{*}}}\xi^{-0.027}}{\beta_3}\Big).
\end{aligned} \tag{2.45}$$

The factor β_0 is determined by the quality level of the gear $\big($see Eqn. (2.4)$\big)$. The value of α_3, β_3 are found in [4]. Table 2.1 gives β_1. The reliability of the baseline gear, i.e. Y_{Z1} and Y_{Z2} are known from the AGMA reliability analysis. Therefore, to identify Eqn. (2.43)-(2.45), it is only required to have β_4. From customer's perspective, this factor is determined when the cost-size relation Eqn. (2.36) is established. From a manufacturer's perspective, β_4 is known as the manufacturer often has a good understanding of β_5' and β_5'' in Eqn. (2.38) from past experience. This implies that the parameters in Eqn. (2.43)–(2.45) correspond to physical or financial featues of the product and, therefore, these models contain no curve-fitting parameter from a manufacturer's point of view. From a customer's viewpoint, however, since β_5' and β_5'' are not identified, a curve-fitting on the cost-size relation Eqn. (2.36) is required to evaluate β_4.

The CPR models Eqn. (2.43)-(2.45) each correspond to a specific scaling; among d^*, b^* and m^* of the gear $\mathbf{g}^*$, only one differs from the baseline $\mathbf{g}$. If more than one geometry parameter are varied, a combination of Eqn. (2.43)-(2.45) must be used. The baseline $\mathbf{g}$ can first be scaled radially from (d, b, m) to (d^*, b, m). Equation. (2.43) is used for CPR modelling. Next, the (d^*, b, m) gear is mapped to (d^*, b^*, m) by an axial scaling, and Eqn. (2.44) is used for CPR modelling. Finally, a module scaling takes the (d^*, b, m) gear to the (d^*, b^*, m^*) gear, and CPR modelling is done with Eqn. (2.45).

2.2 Numerical examples

Equations (2.43)-(2.45) are derived using the assumptions underlying Eqn. (2.2), (2.31), and (2.36). Three groups of cast iron spur gears by an original equipment manufacturer (OEM) are assessed to justify the assumptions and validate the CPR models [74]. Table 2.2 lists the material properties of the gears. The gear geometry and price are given in Tab. 2.3 [74]. The pressure angle equals 14.5^o. At each group, the module and face width of the gears are identical, but they have different pitch diameters ranging from 203.2 mm to 406.4 mm. The module and face

Table 2.2 Material properties of the gears

Gear material	Hardness (Brinell)	σ_{FP} (MPa) [4]	σ_{HP} (MPa) [4]
ASTM A48 class 30	174	60	455

width changes from one group to the other. As a commercial-quality level, it is assumed that the AGMA quality number is $Q_v = 6$ [4].

2.2.1 Assumption justification

To justify the assumption that A_1 is size-indipendent in Eqn. (2.2), the value of A_1 is presented in Tab. 2.4 for the gears of Tab. 2.3 with $m = 4.23$ mm. For a uniform source of power and a uniform driven machine, $K_o = 1.0$ [4]. As the rim thickness of the gears provides enough support for the teeth, $K_B = 1.0$ [4, 74]. The load distribution factor K_H is calculated using the method given in [4]. To do so, uncrowned teeth, straddle-mounted pinion and gear, and commercial, enclosed unit conditions are considered. The difference between the value of A_1 for the baseline, which is the 66-teeth gear, and the other gears is negligible, justifying the assumption that A_1 is size-independent. The size factor K_s is calculated following the approach given in [4, 73]. It is considered that the pitch diameter of the cutting tool is 5 m, its tip radius is 0.25 mm, tooth thining for backlash is 0.024 mm, the addendum modification factors equal zero, the gear ratio is 1.33. The calculations are for highest point of single tooth contact [73]. The results justify the assumption of neglecting the term $\gamma_1^{0.027\beta_1'}$ in Eqn. (2.22).

For the gears of Tab. 2.3, five data points are used to establish Eqn. (2.36): the three 66-teeth gears, the 48-teeth gear with $m = 4.23$ mm, and the 96-teeth gear with $m = 4.23$ mm, which results $\alpha_5 = 93.81$ CAD, $\beta_5' = 0.0280$ CAD/cm^3, and $\beta_5'' = 1.36$ CAD/cm^3. The 66-teeth gear with $m = 4.23$ mm is the baseline. The result of Eqn. (2.36) and the catalog prices are

Table 2.3 Geometry and price of the gears

Number of teeth	d (mm)	m (mm)	b (mm)	Catalog price (CAD)
40	203.2	5.08	44.5	207.71
45	228.6	5.08	44.5	231.44
50	254.0	5.08	44.5	255.30
55	279.4	5.08	44.5	279.20
60	304.8	5.08	44.5	298.34
70	355.6	5.08	44.5	367.34
80	406.4	5.08	44.5	436.34
48	203.2	4.23	38.1	178.41
54	228.6	4.23	38.1	195.45
60	254.0	4.23	38.1	229.23
66	279.4	4.23	38.1	238.41
72	304.8	4.23	38.1	255.57
84	355.6	4.23	38.1	298.34
96	406.4	4.23	38.1	357.84
64	203.2	3.18	31.8	158.18
72	228.6	3.18	31.8	172.05
80	254.0	3.18	31.8	189.27
88	279.4	3.18	31.8	205.13
96	304.8	3.18	31.8	227.84
112	355.6	3.18	31.8	257.94
128	406.4	3.18	31.8	298.55

illustrated in Fig. 2.1. Maximum difference between Eqn. (2.36) and catalog prices is 4.7% for the 60-teeth gear with $m = 4.23$ mm. Two points can be mentioned as the source of the difference: (a) Although the scaling factors in Eqn. (2.19) are determined from the pitch diameter and the gear facewidth, the scaling of some other features of the gears, such as hub, does not necessarily follow the factors of Eqn. (2.19); and, (b) The gear style, such as web, web with lightning holes, spoke, etc., has an impact on the gear price by influecing the material removal volume (or the mold price in case of die casting the gears). In the catalog, the dimensions of the

Table 2.4 Size factor and load distribution factor versus gear size

Teeth	48	54	60	66	72	84	95
K_H	1.18	1.18	1.18	1.18	1.18	1.18	1.18
K_s	1.59	1.60	1.60	1.60	1.60	1.60	1.60

holes of different gear styles are not provided [74]. Here, to eliminate the influence of the gear style, only spoke style gears (as illustrated in [74]) are addressed.

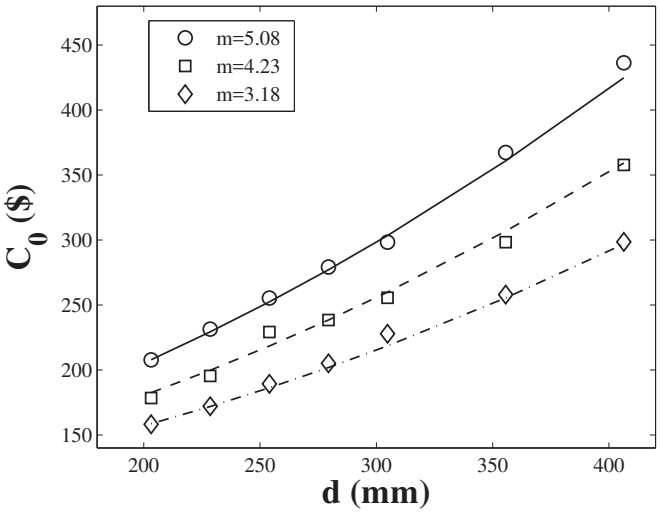

Figure 2.1 Acquisition cost versus pitch diameter and module.

2.2.2 Acquisition cost-reliability of spur gears

The reliability for the gears of Tab. 2.3 undergoing $\tau = 27$ Nm and $S = 900$ rpm is calculated after 10 million revolutions using AGMA equations [4]. None of the simplifying assumptions made for CPR modelling are used in calculating the reliability. The following values are considered for the design parameters. The bending and pitting safety factors are 4.0 and 2.0, respectively.

The baseline is the 66-teeth gear with $m = 4.23$ mm (diametral pitch is 6 in^{-1}). The gear ratio is 1.0. The factors K_s and Y are calculated using the same parameters as Section 2.2.1.

Figure 2.2 illustrates catalog price versus reliability. To better show the model accuracy, horizontal axis is $\text{Ln}\big(1/(1-R)\big)$ instead of reliability, as the reliability of many gears is close to unity. The results of Eqn. (2.43)-(2.45) are also plotted for different modules, demonstrating a good agreement between the cost-reliability data points and the *iso-module* curves. The difference between the catalog price and the model is bounded to 4.8%, which corresponds to the 60-teeth gear with $m = 4.23$ mm. The main source of this deviation is the error of Eqn. (2.36) for this gear.

Figure 2.2 suggests that at a specific reliability, AC decreases by switching from $m = 3.18$ mm to $m = 4.23$ mm, while it increases by going from $m = 4.23$ mm to $m = 5.08$ mm. This non-monotonic behavior can be explained as follows. At a fixed pitch diameter, the reliability increases with module. To maintain the reliability level, the pitch diameter must be reduced. The non-linear cost-size model Eqn. (2.36) suggests that by increasing m and decreasing d, it is possible to find an m to reduce the cost while a specific reliability target is met. For this numerical example, the solution is $m = 4.23$ mm.

In many cases, the pitch diameter is a design input as it is predetermined by system space constraints. In such a case, an alternative method of varying the reliability and cost is changing the module. The results of Fig. 2.2 are plotted again in Fig. 2.3, where *iso-diameter* curves replace the *iso-modules*. Each curve identifies the reliability improvement and the increase in cost by going from $m = 3.18$ mm to $m = 5.08$ mm. The maximum difference between the catalog prices and the model is again 4.8% as the curves are plotted using the same CPR models.

In both iso-module and iso-diameter representations, AC is convex in terms of $Ln\big(1/(1-R)\big)$, implying that AC tends to infinity as reliability approaches unity.

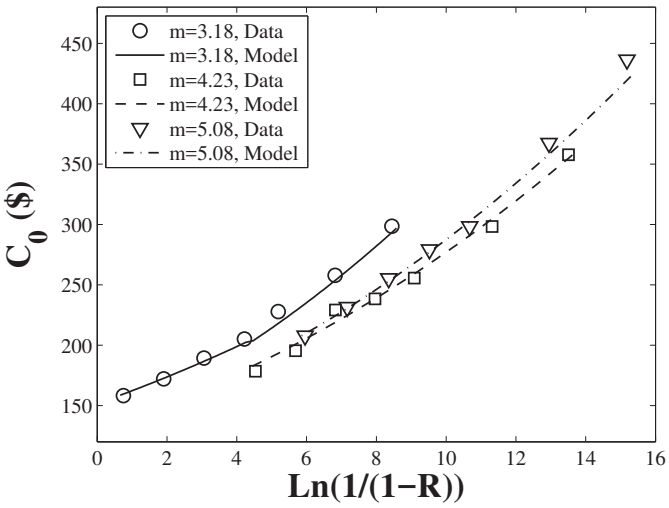

Figure 2.2 Acquisition cost versus reliability; iso-module curves.

2.2.3 Cost-performance-reliability of gears

At different torque levels, the cost-reliability curves of the gears with $d = 279.4$ mm are illustrated in Fig. 2.4. At constant torque, the reliability and the cost increase with module. The model accurately calculates the reliability loss at higher torques. The maximum difference between the model and the catalog price is 1.6% for $m = 3.18$ mm.

2.3 Conclusion

In this chapter, a procedure is proposed to develop CPR models of engineering elements. The procedure, along with the well accepted and broadly used AGMA stress and strength equations and a linear cost-mass-removal volume relation results in the CPR model for spur and helical gears. To establish the model, it is sufficient to: (a) identify the cost-size relation using five gears; and, (b) conduct the AGMA reliability analysis for the baseline gear. The model shows how costly it is to improve the reliability of a gear in a specified performance. Such a CPR

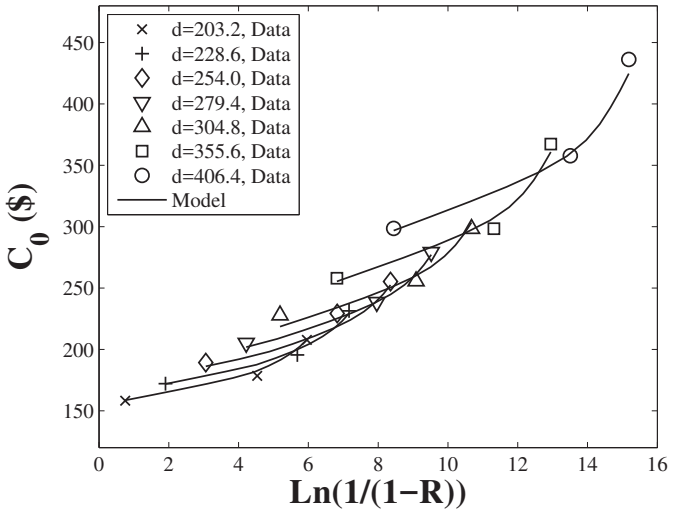

Figure 2.3 Acquisition cost versus reliability; iso-diameter curves.

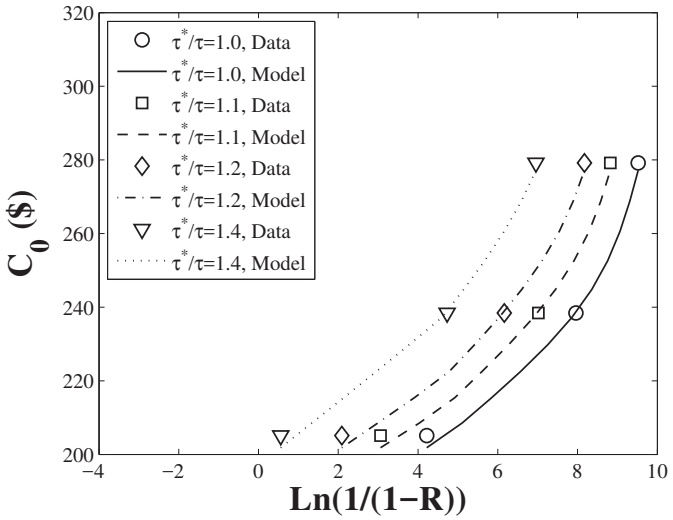

Figure 2.4 Acquisition cost versus reliability and torque, $d = 279.4$ mm.

correlation can be analyzed under radial, axial, or module scaling of the gears. A good agreement is observed between the model and the catalog prices of a manufacturer for a wide range of gear sizes modules. The model has the flexibility to address the CPR modelling of different types of materials and mechanical properties, as well. At constant torque, Eqn. (2.43)–(2.45) imply that

cost is a typically convex function of reliability and tends to infinity as reliability approaches unity. The model can be used by gear designers for reliability allocation and cost reduction.

In the current form, the CPR model only considers the expected value of the reliability function. Therefore, it calculates the cost to reach the expected reliability. To extend the scope of this work, the reliability distribution details, such as the standard deviation of the reliability distribution, can be taken into account. This may be helpful to model the standard deviation of the acquisition cost as well. This is left for a future study. Another interesting aspect to be included in the model is the influence of the manufacturing tolerances, material variability, assembly accuracy, and loading uncertainty.

In the following chapter, after developing the CPR model of rolling bearings, the gear and bearing models are coupled to analyze the CPR behavior of a one-speed gearbox.

Chapter 3

Acquisition Cost-Performance-Reliability Modelling of Bearings and Gearboxes

Similar to gears, roller bearings are broadly used in industry. Bearing damage due to overloading or excessive temperature regimes may be avoided by properly selecting the size and type of the bearing. To quantify the advantage of investing on the acquisition cost of a bearing on its reliability, a CPR analysis is required.

The first objective of this chapter is to develop the CPR model for deep groove ball bearings and cylindrical roller bearings using the procedure proposed in Chapter 2. Next, the CPR model for gearboxes will be established by coupling the bearing model and the gear model from the previous chapter.

3.1 Model formulation

The influence of bearing size and material type of rolling bearings on their performance, reliability and acquisition cost is studied to develop their CPR model. To this end, it is assumed that bearings with different sizes have similar temperature and lubrication condition and, therefore, their temperature and lubrication factors are equal. The influence of these two parameters is left for a future research.

3.1.1 Rolling bearings

For an arbitrary rolling bearing **b**, Standard ISO 281 proposes the following life equation [7]

$$L_b = a_1 f_\theta \left(\frac{C_r}{P}\right)^a, \tag{3.1}$$

where L_b is the bearing rating life in million revolutions, P is the equivalent applied load in kN, C_r is the bearing dynamic load rating in kN, $a = 3$ for ball bearings and $a = 10/3$ for roller bearings. The reliability factor, a_1, is provided in a table in [7]. The data may also be stated in the mathematical form as [76]

$$a_1 = 0.05 + 4.26\left(\text{Ln}\frac{1}{R_b}\right)^{2/3}, \tag{3.2}$$

in which R_b is the reliability of a bearing after L_b million revolutions. The temperature factor f_θ depends on the bearing speed S (in rpm) and temperature θ. In the SI system, it is given by [6]

$$f_\theta = \begin{cases} 600(1.8\theta + 32)^{-1.8} S^{0.38} & ; \ S \geq \dfrac{15000}{d} \\ \\ 3500(1.8\theta + 32)^{-1.8} \left(\dfrac{S}{f_G}\right)^{0.2} & ; \ S < \dfrac{15000}{d} \end{cases} \tag{3.3}$$

in which d is the bore diameter of the bearing in mm, and f_G depends on the geometry of the bearing and is given by the manufacturer. For practical values of d and S, the first condition of Eqn. (3.3) often applies.

Eqn. (3.1)-(3.3) are written for constant values of P, S, and θ. However, these quantities can be time-dependent depending on the application. To generalize Eqn. (3.1) for $P(t)$, $S(t)$, and $\theta(t)$, it may be written in the differential form

$$\frac{S(t)}{60\times 10^6}dt = da_1\ f_\theta(t)(\frac{C_r}{P(t)})^a. \tag{3.4}$$

Some mathematical manipulation and integration yields

$$a_1(t) = \frac{1}{60\times 10^6 C_r^a}\int_0^t \frac{S(s)P^a(s)}{f_\theta(s)}ds. \tag{3.5}$$

Performance of bearings

The dynamic load rating C_r of rolling bearings depends on the diameter of the rolling element D_w, its effective length L_w (for cylindrical roller bearings), and the number of the rolling elements Z [7]. The dynamic load rating equation for single-row deep-groove steel ball bearings and single-row cylindrical steel roller bearings (zero contact angle) are given by [7]

$$C_r = 1.3 f_c Z^{2/3} D_w^{9/5}, \tag{3.6}$$

and

$$C_r = 1.1 f_c Z^{3/4} L_w^{7/9} D_w^{29/27}, \tag{3.7}$$

respectively. The manufacturers use these equations to calculate and report C_r in their catalogs. The factor f_c depends on the bearing type (deep-groove bearing, cylindrical roller bearing, etc.) and the ratio D_w/D_{pw}, where D_{pw} is the diameter of the rollers pitch circle. The value

of f_c is given in [7]. For the range of bearings studied in the numerical examples of Section 3.2, considering that f_c is constant leads to a maximum error of 2%. Therefore, this factor is considered constant in this analysis.

Dimensions of bearings' rolling elements

Dimensions D_w, L_w, and Z are determined as follows:

1. The number of the rolling elements Z for each bearing is obtained from the drawings of the bearings [77].

2. The information provided in the bearing catalogs are not sufficient to calculate the diameter D_w of the rolling elements of the deep groove ball bearings. Knowing C_r from the bearing catalogs and Z from the bearing drawings, D_w for each bearing may be calculated using Eqn. (3.6). For the cylindrical roller bearing, from Fig. 3.1(b) [77] it is evident that D_w equals
$$D_w = \frac{E-F}{2}, \tag{3.8}$$
where E and F are presented in manufacturers' catalogs.

3. The bearing catalogs do not provide the effective length of cylindrical rollers L_w. By substitution of C_r from bearing catalogs, D_w from Eqn. (3.8), and Z from bearing drawings into Eqn. (3.7), L_w may be calculated.

Size, performance and reliability

Now consider another bearing $\mathbf{b}^*$ of the same type whose geometry parameters are related to those of $\mathbf{b}$ through
$$D_w^* = \gamma_1 D_w \ , \ L_w^* = \gamma_2 L_w \ , \ Z^* = \gamma_3 Z. \tag{3.9}$$

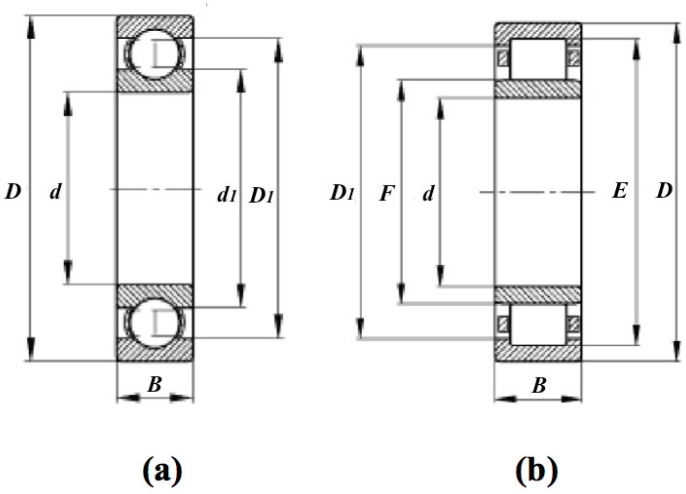

Figure 3.1 (a) Deep groove ball bearings, and (b) cylindrical roller bearings [77]

For the roller bearings studied here, it is observed that

$$B^* = \gamma_2 B, \tag{3.10}$$

is a good approximation. In other words, the bearing's width B is closely scaled with the same scaling factor as the roller's length L_w. Since L_w is only defined for roller bearings, γ_2 for ball bearings is calculated from Eqn. (3.10).

Rewriting Eqn. (3.5) for the bearing $\mathbf{b}^*$ gives

$$a_1^*(t) = \frac{1}{60 \times 10^6 C_r^{*a}} \int_0^t \frac{S^*(s) P^{*a}(s)}{f_\theta^*(s)} ds. \tag{3.11}$$

For deep-groove ball bearings (i.e. $a = 3$), Eqn. (3.5), (3.11), (3.9) along with Eqn. (3.6) give the following relation for two ball bearings $\mathbf{b}$ and $\mathbf{b}^*$

$$\frac{a_1^*(t)}{a_1(t)} = \frac{\int_0^t \frac{S^*(s) P^{*3}(s)}{f_\theta^*(s)} ds}{\int_0^t \frac{S(s) P^3(s)}{f_\theta(s)} ds} \gamma_1^{-27/5} \gamma_3^{-2}. \tag{3.12}$$

Equation (3.12) is the performance-reliability-size equation of deep-groove ball bearings. For the cylindrical roller bearings (with $a = 10/3$), Eqn. (3.5), (3.11), (3.9) along with Eqn. (3.7) yield

$$\frac{a_1^*(t)}{a_1(t)} = \frac{\int_0^t \frac{S^*(s)P^{*3}(s)}{f_\theta^*(s)}ds}{\int_0^t \frac{S(s)P^3(s)}{f_\theta(s)}ds}\gamma_1^{-290/81}\gamma_2^{-70/27}\gamma_3^{-5/2}, \tag{3.13}$$

which is the performance-reliability-size equation of cylindrical roller bearings.

In section 3.2.1 it is shown that

$$\gamma_2 = \gamma_1, \tag{3.14}$$

is a good approximation for the bearings studied in this research. Also, in each bearing type a wide range of bearings have equal number of rolling elements, which implies $\gamma_3 = 1$. Substitution of Eqn. (3.14) and $\gamma_3 = 1$ into Eqn. (3.12) and (3.13) yields

$$\frac{a_1^*(t)}{a_1(t)} = \frac{\int_0^t \frac{S^*(s)P^{*3}(s)}{f_\theta^*(s)}ds}{\int_0^t \frac{S(s)P^3(s)}{f_\theta(s)}ds}\gamma_1^{-27/5} \text{ ; Deep-groove ball bearings,} \tag{3.15}$$

and

$$\frac{a_1^*(t)}{a_1(t)} = \frac{\int_0^t \frac{S^*(s)P^{*3}(s)}{f_\theta^*(s)}ds}{\int_0^t \frac{S(s)P^3(s)}{f_\theta(s)}ds}\gamma_1^{-290/81} \text{ ; Cylindrical roller bearings,} \tag{3.16}$$

which are the simplified size-performance-reliability models.

Size and cost

A linear relation is considered here between the price or the AC of a bearing **b** and its mass M

$$c_0 = \alpha_5 + \beta_5 M. \tag{3.17}$$

In Eqn. (3.17), β_5 depends on the material, bearing type and the manufacturing process, whereas α_5 lumps the non-production costs such as administration, sales, and depreciation [28]. The validity of this equation is assessed in Section 3.2.1. For bearings **b** and $\mathbf{b}^*$ of the same type, the relation between their masses is

$$M^* = \frac{D^{*2} - d^{*2}}{D^2 - d^2} \frac{B^*}{B} M. \tag{3.18}$$

where d and D are the bore and outer diameter of the bearing, respectively (see Fig. 3.1). In writing Eqn. (3.18) it is assumed that the bearings have equal apparent density.

Equation (3.10) indicates that B^*/B in Eqn. (3.18) equals γ_2. Dimensions D and d are not necessarily scaled with γ_1, which is the scaling factor of D_w. However, since these two dimensions are scaled in the radial direction, it may be assumed that

$$\frac{D^{*2} - d^{*2}}{D^2 - d^2} = \gamma_1^2, \tag{3.19}$$

The validity of Eqn. (3.19) is studied in Section 3.2.1. According to Eqn. (3.19), (3.14) and (3.10), Eqn. (3.18) may be rewritten as

$$M^* = \gamma_1^3 M. \tag{3.20}$$

By defining normalized cost ξ as

$$\xi = \frac{c_0^* - \alpha_5}{c_0 - \alpha_5}, \tag{3.21}$$

equations (3.20) and (3.17) yield

$$\xi = \frac{M^*}{M} = \gamma_1^3, \tag{3.22}$$

which relates the normalized cost to the size scaling factors.

Cost-performance-reliability correlation

Substitution of Eqn. (3.22) into Eqn. (3.15) results in

$$\xi = \left(\frac{a_1^*}{a_1}\right)^{-5/9} \left(\frac{\int_0^t \frac{S^*(s)P^{*3}(s)}{f_\theta^*(s)} ds}{\int_0^t \frac{S(s)P^3(s)}{f_\theta(s)} ds}\right)^{5/3}, \tag{3.23}$$

which is the CPR model of deep-groove ball bearings. The CPR model of cylindrical roller bearings is derived by substitution of Eqn. (3.22) to (3.16)

$$\xi = \left(\frac{a_1^*}{a_1}\right)^{-243/500} \left(\frac{\int_0^t \frac{S^*(s)P^{*3}(s)}{f_\theta^*(s)} ds}{\int_0^t \frac{S(s)P^3(s)}{f_\theta(s)} ds}\right)^{81/50}. \tag{3.24}$$

Consider the following duty cycles for the bearings $\mathbf{b}$ and $\mathbf{b}^*$

$$P^*(t) = P_0^* f(t),\ P(t) = P_0 f(t),\ S^*(t) = S(t),\ \theta^*(t) = \theta(t), \tag{3.25}$$

where f is an arbitrary function. The last relation of Eqn. (3.25) can be justified by noting that the energy efficiency (and the heat loss factor) of bearings is almost independent of the bearing size, which implies that the heat production rate is not significantly influenced by the bearing size. Moreover, the lubrication/cooling systems of bearings are often equipped with a closed-loop temperature control unit. This way, even if the heat generation is altered by the bearing size, it may be assumed that the cooling system manages the bearing temperature. Equation (3.25) implies that the only difference between the duty cycle of the bearings is the amplitude of the applied load. An example is when in a gearbox with a specified throughput torque, gear ratio and shaft speed, the designer considers two different gear sizes. Changing the gear size not only affects the gear reliability, but also the bearing reliability by varying the force on each bearing.

The simplified CPR model are achieved by substitution of Eqn. (3.25) into Eqn. (3.23) and (3.24)

$$\xi = \left(\frac{a_1^*}{a_1}\right)^{-5/9}\left(\frac{P_0^*}{P_0}\right)^{5/3} \text{ ; Ball bearings,} \tag{3.26}$$

$$\xi = \left(\frac{a_1^*}{a_1}\right)^{-243/500}\left(\frac{P_0^*}{P_0}\right)^{81/50} \text{ ; Roller bearings.} \tag{3.27}$$

These models may be further simplified in the following three scenarios:

1. If the performance of the bearings are identical, i.e. $P^* = P$, Eqn. (3.26) and Eqn. (3.27) will be reduced to the cost-reliability (CR) models

$$\xi = \left(\frac{a_1^*}{a_1}\right)^{-5/9} \text{ ; Ball bearings,} \tag{3.28}$$

$$\xi = \left(\frac{a_1^*}{a_1}\right)^{-243/500} \text{ ; Roller bearings.} \tag{3.29}$$

   The resulting power-law *isoperformance* curves indicate the incremental cost associated with increasing the reliability of the bearings.

2. If a specific end-of-cycle reliability is targeted for the bearings, i.e. $R^* = R$, the cost-performance (CP) models will be achieved

$$\xi = \left(\frac{P_0^*}{P_0}\right)^{5/3} \text{ ; Ball bearings,} \tag{3.30}$$

$$\xi = \left(\frac{P_0^*}{P_0}\right)^{81/50} \text{ ; Roller bearings.} \tag{3.31}$$

   These *isoreliability* curves determine the cost of increasing the performance of the bearings keeping the reliability unchanged.

3. Finally, the performance-reliability (PR) model of a single bearing, i.e. $\xi^* = \xi$, is

$$\left(\frac{a_1^*}{a_1}\right)^{-1}\left(\frac{P_0^*}{P_0}\right)^{3} = 1 \text{ ; Ball bearings,} \tag{3.32}$$

$$\left(\frac{a_1^*}{a_1}\right)^{-1}\left(\frac{P_0^*}{P_0}\right)^{10/3} = 1 \ ; \text{ Roller bearings.} \tag{3.33}$$

These *isocost* curves may also be directly derived from Eqn. (3.1).

In Section 3.2, the three approximations Eqn. (3.14), (3.17), and (3.20) are justified. Furthermore, the validity of the CPR models Eqn. (3.26) and Eqn. (3.27) and the resulting CR, CP and PR models are assessed for two types of bearings.

3.1.2 Gearboxes

The CPR model of a gearbox can be achieved by coupling the CPR model of its components. As a case study, a one-speed gearbox is addressed here. The method used in this section can be applied to any arbitrary gearbox configuration for CPR modelling of the product.

Consider a one-speed gearbox. As illustrated in Fig. 3.2, it is composed of two shafts, two spur gears, and four bearings. Since no axial force will be transmitted between the spur gears, four deep groove ball bearings can be selected for this application. On each shaft, the gear is mounted exactly between the bearings. If the gear pitch diameter on the shaft is d, the force applied on the shaft bearings is

$$P = \frac{\tau}{d\,\cos\phi_n}, \tag{3.34}$$

where τ is the throughput torque on the pinion, and ϕ_n is the pressure angle of the gears. In writing Eqn. (3.34), the weight of the gears are neglected as they are generally much smaller than P.

To explore the design space of the gearbox, suppose that: (a) the gears are scaled radially while the gear ratio is kept constant; and, (b) the size of the bearings are varied. Also, suppose that the torque and the forces meet the conditions of Eqn. (2.25) and (3.25). Therefore, the gear CPR model is Eqn. (2.43) and the bearing CPR model is Eqn. (3.26). The CPR model

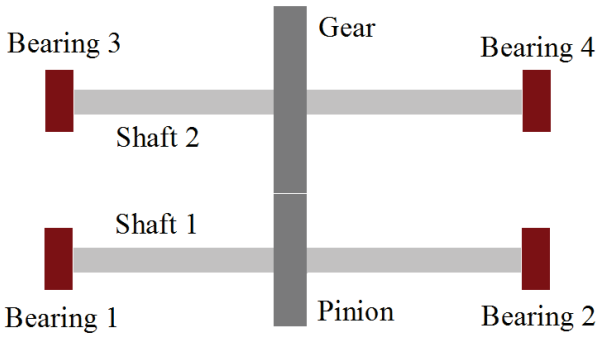

Figure 3.2 Schematic of the conceptual one-speed gearbox

of the gearbox will be

$$c_{0,GB} = c_{0,p} + c_{0,g} + 2c_{0,bi} + 2c_{0,bo},\ R_{GB} = R_p R_g R_{bi}^2 R_{bo}^2, \tag{3.35}$$

where $c_{0,p}$ and $c_{0,g}$ are the AC of the pinion and the gear, respectively. The terms $c_{0,bi}$ and $c_{0,bo}$ denote AC of the bearings on the input shaft and the bearings on the output shaft, respectively. The reliability of the pinion and the gear are denoted by R_p and R_g, while R_{bi} and R_{bo} are the reliability of the bearings on the input shaft and the bearings on the output shaft, respectively.

Except for the gears and the bearings, other features of the gearbox are not reflected in the CPR model Eqn. (3.35). In other words, the AC of other components are assumed constant and, therefore, they are not taken into the account from a comparative cost analysis perspective. Also, only the failure of the gears and bearings are included in Eqn. (3.35) as they are the main failure modes of gearboxes [8, 9]. When the CPR model of shafts are developed, Eqn. (3.35) can be extended to

$$c_{0,GB} = c_{0,p} + c_{0,g} + 2c_{0,bi} + 2c_{0,bo} + c_{0,si} + c_{0,so},\ R_{GB} = R_p R_g R_{bi}^2 R_{bo}^2 R_{si} R_{so}, \tag{3.36}$$

where $c_{0,si}$ and $c_{0,so}$ are the AC of the input and output shafts, and R_{si} and R_{so} are the reliability of the input and output shafts, respectively. This is left for a future research.

3.2 Numerical examples

The ABMA equation Eqn. (3.1) is used here to study the effect of bearing size on its performance or reliability for the 63xx series deep groove ball bearings (hereafter called 63xx) and the NU3xx-E-TVP2 series cylindrical roller bearings (hereafter called NU3xx), manufactured by an OEM [77]. The OEM's price list [78] is consulted for the acquisition cost of the bearings. The acquisition cost is in Canadian Dollars. Here, the Euro/CAD exchange rate is 1.46 as of September 2016 [79]. Next, the cost-performance-reliability data set of the bearings is used in validity assessment of the models Eqn. (3.26) and Eqn. (3.27).

The studied bearings are listed in Tables 3.1 and 3.2 [77]. In each series, the bearing with d =40 mm is selected as the baseline. The size scaling factors γ_1 and γ_2 are calculated using Eqn. (3.9) and Eqn. (3.10) following the argument provided in Section 3.1.1.

Table 3.1 Details of the 63xx series deep groove ball bearings

Part no. 63xx	Mass (kg)	d (mm)	B (mm)	D_w (mm)	c_0 (CAD)	γ_1 (-)	γ_2 (-)
04	0.15	20	15	9.8	21.83	0.61	0.65
05	0.23	25	17	11.8	27.33	0.74	0.74
06	0.36	30	19	12.8	36.94	0.80	0.83
07	0.47	35	21	14.0	49.49	0.87	0.91
08	0.64	40	23	16.0	70.23	1.00	1.00
09	0.85	45	25	18.0	88.62	1.12	1.09
10	1.10	50	27	19.7	117.38	1.23	1.17
11	1.39	55	29	22.1	147.46	1.38	1.26
12	1.75	60	31	23.0	186.15	1.43	1.35

Table 3.2 Details of the NU3xx-E-TVP2 series cylindrical roller bearings

Part no. Nu3xx	Mass (kg)	d (mm)	L_w (mm)	D_w (mm)	c_0 (CAD)	γ_1 (-)	γ_2 (-)
04	0.153	20	11.2	9.0	88.04	0.64	0.67
05	0.245	25	12.4	10.0	101.03	0.71	0.73
06	0.368	30	13.1	11.0	114.17	0.79	0.78
07	0.486	35	15.4	12.0	133.01	0.86	0.91
08	0.659	40	16.8	14.0	157.68	1.00	1.00
09	0.893	45	18.0	15.0	197.10	1.07	1.07
10	1.16	50	19.3	16.0	233.60	1.14	1.14
11	1.48	55	21.0	18.0	273.02	1.29	1.25
12	1.85	60	22.4	19.0	324.12	1.36	1.33

3.2.1 Validation of assumptions

For the NU3xx bearings, γ_2-γ_1 data from Table 3.2 is plotted in Fig. 3.3. The linear model in this figure is $\gamma_2 = 1.00\ \gamma_1$. The same plot may be drawn for the 63xx bearings based on the data of Table 3.1. In that case, $\gamma_2 = 0.97\gamma_1$ is the best linear fitting on the data series. Hence, Eqn. (3.14) may be used as an approximate relation between the size scaling factors.

The acquisition cost of the bearings are plotted versus their mass in Fig. 3.4. For the linear model Eqn. (3.17) plotted in this figure, $\alpha_5 = 2.37$ CAD for deep groove bearings and $\alpha_5 = 66.03$ CAD for cylindrical roller bearings.

For the ball bearings in the range of 6300 to 6317, and for the roller bearings in the range of NU304 to NU322 [77], Fig. 3.5 illustrates the mass-γ_1 data points. The 6308 and the NU308 are selected as the baselines. Note that instead of the nine bearings listed in Tables 3.1 and 3.2, for each bearing type eighteen bearing are included in the analysis. The good agreement between Eqn. (3.5) and the catalog data justifies the assumptions used to derive Eqn. (3.20).

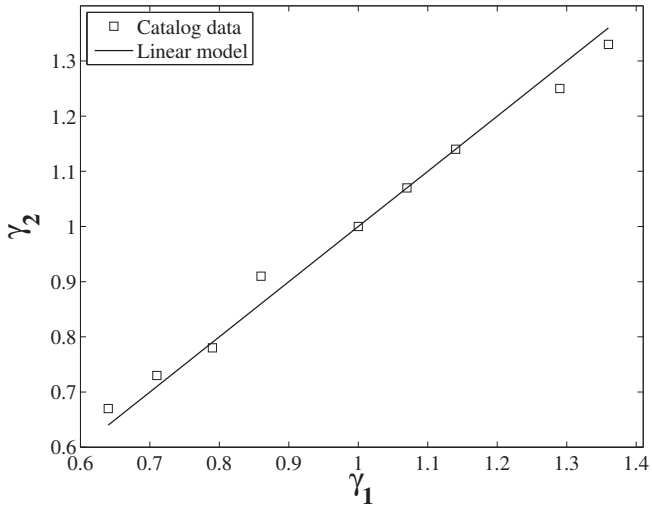

Figure 3.3 γ_2 vs. γ_1 for NU3xx bearings

3.2.2 Cost-performance of the bearings

In the example of this section, the validity of the present CP model is studied for 63xx and NU3xx bearings. The reliability of each bearing is 0.99 after one million revolutions. The baseline bearings are 6308 and NU308. The performance of each bearing is calculated using Eqn. (3.1). The normalized cost ξ is calculated from Eqn. (3.21) and plotted versus P^*/P in Fig. 3.6. The predictions of Eqn. (3.30) and Eqn. (3.31) are also plotted in this figure. Fig. 3.7 presents the same data as Fig. 3.6 where the vertical axis is the acquisition cost instead of ξ. The maximum deviation of the present model from the catalog prices is 29% in 6304 at $P^*/P = 0.37$, followed by a 22% error in 6311 at $P^*/P = 1.78$. Aside from these two bearings, the model prediction is close to the catalog data. For all of the NU3xx bearings, the error is bounded to 7%.

As the final point, note that in Fig. 3.6 the CP models of the ball bearings and the roller bearings are close to each other for the range of P^*/P studied here. Hence, it is possible to consider reformulating Eqn. (3.30) and Eqn. (3.31) and propose the following form for both

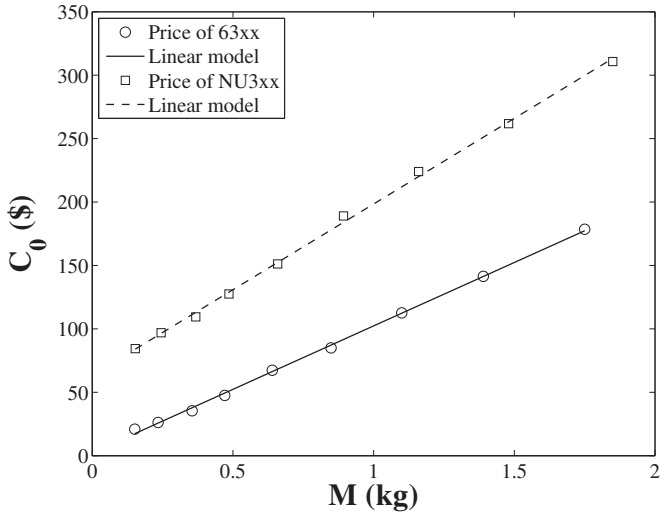

Figure 3.4 Acquisition cost vs. mass of 63xx and NU3xx bearings

types

$$\xi = \left(\frac{P_0^*}{P_0}\right)^{1.65}. \tag{3.37}$$

3.2.3 Cost-reliability of the bearings

In this example the radial load on the 63xx and NU3xx bearings are 39.2 kN and 83.9 kN, respectively. The reliability of each bearing is calculated using Eqn. (3.1) after one million revolutions. The acquisition cost is obtained from the manufacturer's catalog [78]. The normalized cost-reliability factor points as well as the models Eqn. (3.28) and (3.29) are illustrated in Fig. 3.8. Fig. 3.9 depicts the cost-reliability factor data points as well as the prediction of the present model. The maximum deviation of the model is 29 % in 6304 bearing at a^*/a=19.5. The cost versus the reliability of the 63xx and NU3xx bearings are plotted in Fig. 3.10. This CR curve is of high practical importance as it is the acquisition cost curve of Fig. 1.1 which may be used by the designers in the LCC analysis of the product.

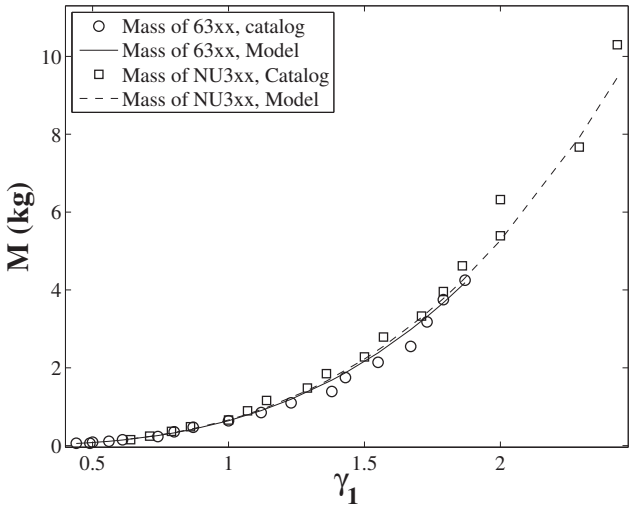

Figure 3.5 Mass vs. size scaling factor of 63xx bearings

Finally, note that in Fig. 3.8, the models Eqn. (3.28) and Eqn. (3.29) are close in the reliability range studied here. Therefore, they may be replaced by the following simplifying model for the both types of bearings

$$\xi = \left(\frac{a_1^*}{a_1}\right)^{-0.5}. \tag{3.38}$$

Combining Eqn. (3.37) and Eqn. (3.38) gives the simplified CPR model of both the deep groove ball bearings and the cylindrical roller bearings

$$\xi = \left(\frac{P_0^*}{P_0}\right)^{1.65}\left(\frac{a_1^*}{a_1}\right)^{-0.5}. \tag{3.39}$$

Rewriting the latter in terms of the acquisition cost yields a two-parameter CPR model

$$c_0^* = \alpha_5 + (c_0 - \alpha_5)\left(\frac{P_0^*}{P_0}\right)^{1.65}\left(\frac{a_1^*}{a_1}\right)^{-0.5}. \tag{3.40}$$

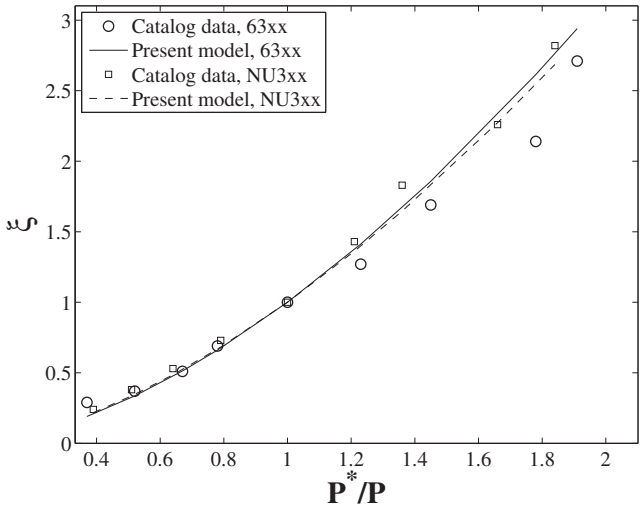

Figure 3.6 Normalized cost vs. normalized performance of bearings

3.2.4 Cost-performance-reliability of the bearings

In Sections 3.2.2 and 3.2.3 either the performance or the reliability of the bearings is constant. In the example of this section, the reliability and performance are variables and the interplay between the acquisition cost of NU3xx bearings and their performance and reliability is studied. The performance is treated as a discrete variable with values $P = 72$ kN, 96 kN, and 144 kN. The reliability is calculated after one million revolutions under each of the three applied loads. The span of the CPR results are shown in Fig. 3.11. It should be noted that the iso-cost points correspond to a specific bearing. As the applied load increases, the CPR curve shifts to lower reliabilities. Evidently, as the reliability approaches unity, the marginal cost of reliability improvement increases much faster.

3.2.5 Cost-reliability of a one-speed gearbox

In the example of this section, the cost-reliability correlation of a conceptual one-speed gearbox is studied. The gearbox is schematically shown in Fig. 3.2. The AGMA equation from [4] and

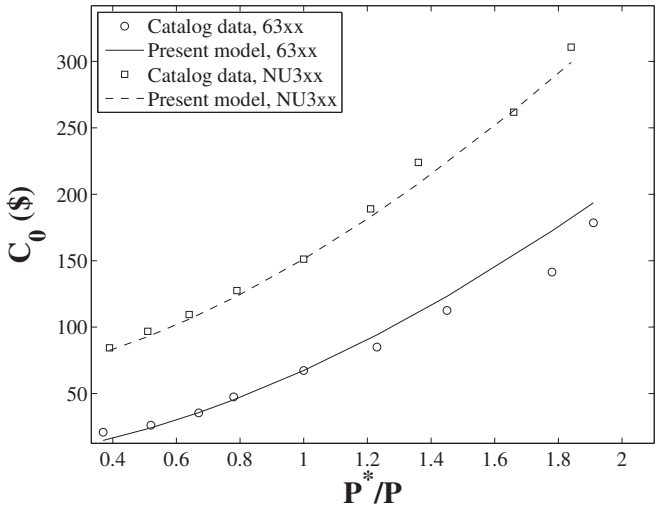

Figure 3.7 Acquisition cost vs. normalized performance of bearings

the ABMA equation from [6] are used to calculate the reliability of the gears and the bearings, respectively. The price of the parts are found in the manufacturers catalogs [78, 74]. The CR model of gears developed in Chapter 2 and the CPR model of bearings established in this chapter are then coupled to predict the cost-reliability correlation of the gearbox and the results are compared with the catalog prices of the manufacturers.

For the gears of an OEM [74], the pressure angle is 14.5^o, the module is 4.23 mm (the diametral pitch is 6 in^{-1}) and the face width is 38.1 mm (1.5 in). The gears are made of ASTM A576 1117 steel, carburized to reach the hardness of 320 Brinell. Therefore, the bending and contact fatigue strength will be $\sigma_{FP} = 250$ MPa and $\sigma_{HP} = 920$ MPa, respectively [4]. The density of the gears material is 7.8 g/cm^3. In the analysis, the transmission accuracy level number Q_v is 7. On each shaft, two deep groove ball bearings manufactured by an OEM are used, and the four bearings in the gearbox are identical.

The speed of the input shaft is 1800 rpm (clockwise) and the applied torque is 150 Nm. The desired gear ratio is 1.33. The required minimum safety factors against bending and wear are $S_F = 3.0$ and $S_H = 1.25$. The minimum reliability target for each gear and bearing is 0.995

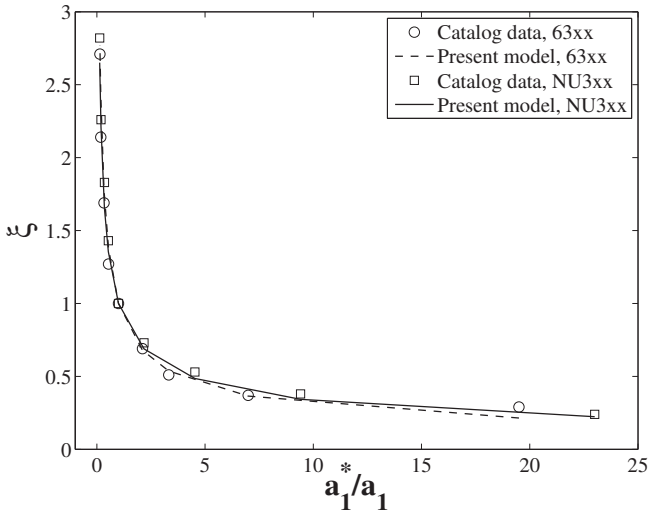

Figure 3.8 Normalized cost vs. normalized reliability factor of bearings

after 10 million revolutions of the input shaft. The gearbox will operate at room temperature and the gears and bearings will be lubricated to ensure the safety of the parts during operation. In absence of information on the mass of the gears, it is assumed that each gear is a uniform disc with no holes. The weight of the gears is included in the bearing loads. It is assumed that the mass of the shaft is negligible.

The aforementioned design considerations may be met by selecting the OEM's NJ30A gear as pinion (30 teeth) meshed with NJ40A gear (40 teeth) [74], along with deep groove ball bearings with serial number 6000 [77]. This design is selected as the baseline design. Its parameters and the result of calculations can be found in the 9th row of Table 3.3.

Next, while keeping the gear ratio in the range of 1.33 ± 0.01, the reliability constraints are relaxed. This way, it is possible to change the size of gears and bearings and study its influence on the cost and reliability of the gearbox. Aside from the pair of 30-teeth and 40-teeth gears, two other pairs of gears are considered. In the first pair, a 29-teeth pinion is meshed with a 39-teeth gear. The second pair of gears have 31 and 41 teeth. These three sets of gears are hereafter referred to as (29,39), (30,40), and (31,41). Aside from the baseline bearing 6000, two

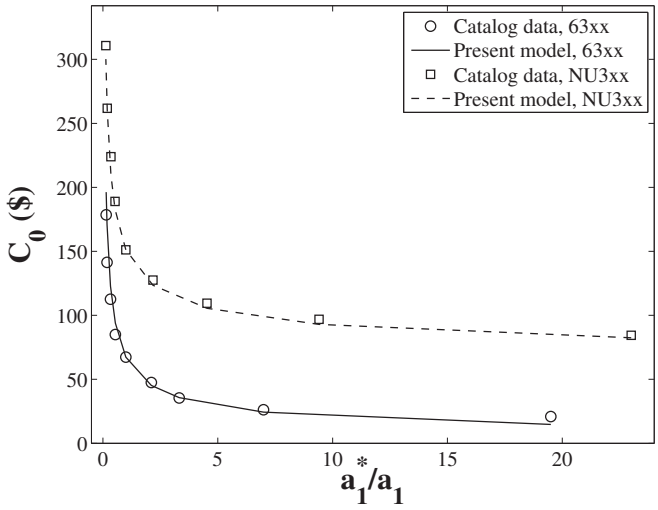

Figure 3.9 Acquisition cost vs. reliability factor of bearings

smaller bearings 608 and 609, and three larger bearings 6001, 6002 and 6003 are considered. Having three sets of gears and six choices of bearings, eighteen different designs are studied and reported in Table 3.3.

The rows 1–8 and 10–18 of Table 3.3 are the neighboring design points of the baseline design (row 9). In these designs, the size of the baseline gears and bearing is varied slightly. Therefore, it is assumed that it is not necessary to significantly change the size and shape of other components of the gearbox, e.g. the shafts, the housing, and the lubrication system. Hence, the presented cost analysis concentrates on the influence of the gears and the bearings on the total cost, and considers that the cost of other parts of the gearbox is not altered. In that sense, this is a comparative cost analysis. Furthermore, it is assumed that the only failure modes are that of gears and bearings. In other words, the reliability of other components of the gearbox is unity.

The reliability of each part calculated using AGMA and ABMA equations is reported in Table 3.3. Failure of any of the gears and bearings leads to the failure of the whole gearbox, which implies that these parts operate in series from the reliability analysis viewpoint. Hence, the total reliability of the gearbox equals the product of the reliabilities of the six parts. The

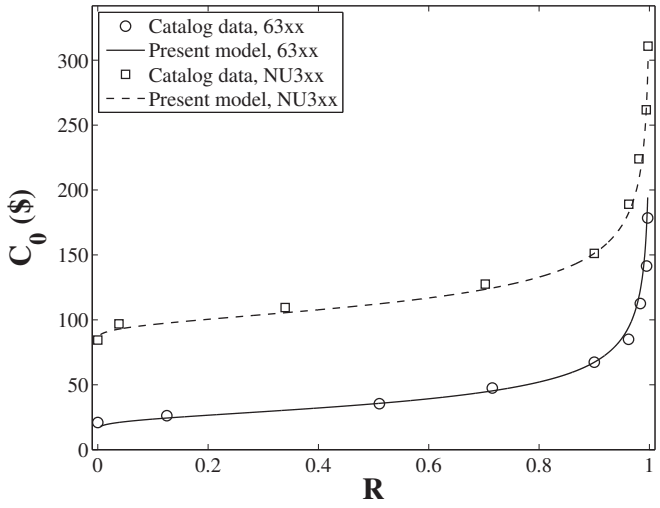

Figure 3.10 Cost-reliability correlation of 63xx and NU3xx bearings

acquisition cost of the gearbox is considered to be equal to the sum of the price of the gears and bearings, which is reported in the last column of Table 3.3.

The gearbox cost-reliability data points, as well as the prediction of the developed CR model are plotted in Fig. 3.12. The baseline design is the square with $R_T = 0.974$ and $c_0 = 368.32$ CAD. For each set of gears, the total reliability and the acquisition cost are both increased by increasing the size of the bearings. If the bearings larger than the 6003 are also used, it is possible to show that the (29, 39) curve would lie above the (30, 40) curve, and similarly the (30, 40) curve would go above the (31, 41) curve. As a result, selecting a bearing larger than the 6003 violates the optimization objectives, which are to reduce the acquisition cost and improve the reliability. This way, the points on the envelope of the curves shown in Fig. 3.12 are the optimum solutions among the design points studied here. In Table 3.3, the points on the envelope are shown bold face. Depending on how the designer weights the cost and the reliability objectives, any of the design points on the envelope may be selected. If the total reliability target is below 0.985, the gear set (29, 39) minimizes the total acquisition cost of the gearbox. If the total reliability shall be in the range of 0.986 to 0.990, the acquisition cost is lowest by selecting

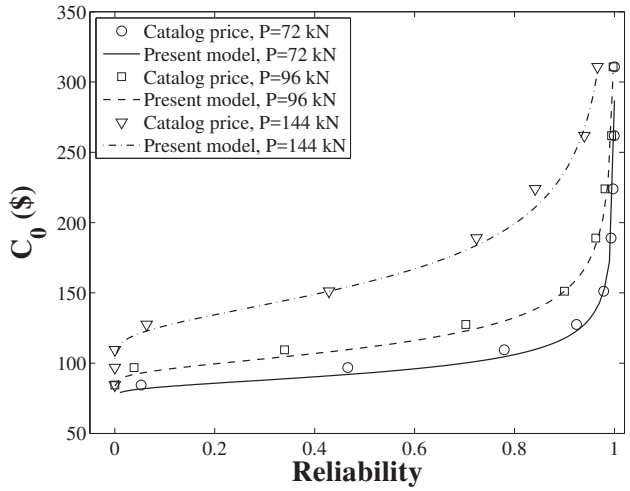

Figure 3.11 Cost-performance-reliability of NU3xx bearings

the (30, 40) gear set. If the reliability target is above 0.990, the designer shall select the (31, 41) gear set to obtain the lowest acquisition cost for the gearbox.

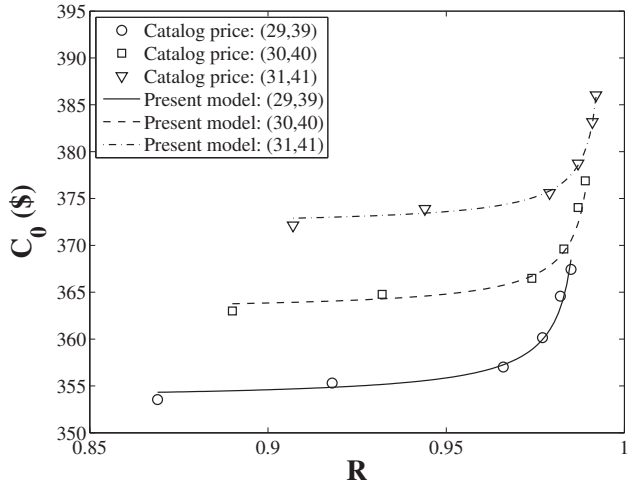

Figure 3.12 Cost-reliability of the one-speed gearbox

Table 3.3 Details of the gearbox

Design no.	Gear set & bearing	Reliability (pinion, gear)	Bearings reli. (in., out. shaft)	Price ($) (pinion , gear, bearing)	Total reliability	Total cost ($)
1	**(29, 39, 608)**	(0.992, 0.995)	(0.972, 0.966)	(118.17, 195.67, 10.36)	0.869	355.28
2	**(29, 39, 609)**	(0.992, 0.995)	(0.984, 0.980)	(118.17, 195.67, 10.81)	0.918	357.08
3	**(29, 39, 6000)**	(0.992, 0.995)	(0.995, 0.994)	(118.17, 195.67, 11.25)	0.966	358.84
4	**(29, 39, 6001)**	(0.992, 0.995)	(0.998, 0.997)	(118.17, 195.67, 12.08)	0.977	362.16
5	**(29, 39, 6002)**	(0.992, 0.995)	(0.999, 0.999)	(118.17, 195.67, 13.22)	0.982	366.72
6	**(29, 39, 6003)**	(0.992, 0.995)	(1.000, 0.999)	(118.17, 195.67, 13.97)	0.985	369.72
7	(30, 40, 608)	(0.995, 0.996)	(0.976, 0.971)	(122.30, 201.00, 10.36)	0.890	364.72
8	(30, 40, 609)	(0.995, 0.996)	(0.986, 0.983)	(122.30, 201.00, 10.81)	0.932	366.53
9	(30, 40, 6000)	(0.995, 0.996)	(0.996, 0.995)	(122.30, 201.00, 11.25)	0.974	368.32
10	(30, 40, 6001)	(0.995, 0.996)	(0.998, 0.998)	(122.30, 201.00, 12.08)	0.983	371.61
11	**(30, 40, 6002)**	(0.995, 0.996)	(0.999, 0.999)	(122.30, 201.00, 13.22)	0.987	376.20
12	**(30, 40, 6003)**	(0.995, 0.996)	(1.000, 1.000)	(122.30, 201.00, 13.97)	0.989	379.17
13	(31, 41, 608)	(0.996, 0.997)	(0.980, 0.975)	(126.43, 206.00, 10.36)	0.907	373.85
14	(31, 41, 609)	(0.996, 0.997)	(0.989, 0.986)	(126.43, 206.00, 10.81)	0.944	375.66
15	(31, 41, 6000)	(0.996, 0.997)	(0.997, 0.996)	(126.43, 206.00, 11.25)	0.979	377.44
16	(31, 41, 6001)	(0.996, 0.997)	(0.999, 0.998)	(126.43, 206.00, 12.08)	0.987	380.74
17	**(31, 41, 6002)**	(0.996, 0.997)	(1.000, 0.999)	(126.43, 206.00, 13.22)	0.991	385.32
18	**(31, 41, 6003)**	(0.996, 0.997)	(1.000, 1.000)	(126.43, 206.00, 13.97)	0.992	388.30

3.3 Conclusion

The cost-performance-reliability (CPR) models for the deep groove ball bearings and the cylindrical roller bearings are derived in this chapter. The derivation of the CPR models is based on the ABMA life equation and a linear cost-mass relation. The model indicates the incremental cost associated with improving the reliability or the performance of a rolling bearing. The predictions of the model are in good agreement with the catalog prices of a manufacturer for a wide range of bearing sizes.

Next, the CPR model of bearings is coupled with the CPR model of gears from Chapter 2 to study the cost-reliability behavior of a one-speed gearbox. The design space of the gearbox is two-dimensional, one dimension referring to either the pinion size or the gear size, and the second dimension as the size of the bearings. This design space leads to a wide distribution of the cost-reliability points. The result implies that the size of the gears and the bearings shall be determined based on how the designer weights the system-level reliability and the total acquisition cost. If reliability can be lower than 0.985, the gearbox cost is lowest by selecting the smallest bearing, whereas for reliability targets above 0.990, the largest bearing must be selected to minimize the gearbox cost. If the CPR model of the shafts are developed, the gearbox CPR model can be extended by including the shafts into the design space. This problem is left for a future research.

The scope of the CPR modelling may be extended by considering dynamic response of the components, uncertainty in the material properties, and the assembly variability/accuracy. This may be a topic for future research.

In the next chapter, the CPR model of electrical insulations are developed first. Next, bearing and insulation models are used in assessing the CPR of an electric motor.

Chapter 4

Acquisition Cost-Performance-Reliability Modelling of Electric Motors

As another type of broadly used engineering product, electric motors are addressed in this chapter. Similar to the gearbox studied in the previous chapter, electric motors are composed of different components and, therefore, their cost and reliability analysis should be conducted from a system-level perspective. The first objective here is the CPR modelling of electric insulations. Next, the insulation model along with the bearing model from Chapter 3 are used for CPR modelling of electric motors.

4.1 Model formulation

As the bearing and insulation failures are reported as the dominant failure modes of electric motors [10–16], the CPR model of electric motors are derived by studying the influence of the design variables of these two elements on reliability, performance and AC of the product.

4.1.1 Failure modes of electric motors

The broad industrial application of electric motors necessitates having a good understanding of their reliability. In an extensive reliability survey of the electric machines [10, 11], among the specified failure modes, the bearing and the insulation damage comprised 72% of the failures; oil leakage and the oil system failure were responsible for 9% of the failure cases, while the remaining 19% of failures are caused by the damage of other elements such as the frame, wedges, cables, shaft, cage, etc [11]. There are thorough reliability models for the failure analysis of the bearings and the insulation. On the contrary, modelling of other failure mechanisms are not as deeply addressed. In the absence of such reliability models, only the two dominant failure modes are taken into account here. In other words, it is assumed that the reliability of other components of the product equals unity.

Cost-performance-reliability of bearings

The CPR models Eqn. (3.26) and (3.27) are used here for AC analysis of bearings.

Cost-performance-reliability of insulation

Motor winding insulation is used to avoid phase-to-chassis and phase-to-phase short circuits. The quality of the insulation depends on the insulating material, and is often characterized by the insulation class, e.g. A, B, F, and H [18]. The insulation reliability is modelled by [17]

$$R_i(t) = \exp(-\frac{t}{L_i}), \tag{4.1}$$

where the average expected life is

$$L_i = L_{i\theta}\ \exp[-\alpha_\theta(\theta_i - \theta_{max})] \tag{4.2}$$

For each insulation class, the maximum allowable temperature θ_{max} and exponent factor α_θ are presented in Table 4.1 [17]. In Eqn. (4.2) $L_{i\theta}$=20,000 hours, which is the average life of the insulation if the hot spot temperature θ_i equals θ_{max} [18]. As the temperature increases, the average life of the insulation is reduced because of an increased insulation degradation rate.

Table 4.1 Insulation classes [17]

Class	A	B	F	H
θ_{max} (^oC)	105	130	155	180
α_θ $(1/^oC)$	0.032	0.073	0.078	0.085

In Eqn. (4.2), it is assumed that θ is time-independent. This results in a constant hazard function, $1/L_i$ [42]. In practice, the temperature of the insulation may fluctuate considerably depending on the motor load cycle and the cooling system performance. For time-dependent temperatures, $\theta_i(t)$, Eqn. (4.2) is rewritten as the hazard function

$$h(t) = \frac{1}{L_i(t)} = \frac{1}{L_{i\theta}} \exp\big[\alpha_\theta\big(\theta_i(t) - \theta_{max}\big)\big]. \tag{4.3}$$

The reliability is then given by [42]

$$R_i(t) = \exp\Big(-\int_0^t h(s)ds\Big) = \exp\Big(-\frac{1}{L_{i\theta}}\int_0^t \exp\big[\alpha_\theta\big(\theta_i(s) - \theta_{max}\big)\big]ds\Big). \tag{4.4}$$

In Eqn. (4.4), the insulation performance is the time-dependent temperature. Hence, this equation couples the performance and the reliability of insulation. Also, θ_{max} and α_θ depend on the insulation material, which itself determines the acquisition cost. Hence, Eqn. (4.4) is the CPR model of insulation. This model is further discussed in numerical examples of Section 4.2.3.

4.1.2 Cost-performance-reliability of electric motors

In the CPR modelling of bearings and electrical insulations, the bearing size and the insulation class are varied keeping other design parameters fixed. This *local* exploration of the design space results in a *family* of motors with the same characteristics as the baseline motor. On the other hand, in a *global* exploration, the motor size is varied in search of new characteristics within the same motor type as the baseline motor.

One approach to the CPR modelling of a global exploration is a component-level analysis. Such an analysis can be challenging due to the system complexity and the design non-linearity. In such a case, the performance analysis requires precise motor models and the cost analysis depends on having a detailed bill of material (BOM). This level of complexity may be avoided by switching to a system-level analysis. In this approach, the manufacturer catalog is consulted to understand the interplay between the size of the motor and its characteristics. For the cost analysis, the simplest model is a linear cost-mass

$$c_0 = \alpha_5 + \beta_5 M, \tag{4.5}$$

or a linear cost-characteristic correlation [26, 28]

$$c_0 = \alpha_6 + \beta_6 X, \tag{4.6}$$

where X denotes the characteristics of the product, β_6 is the marginal variable cost accounting for the material and manufacturing expenses, whereas α_6 is the fixed cost associated with indirect expenses, e.g. sales, administration, etc. [26, 28]. For electric motors, the validity of Eqn. (4.5) and Eqn. (4.6) is demonstrated in Sections 4.2.1 and 4.2.2.

As pointed out in the introduction, the results of the motor reliability survey [14, 15] shows that the reliability of the product is not significantly influenced by the motor size.

Therefore, it is possible to assume that the CPR model of motors reduces to the CP model Eqn. (4.6). The numerical example of Section 4.2.3 supports this assumption.

4.2 Results and discussion

For the global exploration of the design space, the validity of Eqn. (4.5) and Eqn. (4.6) for electric motors is presented in Sections 4.2.1 and 4.2.2. To this purpose, the acquisition cost of the motors is obtained from the list price catalog of two original equipment manufacturers (OEMs). Furthermore, the BOM cost of another OEM is used for verification of Eqn. (4.5). The mass and the characteristics of the product are found in the manufacturers' catalog. Section 4.2.3 studies the local exploration of the design space. To do so, first the CPR models of the bearings and the insulation are examined. Next, the bearing and insulation models are coupled to build the CPR model of an electric motor.

4.2.1 Cost–mass relation

For three motors of the same family manufactured by OEM1, Fig. 4.1 illustrates the BOM cost versus the mass of the motors. The BOM information are provided by OEM1's engineering team and the mass is found in OEM1's website [81]. The motors, here denoted by M20, M35, and M60, are permanent magnet high-speed machines. The nominal torque range of the motors is 45-90 Nm, and the nominal power span of the motors is 18-45 kW [81]. The results are provided for a production volume of 5 and 500 machines. The values of the vertical axis is omitted and the vertical axis is not to scale, as per request of the OEM1. This figure suggests that a linear cost model is a good approximation for the range of the motors, with a maximum error of 4.4% for the M35 when the production volume equals five hundred units.

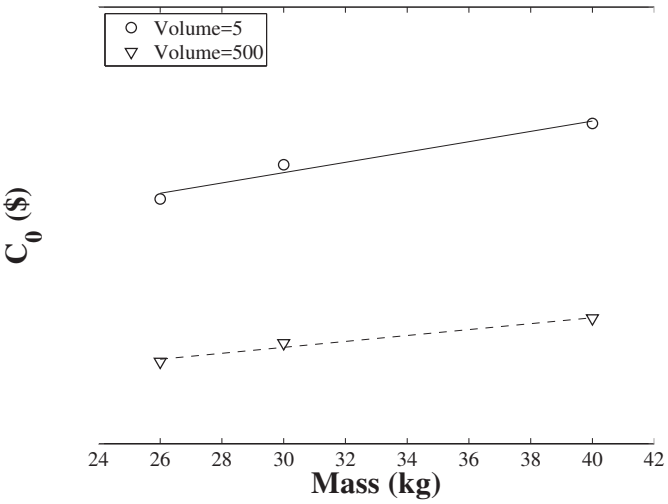

Figure 4.1 BOM cost vs. mass of permanent magnet motors in different production volumes

The acquisition cost versus the mass of wound rotor induction motors and controllers of a series manufactured by OEM2 is presented in Fig. 4.2. The price and the mass of the machines are given in the Pricebook of the OEM2 [82]. It is assumed that the USD/CAD conversion rate is 1.26 as of February 2015 [79]. The power range of the motors is from 112 kW to 597 kW, and the machines have either four or eight poles. The maximum error of the linear cost models is 11% for the four-pole motor with mass of 2322 kg. The r^2 of the linear models is 0.96 for the four-pole machines, and 0.99 for the eight-pole machines.

Many OEMs provide a list price for induction or doubly-fed syncronous machines. In contrast, such information is not available for the permanent magnet machines. In absence of such data from OEMs, it is assumed that the linear BOM cost of Fig. 4.1 extends to a linear correlation between the mass and the acquisition cost in permanent magnet machines. The reason is that the BOM expenses are often multiplied by the overhead factors and profit margins to determine the price of a product [26, 28, 29]. A linear BOM-mass multiplied by constant factors result in a linear acquisition cost-mass relationship for the product.

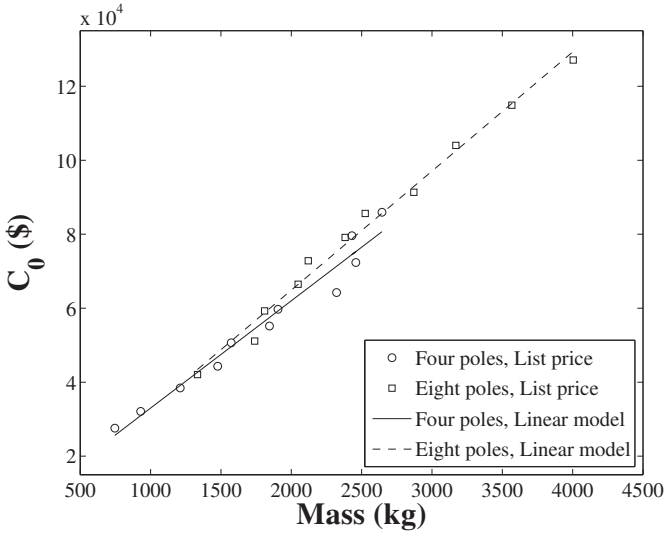

Figure 4.2 Acquisition cost versus mass of induction motors of OEM2

4.2.2 Cost–characteristics correlation

The validity of Eqn. (4.6) is studied for induction motors and controllers by OEM2 and OEM3. The motors of OEM2 are energy efficient level machines of a specific type with class F insulation [82]. The motors of OEM3 are also from a similar class, which are high efficiency level motors with class F insulation [83]. It is assumed that the Euro/CAD conversion rate is 1.42 as of February 2015 [79]. The motors have either two or eight poles. The price and the rated power of the motors are given in the OEMs' catalogs [82, 84]. The cost-rated power results are shown in Fig. 4.3. The power range is from 18.5 kW to 90 kW for the motors of OEM3, and from 112 kW to 373 kW for the motors of OEM2. The maximum error of the linear models is 5.1% for the 112 kW motor of OEM2. Figure 4.4 illustrates the linear behavior of the AC with respect to the rated torque for induction machines of OEM3 with different pole numbers [83, 84].

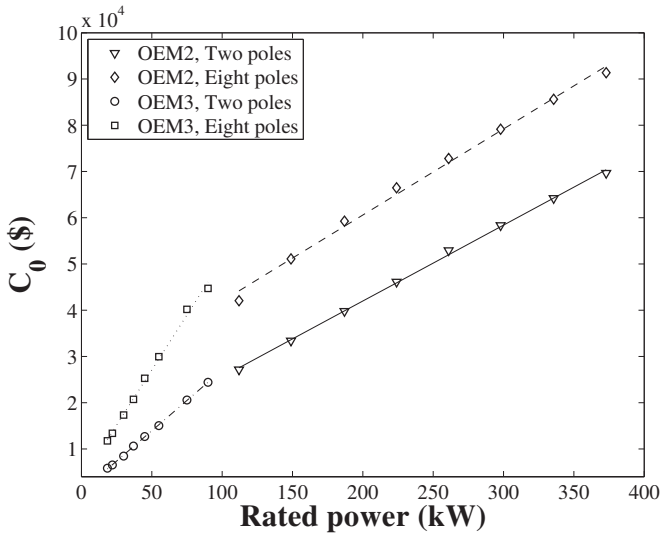

Figure 4.3 Acquisition cost vs. rated power of induction motors

4.2.3 Cost–reliability correlation

As pointed out in the introduction and in Section 4.1.2, the reliability survey results of [14–16] imply that the influence of the size on the reliability of motors of the same type is insignificant and, therefore, here it is assumed that in a global exploration, the CPR model reduces to a CP model Eqn. (4.6). On the other hand, in a local exploration the reliability comes into play as changing the bearing size and the insulation class influences the reliability of the motor.

Motor details

Consider the 1LE1501-3AA4 SIMOTICS induction motor (hereafter called 3AA4) manufactured by the OEM3 (see Table 4.2). This is a high efficiency (IE2) motor with cast iron housing. The motor has two poles and runs at 3000 rpm [83].

No data on the temperature of the bearings and the insulation of the 3AA4 motor is currently available. Instead, the temperature cycles of a motor produced by OEM1 with the rated power of 155 kW and the speed of 3250 rpm is used [81], assuming that the 3AA4 motor

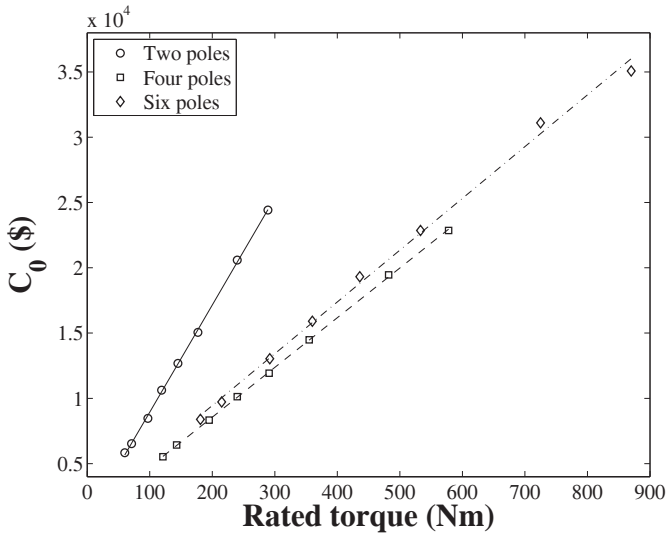

Figure 4.4 Acquisition cost vs. rated torque for induction motors of OEM3

Table 4.2 Motor details [83, 84]

Catalog number	Insulation class	Bearing number	Mass (kg)	Rated power (kW)	Price (CAD)
1LE1501-3AA2	F	6316	880	132	35074
1LE1501-3AA4	F	6316	930	160	43594
1LE1501-3AA5	F	6316	1130	200	54386

faces similar thermal loads. The temperature of the bearings and the hot spot temperature of the insulation are shown in Fig. 4.5 for an operation cycle of 4800 seconds. This cycle is repeated throughout the life of the motor.

Furthermore, it is assumed that the weight of the rotor assembly is equally distributed on the two bearings of the motor. To estimate the weight of the rotor assembly, the BOM of an induction motor is consulted [29]. In the BOM, the housing is made of Magnesium with the density of 1.74 g/cm^3. The mass of the rotor assembly comprises 40% of the mass of the motor. To adjust the BOM of [29] for this example, the magnesium of the housing is replaced by cast

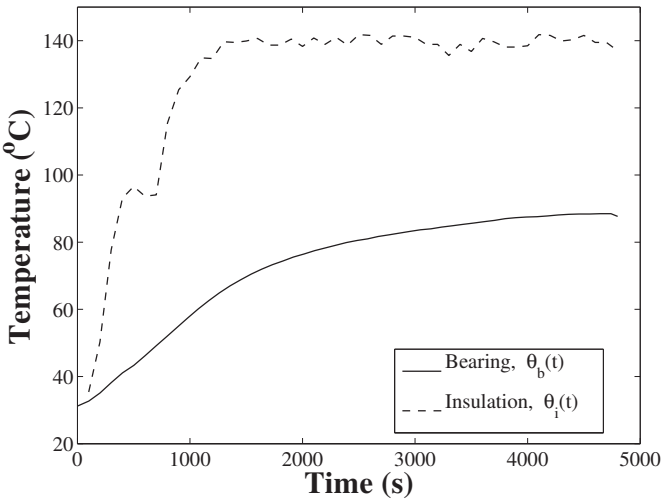

Figure 4.5 Temperature regime of the motor bearings and insulation

iron with the density of 7.64 g/cm^3. Consequently, the mass of the rotor assembly would be 32% of the adjusted BOM. The weight of the rotor assembly is then multiplied by a load factor of 2.5 to account for the transient electromagnetic and mechanical loads. Therefore, the load on each bearing is

$$P_0 = \frac{2.5 \times 0.32}{2} Mg, \tag{4.7}$$

where M is the motor mass. For the 3AA4 motor, the bearing load is 3.65 kN.

Bearing model

In the CPR analysis of the bearings, six deep groove ball bearings of 63xx series are studied (see rows 2 to 7 of Table 4.3). For these bearings, the aforementioned load and temperature cycle is substituted to the bearing life equation Eqn. (3.5) to calculate the reliability of each bearing after 60,000 hours, i.e. 45,000 cycles of Fig. 4.5. The list price of the manufacturer is consulted to report the acquisition cost of the bearings in Table 4.3. Aside from the original temperature regime $\theta_b(t)$ of Fig. 4.5, the reliability analysis is conducted for two temperature regimes of $\theta_b(t) + 10\ ^o$C and $\theta_b(t) - 10\ ^\circ$C, as well. The corresponding cost-reliability results, as well as

the prediction of the CPR model Eqn. (3.23), are plotted in Fig. 4.6. For each of the temperature regimes, as the bearing size increases from the 6312 bearing to the 6317 bearing, the reliability is increased. As the temperature is increased, the CR curve shifts towards lower reliabilities (left). The maximum error of the present CPR model from the catalog prices is 7.9% for the 6313 bearing.

Table 4.3 Deep groove ball bearings [77, 78]

Catalog no.	6312	6313	6314	6315	6316	6317	16016	6016	6216	6416
Bore (mm)	60	65	70	75	80	85	80	80	80	80
C_r (kN)	89	100	115	123	131	141	34	51	77	173
c_0 ($)	181.05	251.34	293.93	357.84	421.03	510.49	166.14	164.72	213.71	1124.58

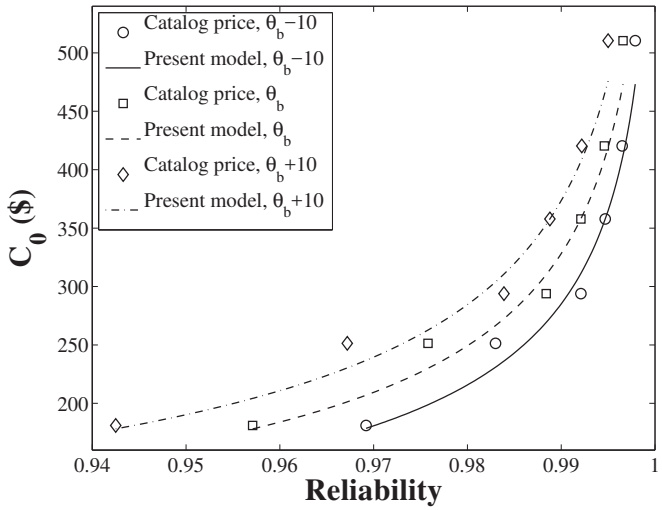

Figure 4.6 CPR of the bearings

Insulation model

The BOM of the 3AA4 motor is not available to get details on the cost of the insulation. Instead, the catalog of OEM4 allows the inference that if the insulation class of a motor is switched from

B to F, its price is increased by 5% [85] . This number is 10% if the class H insulation is used instead of the class B. Here, it is assumed that the motors of OEM3 follow the same pattern as the OEM4 motors. Furthermore, it is assumed that by switching from the class B to the class A, the motor price is reduced by 5%. Although without a BOM it is not possible to conduct an accurate cost analysis, the suggestion of the OEM4 may be used to perform a comparative cost analysis for the insulation classes of Table 4.1. To this end, the zero level of the cost is set at the class F insulation, and the 5% factor is used to evaluate the comparative cost of the other insulation classes.

The insulation reliability is calculated using Eqn. (4.4) for four temperature regimes; the original regime of Fig. 4.5, $\theta_i(t)$, as well as $\theta_i(t) - 20\ ^o$ C, $\theta_i(t) - 10\ ^o$ C, and $\theta_i(t) + 10\ ^o$ C. The reliability is reported after 20,000 hours of operation, which includes 15000 cycles of 4800 seconds (See Fig. 4.5). The result is shown in Fig. 4.7. At each temperature, by going from the insulation class A to the insulation class H, the reliability increases monotonically. Note that the iso-cost points are the same insulation class under different temperature regimes. As expected, increasing the temperature shifts the cost-reliability curve to the left. Except for the class H insulation, the reliability is significantly affected by the temperature regimes. Furthermore, note that compared to the class F operating at $\theta_i(t) - 20\ ^o$ C, the class H at $\theta_i(t) + 10\ ^o$ C has a higher cost and a lower reliability. This underlines that selecting the optimum insulation class requires a good understanding of the temperature regime.

Motor model

In the local exploration of the baseline 3AA4 motor, five bearings with the bore of 80 mm (columns 6 and 8-11 of Table 4.3), and four insulation classes (see Table 4.1) are considered. It is assumed that none of the bearings violates the space limitations. The baseline motor has the 6316 bearing and the class F insulation. The combination of five bearings and four insulation classes leads to a family of twenty different solutions.

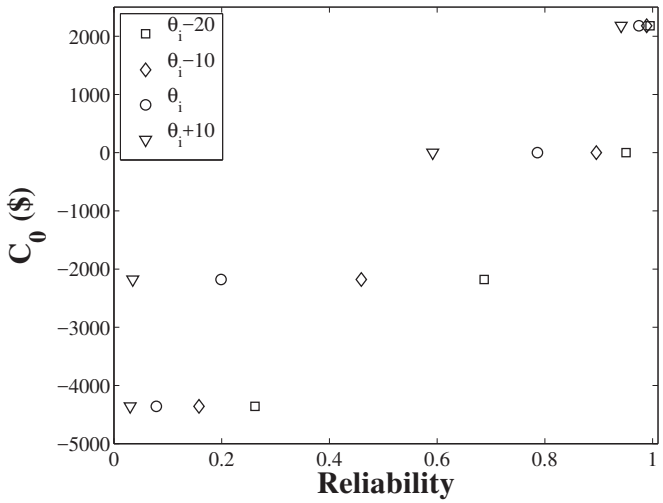

Figure 4.7 CPR of the insulation

For each member of the 3AA4 family, the reliability is calculated after 20000 hours of operation, which includes 15000 cycles of the temperature regimes of Fig. 4.5. The speed of the motor is 3000 rpm. The load on each bearing is given by Eqn. (4.7). The reliability of the bearing and the insulation is calculated using Eqn. (3.1) and Eqn. (4.4), respectively. The failure of a bearing or the insulation leads to the failure of the motor. Therefore, the reliability of the motor, R_m equals

$$R_m = R_b^2 R_i. \tag{4.8}$$

The acquisition cost of the bearings is collected in Table 4.3 [78]. The price of the 6416 bearing is not presented in the price catalog. Instead, for the 64xx series bearings, the price of the bearings from 6405 to 6412 are given. This data is substituted into Eqn. (4.5) to develop the cost-mass correlation of the 64xx bearings. This correlation is then used to estimate the price of the bearing 6416.

The bearings price appear in the BOM of the motor as a material cost. The BOM is then multiplied by the overhead and the profit margin factors to calculate the acquisition cost of the product. Here, similar to Cuenca, Gaines, and Vyas [29], it is assumed that these factors are

1.35 and 1.20, respectively, resulting in a total multiplier of 1.62. Hence, if the bearing 6316 is replaced by another bearing, the difference of the price of the latter and the former is multiplied by 1.62, and the result is added to the price of the baseline motor to get the acquisition cost of the new motor. If the baseline insulation class is changed, the aforementioned “5% insulation cost" rule is applied to the acquisition cost analysis.

The results of the local exploration of the 3AA4 motor are presented in Fig. 4.8. As expected, by going from the insulation class A toward H, higher reliability is achieved. In each insulation class, as the dynamic rating load is increased from the 16016 bearing to the 6416 bearing, the reliability increases. However, switching between the bearings 16016, 6016, and 6216 leads to no significant change in the acquisition cost. Therefore, among these three options, the 6216 bearing is the best solution. Furthermore, switching from the bearing 6316 to 6416 increases the acquisition cost with no considerable effect on the reliability. The reason is that the reliability of the bearings 6314 and 6414 are 0.9999 and 1.0000, respectively, which implies that the system reliability is mainly determined by the insulation. Therefore, it is not reasonable to invest on increasing the reliability of the bearing by going from the 6316 to the 6416.

It is interesting to compare the baseline motor and the motor with the 6016 and the class H insulation. The reliability of the two motors equal 0.786 and 0.782, respectively. This implies that if the reliability target of the motor is around 0.8, the baseline motor is the best solution. On the other hand, higher levels of reliability are not achievable by the class F insulation. In that case, the class H insulation and either the 6216 or the 6316 shall be used, depending on the reliability target and the cost considerations.

In Fig. 4.8, all of the 3AA4 family machines have the same characteristics as the original. To include the influence of the characteristics, the local exploration procedure is conducted for the 3AA2 and 3AA5 motors. Figure 4.9 illustrates the span of each family in the cost-reliability plane.

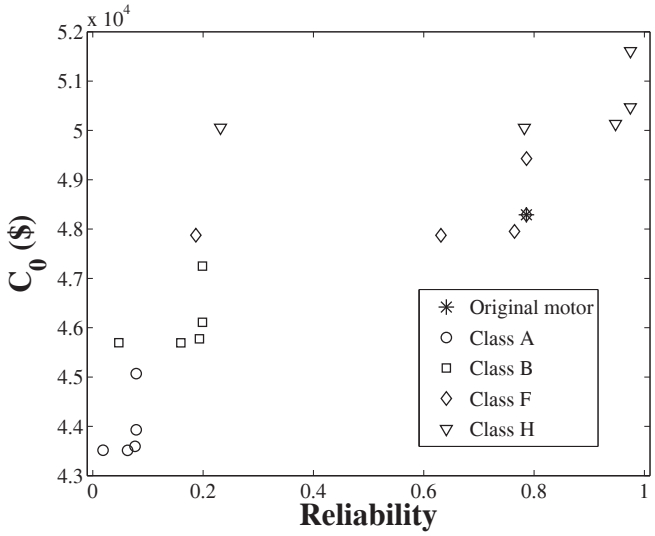

Figure 4.8 CR of the 3AA4 motor

Equation (4.4) implies that R_i is independent of the motor size, as long as the temperature regime is not varied. On the other hand, substitution of Eqn. (4.7) into Eqn. (3.26) and (3.27) results in R_b being reduced when the bearing is mounted on a larger motor. Thus, between two motors of different families but with identical bearings and insulation class, the larger motor has a lower reliability. Equation (3.1) implies that increasing the bearing size (or C_r) reduces the sensitivity of the bearings reliability to the load variation. Therefore, when high reliability bearings (with large C_r) are used, the influence of the motor size on R_b and, consequently, on R_m is negligible. As an example, R_m of the 3AA2, 3AA4, and 3AA5 motors with the 6316 bearing and the class F insulation is 0.786, 0.786, and 0.784, respectively, whereas for the 3AA2, 3AA4, and 3AA5 motors with the 6016 bearing and the class F insulation, R_m is 0.664, 0.631, and 0.455, respectively. This validates the assumption that, in practical cases, where the motor elements are designed for high reliability, the CPR model is reduced to a CP model in a global exploration.

As the final note, the reliability of the motors is calculated assuming that the temperature and mechanical loads are as given in Fig. 4.5 and Eqn. (4.7). The original product of OEM3 does not necessarily undergo such thermal and mechanical loads. Consequently, depending on

the application and the applied loads, the reliability of the product may be different from what is reported here.

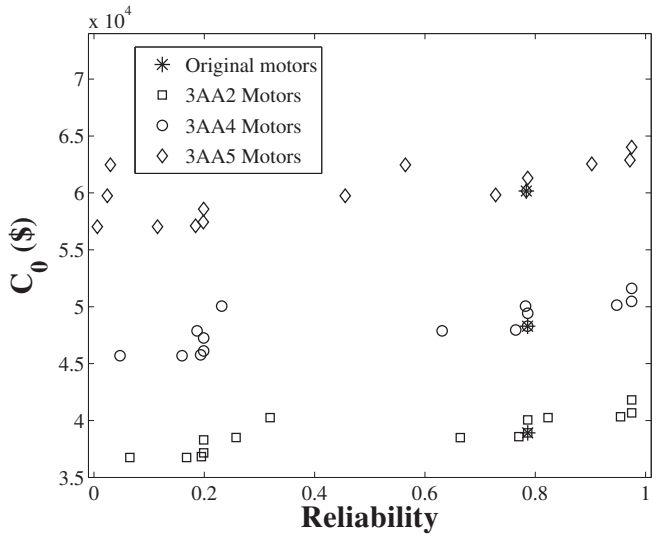

Figure 4.9 CPR of the motors

4.3 Conclusions

This chapter studies the acquisition cost-performance-reliability (CPR) relation of electric motors. This problem is addressed from two perspectives. In a *global* exploration perspective, the motor size is scaled to define new motors with different characteristics. The second approach is a *local* exploration where the general features of the motor that affect its characteristics are left unchanged, whereas its bearing size and insulation class are altered to vary the motor reliability. This process results in new motors as neighboring design points with the same characteristics as the original motor.

The motor failure is mainly caused by the damage of the bearings or the electrical insulation. To derive the CPR model of electric motors, the CPR model of electrical insulations is

developed first. The insulation model illustrates the sensitivity of the reliability to the temperature regime, resulting in a wide span of the data points on the cost-reliability plane.

The bearing and the insulation models are next coupled to built up the CPR model of motors. This model is used in the local exploration of the design space of a motor. The results indicate that, depending on the system-level reliability target and the duty cycle, either the original motor or a neighboring design point may have the lowest acquisition cost.

In the global exploration, for different motors of the same type and class, the influence of the motor size on its acquisition cost, reliability, and characteristics is addressed. The previous empirical data indicates that the reliability of the motor is not significantly affected by its size. This implies that in a global exploration, the CPR model of a motor is reduced to a cost-performance (CP) model. The results of the present cost model is in agreement with the empirical observation.

In Chapters 2–4, the AC modelling of gears, rolling bearings, gearboxes, and electric motors are addressed. To add the maintenance cost into the cost analysis, the next chapter is dedicated to MC modelling of engineering elements.

Chapter 5

Maintenance Cost Modelling and Life-Cycle Cost Assessment of Engineering Systems

Chapters 2–4 study the acquisition cost of gears, rolling bearings, electrical insulations, gearboxes and electric motors. As the next step for the life-cycle cost analysis of the aforementioned components/systems, it is important to quantify the interplay between their maintenance cost and their reliability. The objective is to derive cost models for a post-failure and two preventive maintenance strategies. The models will be generic in the sense that the expected maintenance cost of an arbitrary component can be calculated by having its reliability function $R(t)$, the maintenance downtime, the price of spare parts, the downtime cost associated with the loss of productivity, and the inflation rate. The convergence of the models, as well as the conditions for selecting one maintenance strategy over the other are addressed. In a case study, the maintenance cost model as well as the CPR models of previous chapters are used in the life-cycle cost assessment a one-speed gearbox.

5.1 Model formulation

The reliability, $R(t)$, of an element is defined as the probability that the element is properly operational up to instant t [3]. This definition implies that the failure probability between t and $t+\Delta t$ equals $R(t)-R(t+\Delta t)$. If the cost of failure of the element at instant t is $c_f(t)$, its discounted maintenance cost in this interval equals

$$\text{Discounted maintenance cost} = -\Big(R(t+\Delta t)-R(t)\Big)c_f(t)e(t), \tag{5.1}$$

where $e(t)$ is the discount factor at instant t, and is applied to calculate the present value of the maintenance cost. As $\Delta t \to 0$, the rate of the discounted maintenance cost, $\dot{c}$, is

$$\dot{c} = p(t)c_f(t)e(t), \tag{5.2}$$

in which $p(t)$ is the failure probability density function (FPDF) defined by

$$p(t) = -\frac{\partial R(t)}{\partial t}. \tag{5.3}$$

By taking the integral of Eqn. (5.2) over the life cycle of the element, its total discounted maintenance cost is calculated. In other words, the FPDF is the kernel for calculation of the total maintenance cost of the part throughout its life cycle. This idea will be used in the following sections to establish the maintenance cost model associated with multiple failures for three maintenance strategies. The cost models are then used in several component-level and system-level reliability allocation and cost reduction problems.

5.1.1 Post-failure maintenance

The post-failure maintenance (PFM) strategy has the following properties:

1. The life target for the element is T.

2. The reliability of the element is given by $R(t)$.

3. A failed element is replaced by a new, identical one.

4. The failure downtime is δ_f.

5. The cost of a failure at instant t is $c_f(t)$, paid at t.

Equation (5.2) is written for one failure at instant t. To study the cost associated with multiple failures, this equation is generalized. Consider k failures as shown in Fig. 5.1. The initial element fails at t_1. The downtime is δ_f to replace the failed element with a new, identical one. The operation time of the second element is t_2 whereupon it fails. After downtime of δ_f, the third element operates until it faces failure after t_3. This process repeats up to the failure of the k-th element. The element $k+1$ will then safely operate up to the end of the life target. The instant of i-th failure is given by

$$\tilde{t}_i = \sum_{j=1}^{i} t_j + (i-1)\delta_f. \tag{5.4}$$

The FPDF of having exactly k failures is

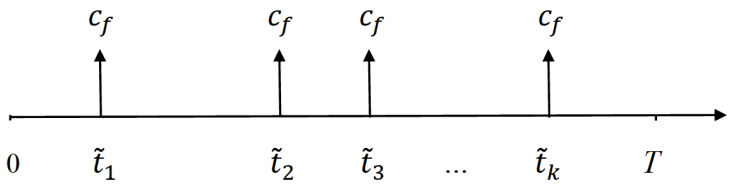

Figure 5.1 Monetary cash flow of the PFM strategy

$$f_k = p(t_1)p(t_2)\cdots p(t_k)R(T-\tilde{t}_k-\delta_f), \tag{5.5}$$

where $p(t_i)$ is the failure probability of i-th failure at $\tilde{t}_i$. The term $R(T-\tilde{t}_k-\delta_f)$ ensures that the $(k+1)$-th element, which starts operating at $\tilde{t}_k+\delta_f$, faces no failure up to T. The cash flow of

such event is given by

$$\varsigma_k = \sum_{i=1}^{k} c_f(\tilde{t}_i) e(\tilde{t}_i). \tag{5.6}$$

where the term $e(\tilde{t}_i)$ is added to calculate the net present value (NPV) of the cash flow. Similar to the idea used in Eqn. (5.2), f_k may be used as the kernel to write the rate of the cost of exactly k failures as

$$\dot{c}_k = f_k \varsigma_k, \tag{5.7}$$

Before proceeding to taking the integral of $\dot{c}_k$ over the time domain, the limits of the integrals should be determined. Equation (5.4) may be rewritten as

$$\tilde{t}_{i+1} = \tilde{t}_i + \delta_f + t_{i+1}. \tag{5.8}$$

Failures happen in the interval $(0,T)$, implying $0 < \tilde{t}_i < T$ for any i. Hence, Eqn. (5.8) determines the range of t_i as $0 < t_1 < T$ and $0 < t_{i+1} < T - \tilde{t}_i - \delta_f$ for $i > 1$. The discounted maintenance cost of exactly k failures, therefore, equals

$$\bar{c}_k = \int_0^T \int_0^{T-\tilde{t}_1-\delta_f} \cdots \int_0^{T-\tilde{t}_{k-1}-\delta_f} \dot{c}_k \, dt_k \cdots dt_2 dt_1. \tag{5.9}$$

Summing up the maintenance cost of any possible number of failures gives the total discounted maintenance cost as

$$\bar{C}_M = \sum_{k=1}^{\infty} \bar{c}_k. \tag{5.10}$$

The term $\dot{c}_k$ and, consequently, the discounted maintenance cost $\bar{C}_M$ depends on the reliability function, $R(t)$, the cost of a failure, $c_f(t)$, and the time value of money, $e(t)$. Among these three parameters, a designer often has no control over the latter two because they are determined by the market and the economy. Hence, in a PFM strategy the only cost optimization parameter is the reliability of the part. This cost optimization problem is addressed in Section 5.2.

Equivalent to the approach that leads to Eqn. (5.5)–(5.10), a second formulation of the PFM can be derived. To this end, it is useful to define a new FPDF

$$\hat{f}_k = p(t_1)p(t_2)\cdots p(t_k), \tag{5.11}$$

where higher number of failures are not excluded because the term $R(T-\tilde{t}_k-\delta_f)$ is dropped. In Eqn. (5.7), since both f_k and ς_k correspond to having exactly k failures, $\dot{c}_k$ gives the time rate of only k failures. The definition of $\hat{f}_k$, on the other hand, allows having more than k failures. Hence, if $\hat{f}_k$ is multiplied by $c_f(\tilde{t}_k)$, the result is the time rate of the maintenance cost of the k-th failure

$$\breve{c}_k = \hat{f}_k c_f(\tilde{t}_k). \tag{5.12}$$

Integration of $\breve{c}_k$ over the time domain gives the expected maintenance cost of k-th failure

$$\bar{\bar{c}}_k = \int_0^T \int_0^{T-\tilde{t}_1-\delta_f} \cdots \int_0^{T-\tilde{t}_{k-1}-\delta_f} \breve{c}_k \, dt_k \cdots dt_2 dt_1, \tag{5.13}$$

which calculates the contribution of the k-th failure on the maintenance cost of having k or more failures. The total maintenance cost equals

$$\bar{\bar{C}}_M = \sum_{k=1}^{\infty} \bar{\bar{c}}_k. \tag{5.14}$$

In Section 5.2.1, it is shown that the two formulations Eqn. (5.10) and (5.14) converge to a single solution. Furthermore, in Section 5.2.1 the convergence of the present PFM model to the PFM model in [42, 43] is studied to validate the present model. The PFM model of [42, 43] assumes a zero inflation rate. This implies that the model of [42, 43] is a special case of the work presented here.

As the final note, in most of practical cases, the downtime δ_f is much smaller than the target life [43]. Hence, a simplification of Eqn. (5.10) is to set $\delta_f = 0$ and to lump the capital loss caused by the downtime in c_f. In Section 5.2 it is shown that the influence of this assumption on

the accuracy of the model is negligible and, therefore, in the following sections this assumption is used to simplify the preventive maintenance cost models.

5.1.2 Preventive maintenance

In the PFM strategy, the replacement is conducted when a failure occurs. Since the maintenance activity is unscheduled, the resources required for procedure may not be available. In a preventive strategy, on the other hand, the maintenance team is ready for the procedure as defined by the maintenance schedule. Moreover, in some cases it is possible to schedule the preventive maintenance of several parts of a system at the same time to reduce the system downtime. Consequently, the cost of a preventive maintenance c_p is often lower than that of an unplanned post-failure maintenance c_f. Often, this justifies switching from a PFM strategy to a preventive one. Next, two preventive maintenance strategies are assessed and the corresponding cost models are developed.

Strategy 1– Block replacement policy

The first preventive maintenance (PrM1) strategy is defined by:

1. The life target for the element is T.
2. The reliability of the element is given by $R(t)$.
3. The downtime of a preventive maintenance is negligible compared to T, i.e. $\delta_p/T \to 0$.
4. The downtime of a failure is negligible compared to T, i.e. $\delta_f/T \to 0$.
5. There are n preventive maintenances, dividing the life target into $n+1$ blocks. The length of each block is $t_p = T/(n+1)$.

6. The j-th preventive maintenance is conducted at instant jt_p; $j = 1, ..., n$. The faulty part is replaced by a new, identical one.

7. If a part fails at any instant other than jt_p, it is replaced by an as new part. The reliability resets to unity.

8. The cost of the j-th preventive maintenance is $c_p(jt_p)$, paid at jt_p.

9. The cost of a failure is $c_f(t)$, paid at t.

The monetary cash flow of this strategy is schematically illustrated in Fig. 5.2. The short thick arrows indicate the cash flow corresponding to the preventive maintenance at instants jt_p, whereas the long thin arrows refer to the unexpected failures between the preventive maintenances.

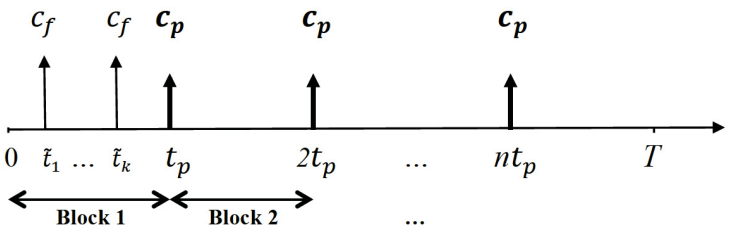

Figure 5.2 Monetary cash flow of the PrM1 Strategy

The total maintenance cost of this strategy is composed of two terms. The first term deals with the cost of the preventive maintenance activities at instants jt_p in the form

$$\bar{C}_P = \sum_{j=1}^{n} c_p(jt_p)e(jt_p). \tag{5.15}$$

The second term considers the direct cost of the failures in the maintenance cost. To develop the model for the second term, consider the time interval $\big((l-1)t_p, lt_p\big)$, hereafter called block l. No preventive maintenance is conducted within each block– a PFM strategy is followed and the model developed in Section 5.1.1 is applicable within each block. To calculate the FPDF of having k failures at block l, replacing T in Eqn. (5.5) by t_p and setting $\delta_f = \delta_p = 0$ yields

$$f_k = p(t_1)p(t_2)\cdots p(t_k)R(t_p - \tilde{t}_k). \tag{5.16}$$

Note that for any block, the FPDF is given by Eqn. (5.16). The reason is that t_i, $\tilde{t}_k$ and t_p are independent of l. Furthermore, it is important to bear in mind that in the PFM strategy the operation starts at $t = 0$, whereas at block l the operation starts at $t = (l-1)t_p$. Therefore, for k failures at block l, Eqn. (5.6) becomes

$$\varsigma_{k,l} = \sum_{i=1}^{k} c_f\big((l-1)t_p + \tilde{t}_i\big)\, e\big((l-1)t_p + \tilde{t}_i\big). \tag{5.17}$$

Having the cash flow in hand, the time rate of the cost of k failures at block l is given by

$$\dot{c}_{k,l} = f_k \varsigma_{k,l}, \tag{5.18}$$

The limits of the t_i are similar to that of the PFM strategy, except that T is replaced by t_p. Integration of Eqn. (5.18) over this time domain gives the discounted maintenance cost of k failure at block l

$$\bar{c}_{k,l} = \int_0^{t_p} \int_0^{t_p - \tilde{t}_1} \cdots \int_0^{t_p - \tilde{t}_{k-1}} \dot{c}_{k,l}\, dt_k \cdots dt_2 dt_1. \tag{5.19}$$

Summation of Eqn. (5.19) over all possible number of failures and over the $n+1$ blocks gives the discounted cost of failure

$$\bar{C}_F = \sum_{k=1}^{\infty} \sum_{l=1}^{n+1} \bar{c}_{k,l}. \tag{5.20}$$

The total discounted maintenance cost is the sum of the preventive maintenance cost Eqn. (5.15) and the failure maintenance cost Eqn. (5.20)

$$\bar{C}_M = \bar{C}_P + \bar{C}_F. \tag{5.21}$$

In this maintenance strategy, the cost optimization variables are the reliability function $R(t)$ and the block length t_p. Increasing t_p reduces the frequency of the preventive maintenance and, therefore, decreases the preventive maintenance cost $\bar{C}_P$. On the other hand, a higher t_p results in a higher chance of failure at each block, resulting in a higher failure maintenance cost $\bar{C}_F$. Hence, t_p should be selected such that a trade-off is made between these two cost terms to minimize the total maintenance cost. Furthermore, investing on the acquisition cost to increase

the reliability leads to a saving on the maintenance cost, which implies that there is an optimum reliability at which a trade-off is achieved between the acquisition cost and the maintenance cost. These problems are addressed in Section 5.2.

One point may be raised about the optimality of the PrM1 strategy. To address this point, consider two blocks l and l'. Consider that no failure occurs at block l and the part operates up to t_p, where it is replaced by a new one. At block l', on the other hand, consider a failure at t_1. The failed part is replaced by a new one which operates for $t_p - t_1$ until it reaches the preventive maintenance point. It is reasonable to ask why the age of the part at block l could be t_p up to the preventive maintenance point, whereas the age of the replaced part at block l' is only $t_p - t_1$ when the preventive maintenance is conducted? In other words, it is more economical to let the replaced part of block l' operate up to age t_p if no failure is observed. This point is the motivation of switching from a block replacement policy (PrM1) to an age replacement policy. This new strategy is discussed next.

Strategy 2– Age replacement policy

The second preventive maintenance (PrM2) strategy is qualified by:

1. The life target for the element is T.
2. The reliability of the element is given by $R(t)$.
3. The downtime of a preventive maintenance is negligible compared to T, i.e. $\delta_p/T \cong 0$.
4. The downtime of a failure is negligible compared to T, i.e. $\delta_f/T \cong 0$.
5. The element will be replaced at age (i.e. after operating for) t_p or upon a failure, whichever happens first.
6. The replaced part is as new. The reliability is reset to unity.

7. The cost of a preventive maintenance at instant t is $c_p(t)$, paid at t.

8. The cost of an unexpected failure at instant t is $c_f(t)$, paid at t.

In the PrM1 case, the preventive maintenance dates are known beforehand (see item 6 of the PrM1 strategy). In contrast, in the PrM2 strategy, after a preventive maintenance event, the next preventive maintenance date depends on whether a failure occurs before t_p or not. If the element fails before operating for t_p, a maintenance is conducted. Next, the item 5 of the PrM2 strategy shall again be consulted to determine the next potential preventive maintenance date. As a result, the derivation of the PrM2 cost model is not as straightforward as that of PrM1.

Consider that t_p is given by $T = (n+1)t_p$. In other words, there will be n preventive maintenances if no failure occurs, which implies there are at least n replacements throughout the total operation cycle. Therefore, $\bar{c}_j = 0$ for $j < n$, where $\bar{c}_j$ denotes the cost of j preventive and/or failure replacements.

Next, consider the case that no failures occur and each part safely operates up to t_p (Fig. 5.2 with no failures in the blocks). This case is composed of n preventive maintenances at instants jt_p ; $j = 1, \ldots, n$. The probability of this event equals $R(t_p)$ to the power of $n+1$ because all of $n+1$ elements (the initial element plus n replaced elements) shall properly operate up to $t = t_p$. Hence, the discounted expected maintenance cost of having only preventive maintenances is

$$\bar{C}_P = R^{n+1}(t_p) \sum_{j=1}^{n} c_p(jt_p) e(jt_p). \tag{5.22}$$

where the subscript P denotes the case of having only preventive maintenances.

Now consider having k failures as depicted in Fig. 5.3. The term t_i denotes the age of the i-th failed part at the failure point. The first question to address is that besides the k failure maintenances, how many preventive maintenances, n', shall be conducted? As explained in the previous paragraph, the operation duration of n' elements with no failure is

$(n'+1)t_p$. The operation duration of the k failed elements equals their accumulated age $\tilde{t}_k$ (see Eqn. (5.4)). Hence, the total operation duration of such event equals $(n'+1)t_p+\tilde{t}_k$. The life target is $T=(n+1)t_p$. This implies that n' is the smallest integer that meets the following condition

$$(n+1)t_p \leq (n'+1)t_p+\tilde{t}_k. \tag{5.23}$$

Now the relation $0 \leq t_i < t_p$ and Eqn. (5.4) with $\delta_f = 0$ yield $0 \leq \tilde{t}_k < kt_p$. Consider that $\tilde{t}_k$ is in the range

$$(l-1)t_p \leq \tilde{t}_k < lt_p, \tag{5.24}$$

where l is an integer between 1 and k. Adding $(n'+1)t_p$ to relation Eqn. (5.24) gives

$$(n'+l)t_p \leq (n'+1)t_p+\tilde{t}_k < (n'+1+l)t_p \ , \ l=1, \ ..., \ k. \tag{5.25}$$

For Eqn. (5.23) to follow from Eqn. (5.25), it is necessary and sufficient to have

$$(n+1)t_p \leq (n'+l)t_p \ , \ l=1, \ ..., \ k, \tag{5.26}$$

where the smallest answer is $n'=n+1-l$; n' depends on both n and l, which itself is bounded to k.

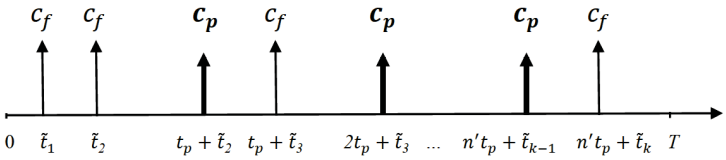

Figure 5.3 Monetary cash flow of the PrM2 Strategy with k failures

The second step is determining the FPDF of such an event. In addition to the k failures in the range $(l-1)t_p < \tilde{t}_k < lt_p$, $n-l+1$ parts will operate up to t_p. This means that the FPDF is

$$f_{k,l} = R^{n-l+1}(t_p)R(lt_p-\tilde{t}_k)\prod_{i=1}^{k}p(t_i), \tag{5.27}$$

where $R(lt_p - \tilde{t}_k)$ is the probability that the last element safely operates up to the end of the life target. Fig. 5.3 illustrates this with the caveat that $T - (n't_p + \tilde{t}_k) = lt_p - \tilde{t}_k$.

The last step is determining the cash flow of the event. To this end, it is useful to define m_i as the number of preventive maintenance before i-th failure. According to Fig. 5.3, after m_1 preventive maintenances, the next element fails at age t_1. The next $m_2 - m_1$ parts meet no failure. The next part fails at age t_2. This process continues until $m_k - m_{k-1}$ parts meet a preventive maintenance right before the k-th failure. The remaining $n - l + 1 - m_k$ parts face no failure. Note that $0 \leq m1 \leq m2 \leq ... < m_k \leq n - l$. The cash flow of the event, therefore, has the form

$$\begin{aligned}
\varsigma_{k,l} =& \Big(\sum_{i=0}^{m_1} - \sum_{i=0}^{0}\Big) c_p(it_p) e(it_p) + c_f(m_1 t_p + \tilde{t}_1) e(m_1 t_p + \tilde{t}_1) \\
&+ \Big(\sum_{i=0}^{m_2} - \sum_{i=0}^{m_1}\Big) c_p(it_p + \tilde{t}_1) e(it_p + \tilde{t}_1) + c_f(m_2 t_p + \tilde{t}_2) e(m_2 t_p + \tilde{t}_2) + \ ... \\
&+ \Big(\sum_{i=0}^{m_k} - \sum_{i=0}^{m_{k-1}}\Big) c_p(it_p + \tilde{t}_{k-1}) e(it_p + \tilde{t}_{k-1}) + c_f(m_k t_p + \tilde{t}_k) e(m_k t_p + \tilde{t}_k) \\
&+ \Big(\sum_{i=0}^{n-l} - \sum_{i=0}^{m_k}\Big) c_p(it_p + \tilde{t}_k) e(it_p + \tilde{t}_k),
\end{aligned} \tag{5.28}$$

The term $\sum_{i=0}^{m_j} - \sum_{i=0}^{m_{j-1}}$ considers the cash flow of the preventive maintenances between the $(j-1)$-th and the j-th failures. It may also be written as $\sum_{i=m_{j-1}+1}^{m_j}$. However, the latter is not well-defined when $m_j = m_{j-1}$. Therefore, the former form is used here. Moreover, in the PrM2 strategy, $\varsigma_{k,l}$ is the cash flow of having k failures when $(l-1)t_p \leq \tilde{t}_k < lt_p$, whereas in the PrM1 strategy $\varsigma_{k,l}$ is the cash flow of having k failures in block l.

The rate of the cost of k failures is then equal to

$$\dot{c}_{k,l} = \sum_{m_1=0}^{n-l} \sum_{m_2=m_1}^{n-l} \cdots \sum_{m_k=m_{k-1}}^{n-l} f_{k,l}\, \varsigma_{k,l}, \tag{5.29}$$

where the summation over m_i's consider all order combinations of the failures and preventive maintenances. Integration of Eqn. (5.29) over the corresponding time domain gives

$$\bar{C}_{F_k} = \sum_{l=1}^{k} \int_0^{t_p} \int_0^{t_p} \cdots \int_0^{t_p} \dot{c}_{k,l}\, dt_k \cdots dt_2 dt_1, \tag{5.30}$$

where the subscript F_k on the left-hand side refers to having k failures. In Eqn. (5.30) the numerical value of $\tilde{t}_k$ and the relation Eqn. (5.24) must be consulted to determine l and the cash flow and the FPDF which corresponds to l.

Summing the preventive and failure maintenance costs gives the discounted maintenance cost

$$\bar{C}_M = \bar{C}_P + \sum_{k=1}^{\infty} \bar{C}_{F_k}, \tag{5.31}$$

adding which to the acquisition cost gives the LCC

$$\bar{C}_T = c_0 + \bar{C}_M. \tag{5.32}$$

As pointed out earlier, the PrM2 model proposed in Blischke et. al. [42] and Jardine et. al. [43] assumes no inflation rate and an infinite horizon for the project. This assumption significantly simplifies the model. The PrM2 model developed here, on the other hand, has a more complex formalism since these assumptions are avoided. In Section 5.2.3 the validity of these assumptions is discussed and the corresponding error associated with the assumptions is studied to assess the advantage of switching from the models in [42, 43] to the model developed here. Moreover, the LCC of the PrM1 and PrM2 strategies are compared to assess the advantage of choosing one over the other.

5.2 Numerical examples

The developed cost models for the maintenance strategies are studied through five classes of numerical examples. In the first class, the sensitivity of the cost model to the model parameters is studied. This analysis is important because it may be difficult to determine the value of some of the model parameters in the early design stages of a project. The interest rate, the downtime, and the future price of the part are three examples of such parameters. The second class of examples examines how many terms should be considered to ensure the convergence of the cost models $\big($See Eqn. (5.10) and (5.14)$\big)$. The third class of examples deals with the comparison of the models developed here with the models presented in Blischke and Murthy [42] and Jardine and Tsang [43]. The next class of examples deals with comparing the results of the PFM, PrM1, and PrM2 strategies to select the best maintenance strategy for different case studies. Lastly, the acquisition cost models developed in Chapters 2 and 3 are coupled with the present cost models to design a one-speed gearbox with low life-cycle cost such that the overall performance and reliability requirements are met.

5.2.1 Post-failure maintenance strategy

For the PFM model Eqn. (5.11)-(5.14), the convergence of the model is studied. Next, the sensitivity of the maintenance cost to the price function $c(t)$, the discount function $e(t)$, and the downtime δ_f is studied. Finally, the behavior of the model is assessed for different reliability functions.

Convergence of the model

As the first example, the PFM strategy is studied for a part with

$$R(t) = e^{-\lambda t}\ ,\ e(t) = e^{-rt}. \tag{5.33}$$

The exponential distribution is important as it is widely used in the reliability modelling of the electronic and electrical parts [42], where λ is the failure rate of the part. The time value of money $\exp(-rt)$ describes the situation of a constant discount rate r. The total life of the project is T. It is assumed that the price of the element and the cost of a failure follow

$$c(t) = c_0 e^{st} \ , \ c_f(t) = (c_0 + c_{f_0}) e^{st}, \tag{5.34}$$

Eqn. (5.34) describe a market where the prices and the service costs continuously increase with the constant rate s. The term c_0 is the present price of the part, and c_{f_0} takes into account other expenses associated with the failure, including the labor cost, loss of productivity, costumer dissatisfaction, etc. Substitution of Eqn. (5.33) and Eqn. (5.34) into Eqn. (5.13) for the first four failures gives

$$c_1^{**} = \frac{\lambda}{\alpha}\Big(\frac{\lambda e^{\lambda\delta_f}}{\alpha}\Big)^0 \Big[e^{\alpha T} - 1\Big], \tag{5.35}$$

$$c_2^{**} = \frac{\lambda}{\alpha}\Big(\frac{\lambda e^{\lambda\delta_f}}{\alpha}\Big)^1 \Big[e^{\alpha T}\Big(\alpha T - e^{\alpha\delta_f}\Big) + e^{\alpha\delta_f}\Big], \tag{5.36}$$

$$c_3^{**} = \frac{\lambda}{\alpha}\Big(\frac{\lambda e^{\lambda\delta_f}}{\alpha}\Big)^2 \Big[e^{\alpha T}\Big(\frac{1}{2}(\alpha T)^2 - (\alpha\delta_f + e^{\alpha\delta})\alpha T + e^{2\alpha\delta_f}\Big) - e^{2\alpha\delta_f}\Big], \tag{5.37}$$

$$\begin{aligned} c_4^{**} = \frac{\lambda}{\alpha}\Big(\frac{\lambda e^{\lambda\delta_f}}{\alpha}\Big)^3 \Big[e^{\alpha T}\Big(\frac{1}{6}(\alpha T)^3 - \frac{1}{2}(2\alpha\delta_f + e^{\alpha\delta_f})(\alpha T)^2 \\ + (\frac{3}{2}(\alpha\delta_f)^2 + \alpha\delta_f e^{\alpha\delta_f} + e^{2\alpha\delta})\alpha T - e^{3\alpha\delta_f}\Big) + e^{3\alpha\delta_f}\Big], \end{aligned} \tag{5.38}$$

where $\alpha = s - r - \lambda$. The normalized maintenance cost of exactly k failures, c_k^*, and the normalized maintenance cost of k-th failure, c_k^{**} are defined as

$$c_k^* = \frac{\bar{c}_k}{c_0 + c_{f_0}} \ , \ c_k^{**} = \frac{\bar{\bar{c}}_k}{c_0 + c_{f_0}}. \tag{5.39}$$

Furthermore, the normalized expected maintenance costs C_M^* and C_M^{**} are defined as

$$C_M^* = \frac{\bar{C}_M}{c_0 + c_{f_0}} \ , \ C_M^{**} = \frac{\bar{\bar{C}}_M}{c_0 + c_{f_0}}. \tag{5.40}$$

To assess the contribution of each number of failures in the maintenance cost, the first four terms of c_k^{**} are plotted in Fig. 5.4 for

$$\delta_f = 0,\ r = 0.03,\ s = 0.01,\ \lambda = 0.051. \tag{5.41}$$

This value of λ corresponds to reliability of 95% after one year. It is observed that $c_1^{**} = 0.3668$, $c_2^{**} = 0.0830$, $c_3^{**} = 0.0133$, and $c_4^{**} = 0.0016$ after $T = 1$ year. This implies that if Eqn. (5.14) is truncated to the first four terms, the contribution of the first failure in the maintenance cost is 78.9%. The contribution falls to 17.9%, 2.9%, and 0.3% for the second, third, and fourth failures, respectively. Evidently, the contribution of higher numbers of failures to the maintenance cost decreases rapidly. To study the validity of this conclusion, setting $\delta_f = 0$ in the limits of the integrals of Eqn. (5.13) yields

$$c_k^{**} = (\frac{\lambda}{\alpha})^k \Big[e^{\alpha T} \sum_{j=1}^{k} (-1)^{k-j} \frac{(\alpha T)^{j-1}}{(j-1)!} + (-1)^k \Big], \tag{5.42}$$

substitution of which into Eqn. (5.14) results in

$$C_M^{**} = \frac{\lambda}{s-r} \Big(e^{(s-r)T} - 1 \Big). \tag{5.43}$$

or equivalently

$$C_M^{**} = \frac{\lambda}{s-r} \Big[(\frac{1}{R(T)})^{\frac{s-r}{\lambda}} - 1 \Big]. \tag{5.44}$$

For the parameters given in Eqn. (5.41), Fig. 5.5 shows the error of truncating Eqn. (5.14) to three terms. The error is calculated with respect to the solution Eqn. (5.43). It is concluded that the cost associated with having four or more failures contribute less than 0.4% to the maintenance cost.

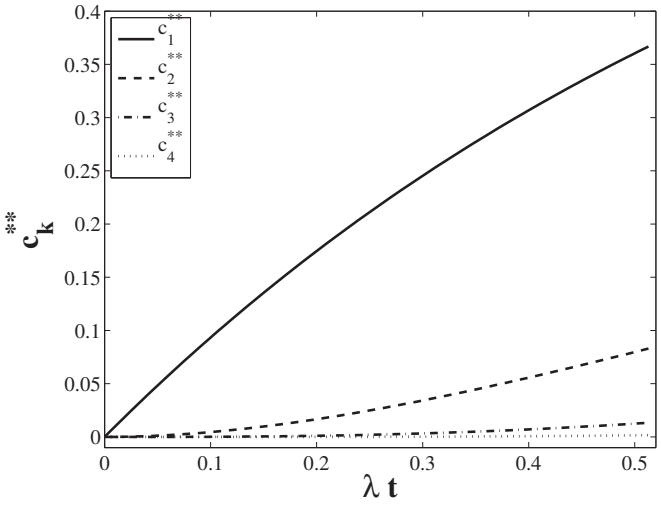

Figure 5.4 Normalized cost of k-th maintenance versus λt; $0 \leq t \leq T$

Sensitivity to the inflation rate and the downtime

In Eqn. (5.35)–(5.38) the parameters s and r do not appear separately, but as $s-r$. Since s is the increase rate of the prices and r is the discount rate, the term $s-r$ may be interpreted as the inflation rate. To study the sensitivity of the maintenance cost to the inflation rate, the solution Eqn. (5.43) is plotted in Fig. 5.6 for $\lambda = 0.051$ and different values of the inflation rate. For the special case of $s-r \to 0$, Eqn. (5.43) is further simplified to

$$C_M^{**} = \lambda T, \tag{5.45}$$

which means that the time rate of the maintenance cost is equal to the failure rate λ, as observed Fig. 5.6. Note that Eqn. (5.33) and Eqn. (5.34) imply that $c_f(t)e(t) = (c_0 + c_{f_0})\exp\big((s-r)t\big)$. As a result, the net present value of the cost of a maintenance in a positive inflation rate scenario is higher than that of a no inflation rate one. That is why the positive inflation rate curves lie above that of $s-r = 0$ 1/year. The same argument justifies the negative inflation rate behaviors. This figure shows the high sensitivity of the solution to the inflation rate, as for an inflation rate

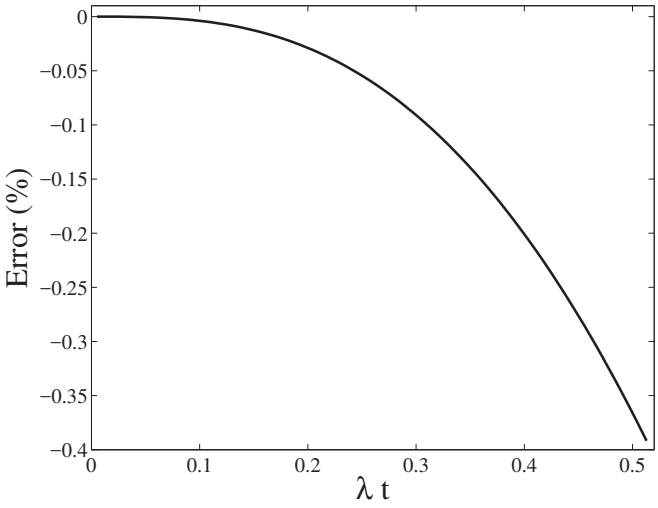

Figure 5.5 Error of truncating Eqn. (5.14) to the first three terms versus λt; $0 \leq t \leq T$

of 5% at $\lambda t = 0.513$, the maintenance cost is 33% higher than that of the case of a zero inflation rate.

Figures 5.4 to 5.6 are plotted for $\delta_f = 0$. Although in many practical cases the downtime is much smaller than T, it is important to study the sensitivity of the model to δ_f. For an element with $\lambda = 0.051$, Fig. 5.7 illustrates that the deviation of Eqn. (5.43) from Eqn. (5.14) for different values of δ_f/T and $s-r$ is less that 1% for most of the range. Assuming a zero downtime leads to no significant error. Hence, in the rest of model derivation the zero downtime assumption is used.

Effect of the reliability function

For an exponential reliability function, the analytic solution to Eqn. (5.9) is expressed in Eqn. (5.35)-(5.38). However, in general it is not possible to provide analytic solutions to Eqn. (5.9). Instead, it may be calculated numerically.

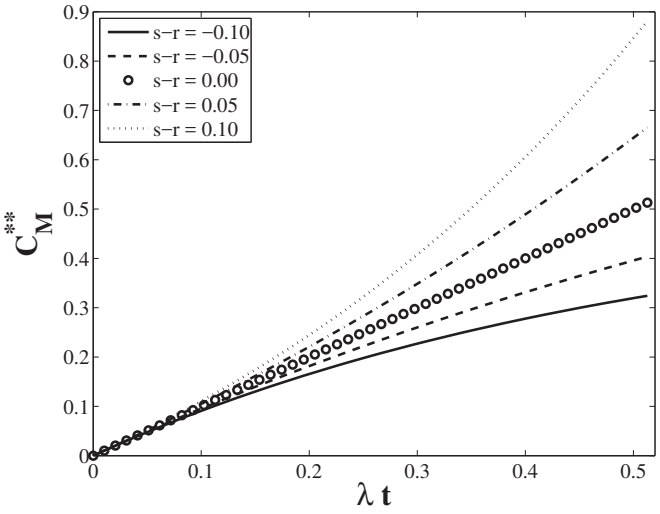

Figure 5.6 Normalized maintenance cost versus the inflation rate

The reliability of many mechanical systems is modeled by the Weibull distribution [86]

$$R(t) = e^{-(\lambda t)^{\gamma}}\ ,\ 0 \leq t \leq T. \tag{5.46}$$

In the first step the convergence of the PFM strategy is studied for the Weibull distributions. Table 5.1 collects the contribution of the first four failures on the LCC of different Weibull distributions. In calculating the LCC, Eqn. (5.14) is truncated to the first four terms. The results are provided for $T = 10$ years, $R(T) = 0.60$, $s - r = -0.02$ 1/year, and $c_0 = 3500$ CAD. In this example, three different orders of magnitudes are chosen for the value of c_{f_0} to assess the influence of this parameter on the convergence of different Weibull distributions. For each value of c_{f_0}, it is observed that by decreasing γ, the contribution of the first failure decreases, whereas the contribution of higher number of failures increase. For $1 \leq \gamma$ and the range of c_{f_0} considered here, the contribution of the fourth failure is at most 1% of the LCC. The maximum value of $\bar{c}_4/\bar{c}_T$ is 2.6% for $\gamma = 0.5$ and $c_{f_0} = 30000$ CAD. According to the trends, it is expected that the contribution of a higher number of failures is bounded to 1%– for the PFM strategy, only four failures are considered in calculating the LCC.

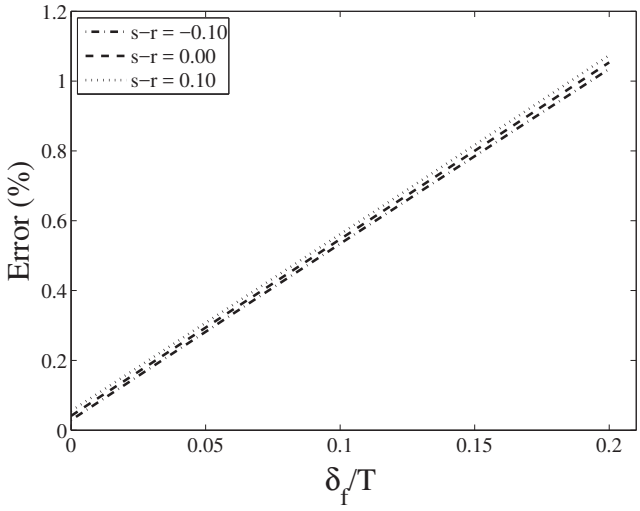

Figure 5.7 Deviation of Eqn. (5.43) from Eqn. (5.14) versus δ_f/T and the inflation rate

Next, the influence of γ on the maintenance cost of Weibull reliabilities is assessed. Fig. 5.8 illustrates the normalized maintenance cost versus dimensionless time for different values of γ. In this example λ=0.051 and $s = r$. Equation (5.45) states that for $\gamma = 1$, the normalized maintenance cost is linearly scaled with time, which agrees with Fig. 5.8. Furthermore, for $\gamma > 1$ the maintenance cost is a concave function which falls below the $\gamma = 1$ curve, whereas the $\gamma < 1$ curves are convex, lying above the $\gamma = 1$ curve. The reason is that for $\gamma < 1$, the reliability function initially decreases faster than the exponential function, which means that its FPDF is higher than that of an exponential function for the most of the operation period. The lower maintenance cost for $\gamma > 1$ is because the FDPF of such reliability function is lower than that of an exponential distribution. Fig. 5.9 shows the same data where the horizontal axis is the reliability. This behavior is of utmost importance in selecting a preventive maintenance strategy as will be discussed in Section 5.2.2 and 5.2.3.

Figures 5.8 and 5.9 are plotted for Weibull distributions in a zero inflation rate scenario. For three Weibull distributions, the influence of the inflation rate on the maintenance cost is illustrated in Fig. 5.10. The curves are for the maintenance cost after 10 years of operation with

Table 5.1 Convergence study of the PFM strategy

c_{f_0} (CAD)	γ	$\frac{\bar{\bar{c}}_1}{\bar{c}_T}$ (%)	$\frac{\bar{\bar{c}}_2}{\bar{c}_T}$ (%)	$\frac{\bar{\bar{c}}_3}{\bar{c}_T}$ (%)	$\frac{\bar{\bar{c}}_4}{\bar{c}_T}$ (%)
300	1.5	22.7	7.3	0.9	0.1
	1.0	20.2	10.1	2.5	0.4
	0.5	17.3	10.3	3.8	1.0
3000	1.5	31.8	10.3	1.2	0.1
	1.0	27.9	14.0	3.4	0.6
	0.5	24.1	14.4	5.2	1.5
30000	1.5	58.5	18.9	2.3	0.2
	1.0	49.5	24.8	6.1	1.0
	0.5	43.1	25.8	9.4	2.6

$R(10) = 0.60$. For each Weibull function, the normalized maintenance cost is monotonically increasing with the inflation rate; the higher the inflation rate, the more expensive a maintenance in future will be. It is observed that the curvature increases with γ. It should be noted that the curve of each of the Weibull distribution lies above the other curves in some range of the inflation rate. The results emphasize the high sensitivity of the maintenance cost to the inflation rate, which indicates the importance of incorporating this parameter in the maintenance model.

Comparison of the two developed PFM model

For three Weibull distributions whose parameters are given in Table 5.2, the normalized maintenance cost after one year of operation is calculated using Eqn. (5.10) and Eqn. (5.14). In this example, each set of Weibull parameters result in $R = 0.80$ after one year of operation. The continuous annual inflation rate is 0.03. The deviation of $\bar{\bar{C}}_M$ from $\bar{C}_M$ is reported in the

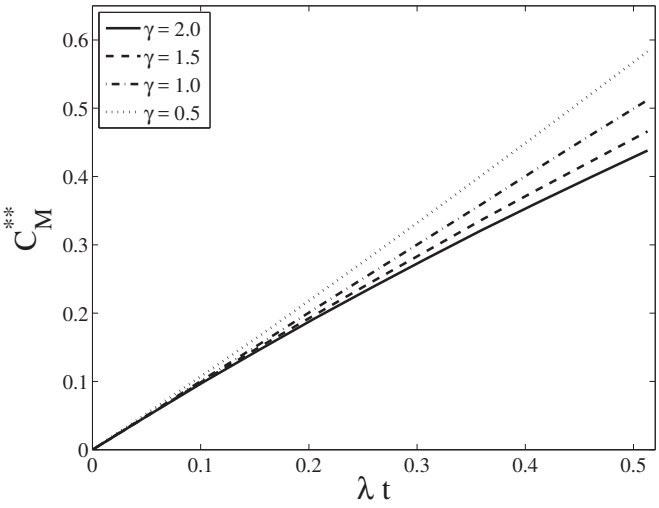

Figure 5.8 Normalized maintenance cost versus normalized time for Weibull distributions

table. The third column corresponds to the case where only the first term of the summation is considered in Eqn. (5.10) and Eqn. (5.14), the fourth column reports the deviation of the models when they are truncated after the second term, and so on. It is observed that as γ decreases, higher number of terms should be considered to assure the convergence of the two models. Regardless, in the range of γ studied here, truncating after the fourth term results in less than 1% deviation between the two models.

Table 5.2 Deviation (%) of $\bar{\bar{C}}_M$ from $\bar{C}_M$ for different Weibull distributions

γ	λ	One term	Two terms	Three terms	Four terms
1.50	0.368	7.0	0.4	0.0	0.0
1.00	0.223	12.0	1.5	0.2	0.1
0.67	0.107	16.5	3.4	1.1	0.8

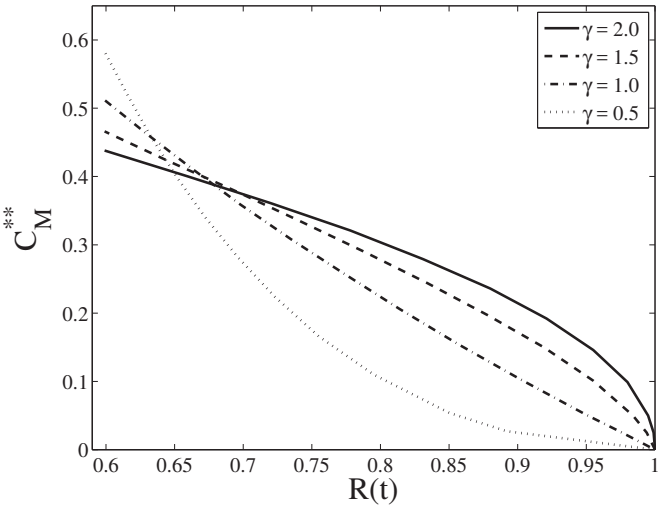

Figure 5.9 Normalized maintenance cost versus reliability for Weibull distributions

Comparison of the present PFM model and the previous models

The PFM model presented in Blischke and Murthy [42] and in Jardine and Tsang [43] is

$$\bar{C}_M = (c_0 + c_{f_0})H(T), \tag{5.47}$$

which gives the expected maintenance cost as the product of the expenses $c_0 + c_{f_0}$ times the expected number of failures $H(T)$ during a cycle $[0,T]$. This solution is valid because it is assumed that $c_0 + c_{f_0}$ is time-independent, as in a zero inflation rate scenario.

Comparing Eqn. (5.40) with Eqn. (5.47) implies that $H(t)$ is equivalent to the concept of the normalized maintenance cost in the present context. After some mathematical manipulation, the Laplace transform of H is derived as [42, 43]

$$L\{H\}(x) = \frac{L\{p\}(x)}{x\Big(1 - L\{p\}(x)\Big)}. \tag{5.48}$$

where $L\{p\}(x)$ denotes the Laplace transform of the FPDF of one failure $p(t)$. If $R(t)$ is known, Eqn. (5.3) may be used to calculate $p(t)$. The Laplace transform of $p(t)$ is substituted in

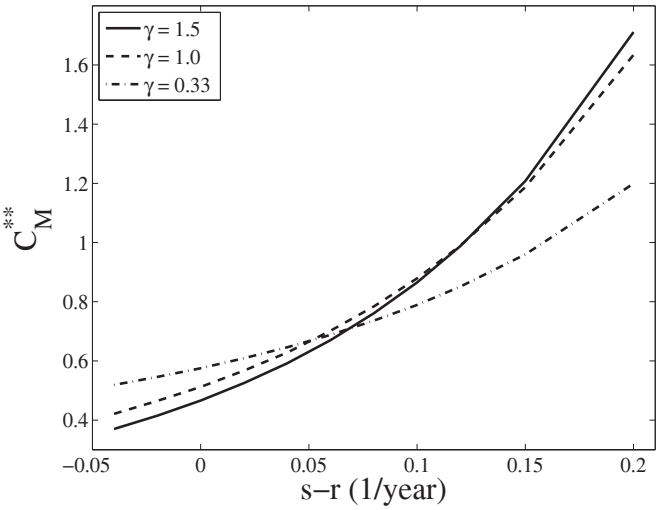

Figure 5.10 Normalized maintenance cost versus inflation rate for Weibull distributions

Eqn. (5.48) to calculate the Laplace transform of $H(t)$. Then, the inverse Laplace transform is taken to obtain $H(t)$.

For an exponential reliability function, $R(t) = \exp(\lambda t)$, Jardine and Tsang [43] provide an analytic solution as $H(t) = \lambda t$. This is in agreement with the result of the present model in Eqn. (5.45). The analytic solution of Eqn. (5.48) may, however, be derived for a limited number of functions. In Jardine and Tsang [43] a numerical method is proposed for solving this equation in general. Here, this method is applied to two Weibull distributions with parameters $\{\gamma = 1.5,\ \lambda = 0.639\}$, and $\{\gamma = 0.67,\ \lambda = 0.367\}$ to calculate $H(t)$. For both distributions, the reliability is 0.60 after one year of operation. As depicted in Fig. 5.11, the present model is validated by its good agreement with Blischke and Murthy [42] and Jardine and Tsang [43]. Since Eqn. (5.48) is a zero inflation rate scenario, the present model may be consider as an extension to the non-zero inflation rate cases.

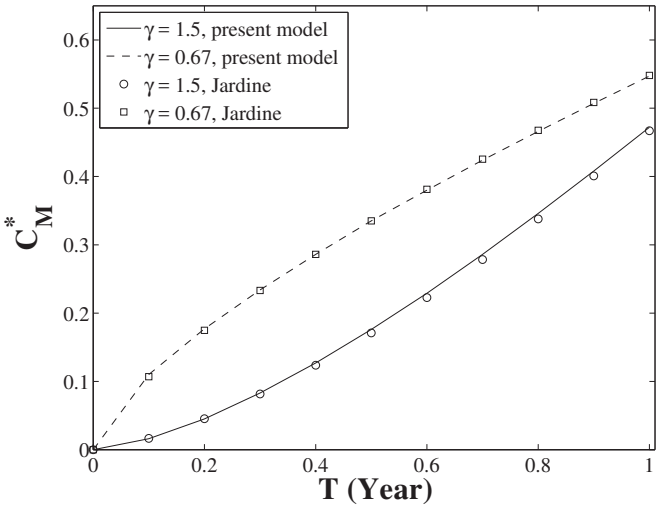

Figure 5.11 The present PFM model versus PFM model of Jardine and Tsang [43]

Case study: Gears- LCC at the PFM strategy

The acquisition cost-reliability (CR) model of gears from Chapter 2 and the maintenance cost model developed here are used to calculate the life-cycle cost of gears. In this example, the goal is to select a gear that would operate 8 hours a day, 250 days a year with 100 rpm undergoing a $\tau = 133$ Nm torque. The reliability under bending and wear shall be at least 0.975 after one year. The safety factor for bending and wear are 2.0 and 4.0, respectively. The gear NJ120B made of ASTM class 30 cast iron manufactured by the OEM1 [74] meets the reliability requirements $\big($see the second column of Table 5.3$\big)$. At this point, it is possible to ask *if the reliability constraint is relaxed, is there another solution that minimizes the LCC of the gear*? To find the answer, the NJ120B gear is considered to be the baseline design. Next, its width is scaled with a factor γ_2– not to be mistaken with the Weibull parameter γ– to get a group of gears with similar pitch diameter but different widths. This example assumes that γ_2 can not exceed 1.20 due to space limitations. The results are collected in Table 5.3. The first column of the table indicates the scaling factor γ_2. For each scaling factor, the reliability of the corresponding gear after one year is calculated using AGMA equations [4] and reported in the second column. The acquisition cost

of the scaled gears are presented in the third column, calculated using Eqn. (3.17) and the catalog prices obtained from the OEM1 [74]. Here, the continuous annual inflation rate is $s - r = 0.03$ 1/year. The LCC is reported in the last three columns for three different orders of magnitude of c_{f_0}. The lowest value of the maintenance cost for each value of c_{f_0} is emboldened in the corresponding column. In no cases, does the baseline gear (with $\gamma_2 = 1.00$) minimize the LCC. As c_{f_0} increases, a gear with a higher scaling factor shall minimize the LCC because as the cost of a failure increases, it is more cost effective to improve the reliability by investing on the size of the gear than to have failures in the future. As the last point on this example, although a specific γ_2 minimizes the LCC of the gear, the LCC may be a flat function in a range of γ_2. As an example, for $c_{f_0} = 500$ CAD, in the range of $0.90 \leq \gamma_2 \leq 1.05$ the LCC is affected by less than 3% compared to the best solution $\gamma_2 = 0.95$.

Table 5.3 LCC of cast iron spur gears after one year

γ_2	$R(T)$	c_0 (CAD)	LCC (CAD)		
			c_{f_0}=500	c_{f_0}=5000	c_{f_0}=50000
0.80	0.807	411.02	620.55	1655.55	12005.55
0.85	0.890	428.16	541.40	1090.40	6580.40
0.90	0.939	445.31	506.94	800.34	3734.34
0.95	0.964	462.46	**498.65**	667.85	2359.85
1.00	0.978	479.60	501.45	601.80	1605.30
1.05	0.985	496.75	511.80	579.75	1259.25
1.10	0.989	513.89	524.84	**573.44**	1059.44
1.15	0.992	531.04	539.29	575.29	935.29
1.20	0.994	548.18	554.49	581.58	**852.48**

Case study: Bearings- LCC at the PFM strategy

Now consider this scenario. The baseline gear of the previous example is mounted on a shaft between two NU22xx cylindrical rolling bearings of the OEM. Using the torque of the previous example, 133 Nm, the force acting on each bearing is 270.4 kN (the weight of the gear and the shaft is neglected). The minimum desired reliability of each bearing is 0.98 after one year of operation, 250 days a year, 8 hours a day at 100 rpm (12 million revolutions per year). As understood from the second column of Table 5.4, the bearing NU2230 meets the reliability requirement. The designer may select this bearing as the baseline design. At this point, it is possible to ask *how the LCC of the bearing would be affected if the reliability constraint is relaxed and another bearing is selected*? The answer can be found in Table 5.4, where the calculation is repeated for three other bearings of the same type. The first column is the catalog number of the bearing. The reliability of each bearing after one year is calculated using the bearing life equation [6] and is presented in the second column. The price list of the OEM2 is used to obtain the acquisition cost c_0 [78], with the conversion rate of 1.40 Euro/CAD. These prices are listed in the third column. For three different values of c_{f_0}, the LCC is presented in the last three columns of the table. The results suggest that for $c_{f_0} = 300$ CAD and $c_{f_0} = 3000$ CAD, switching from the baseline design to the smaller bearing NU2228 reduces the LCC. For the case of $c_{f_0} = 30000$ CAD, selecting the baseline bearing over the smallest bearing is an investment on the acquisition cost that leads to enough savings on the maintenance cost such that the LCC is reduced.

5.2.2 Preventive maintenance strategy– Block policy

In this strategy, n preventive maintenances are conducted at jt_p , $j = 1, \ldots, n$, where the length of the block is $t_p = T/(n+1)$. The goal is finding n such that the LCC is minimized. In this

Table 5.4 LCC analysis of NU22xx bearings after one year

Cat. no.	$R(T)$	c_0 (CAD)	LCC (CAD)		
			c_{f_0}=300	c_{f_0}=3000	c_{f_0}=30000
NU2228	0.957	3514.00	**3680.29**	**3798.01**	4975.21
NU2230	0.982	4074.00	4154.92	4204.87	**4704.37**
NU2232	0.995	5507.60	5539.31	5554.05	5701.47
NU2234	0.999	6022.80	6031.08	6034.62	6069.99

section, the model developed in Section 5.1.2 is applied on a gear and a bearing to find the best PrM1 schedule.

For the NJ120B gear with the scaling factor $\gamma_2 = 1.20$ (see Table 5.3) undergoing the condition of Table 5.5, for different values of n the LCC is collected in Table 5.6. for $T = 10$ years is studied as an example. The torque on the gear is $\tau = 133$ Nm for 12 million cycles each year. The continuous annual inflation rate is 0.02. Similar to Eqn. (5.34), the cost of a preventive maintenance $c_p(t)$ has the form

Table 5.5 Working condition of the NJ120B gear

T (Y)	τ (Nm)	Cycles (rev./Y)	$s-r$ (1/Y)
10	133	12×10^6	0.02

$$c_p(t) = (c_0 + c_{p_0})e^{st}, \tag{5.49}$$

where c_{p_0} lumps all expenses associated with a preventive maintenance, including the labor cost, loss of productivity, etc. In this case, it is assumed that $c_{f_0} = 50000$ CAD and $c_{p_0} = 5000$ CAD,

which means the cost of a failure is much higher than that of a preventive maintenance. The results are presented in Table 5.6. As expected, the preventive maintenance cost, $\bar{C}_P$, increases with n. Therefore, to end up with a convex maintenance cost or LCC, the necessary condition is that the failure maintenance cost, $\bar{C}_F$, decreases with n. To determine when this condition will be met, it is useful to study the FPDF of Eqn. (5.46) for one failure

$$p(t) = \gamma\lambda^{\gamma}t^{\gamma-1}\exp\big(-(\lambda t)^{\gamma}\big). \tag{5.50}$$

When $\gamma \leq 1$, e.g. for gears, p is monotonically decreasing with t. Furthermore, the term $t^{\gamma-1}$ tends to infinity as $t \to 0$. This implies that, after a preventive maintenance, a high failure maintenance cost shall be expected. If no preventive maintenance is conducted, the FPDF of the original element keeps decreasing. In other words, for any element with $\gamma < 1$, the preventive maintenance shall be avoided as it increases the LCC. As seen in Table 5.6, for the NJ120B gear $\bar{C}_F$ increases by n, and the LCC is minimum at $n = 0$.

Table 5.6 LCC of NJ120B gear with γ_2=1.20 after ten years

n	$\bar{C}_P$ (CAD)	$\bar{C}_F$ (CAD)	$\bar{C}_M$ (CAD)	C_T (CAD)
0	0.00	494.36	494.36	**1042.54**
1	6131.68	889.61	7021.29	7569.47
2	12270.18	1243.52	13513.70	14061.88
3	18410.39	1571.62	19982.01	20530.19
4	24551.28	1886.69	26437.97	26986.15
5	30692.50	2185.79	32878.29	33426.47
6	36833.92	2475.12	39309.04	39857.22
7	42975.46	2758.63	45734.09	46282.27
8	49117.09	3033.07	52150.16	52698.34
9	55258.77	3301.82	58560.59	59108.77
10	61400.48	3568.23	64968.71	65516.89

For elements with $\gamma \geq 1$, the term $t^{\gamma-1}$ assures that $p(0) = 0$. As t increases, p increases to reach a maximum, after which decreases monotonically. Since p increases at the start of the operation, investing on a preventive maintenance which brings the FPDF to zero may be helpful in saving on the failure maintenance cost. That possibility depends on the value of γ, λ, the cost of a failure, and the cost of a preventive maintenance. As there is no analytic solution for the PrM strategies of the Weibull distributions in general, it is not feasible to establish a relation to determine the behavior of $\bar{C}_F$ in terms of the above parameters and, therefore, the problem must be solved numerically.

The life-cycle cost of the bearing NU2230-M1 versus the number of preventive maintenances is presented in Table 5.8 for the working condition of Table 5.7. Similar to the NJ120B gear, $\bar{C}_P$ is monotonically increasing with n. On the other hand, $\bar{C}_F$ decreases with n. The reason is that for bearings $\gamma \geq 1$, which imply that the FPDF is initially small, but increases as time passes. Hence, conducting a preventive maintenance prevents going to high FPDF regions and reduces the failure cost compared to the case where no preventive maintenance is conducted. Having a $\bar{C}_F$ that decreases with n is the necessary condition for the possibility of reducing LCC using a preventive maintenance strategy. In this example, it is observed that the LCC is minimized for $n = 2$.

Table 5.7 Working condition of the NU2230-M1 bearing

T (Y)	Load (kN)	Cycles (rev./Y)	$s-r$ (1/Y)	c_0 (CAD)	c_{f_0} (CAD)	c_{p_0} (*CAD*)
10	270.4	12×10^6	0.02	4074	30000	3000

The PrM1 LCC of the NU2230 bearing, as well as that of NU2228, NU2232, and NU2234 are presented in Table 5.9. The values of the inflation rate, c_{p_0}, and c_{f_0} are similar to the example of Table 5.8. The acquisition cost of NU2228, NU2232 and NU2234 are 3514.00 CAD,

5507.60 CAD, and 6022.80 CAD, respectively [78]. For any of the bearings, the best LCC is shown in bold letters in the table. Compare to the PFM strategy, selecting the best PrM1 strategy provides up to 22.1% of savings in case of the NU2230 bearing. The results suggest that, if the space limitations allows the use of any of the four bearings, selecting NU2234 along with the PrM1 strategy where $n = 1$ provides the lowest LCC for the bearing.

Table 5.8 LCC of NU2230-M1 bearing – ten years, PrM1

n	$\bar{C}_P$ (CAD)	$\bar{C}_F$ (CAD)	$\bar{C}_M$ (CAD)	C_T (CAD)
0	0.00	48691.75	48691.75	52765.75
1	7817.98	34036.64	41854.62	45928.62
2	15644.65	23483.90	39128.55	**43202.55**
3	23473.48	17759.92	41233.40	45307.40
4	31303.20	14170.98	45474.18	49548.18
5	39133.34	11733.96	50867.30	54941.30
6	46963.74	9984.67	56948.41	61022.41
7	54794.29	8671.99	63466.28	67540.28
8	62624.94	7654.54	70279.48	74353.48
9	70455.66	6841.51	77297.17	81371.17

5.2.3 Preventive maintenance strategy– Age policy

Convergence of the model

For an element with the parameters listed in Table 5.12, the maintenance cost of the first three failures versus the normalized time are plotted in Fig. 5.12 for $0 < t < T$. For these parameters, $R(T) = 0.60$. If Eqn. (5.31) is truncated to three failures, the contribution of the first three failures on the LCC is 52.8%, 13.8%, and 1.9%, respectively. These results, as well as that of

Table 5.9 LCC of NU22xx-M1 bearings – ten years, PrM1

n	NU2228	NU2230	NU2232	NU2234
0	63805.69	52765.75	37478.64	27697.72
1	58187.99	45928.62	**31676.28**	**24048.12**
2	**55688.43**	**43202.55**	34555.13	30063.51
3	56389.36	45307.40	40809.82	38459.62
4	59066.23	49548.18	48436.61	47647.91
5	62951.26	54941.30	56725.58	57176.93
6	67629.94	61022.41	65376.68	66873.82
7	72843.89	67540.28	74244.74	76665.21
8	78441.32	74353.48	83251.92	86514.16
9	84314.93	81371.17	92350.86	96401.38

Weibull distributions with $\gamma = 1.0$ and $\gamma = 0.5$ are presented in Table 5.11. The values of T, $R(T)$, c_0, c_{f_0}, and c_{p_0} for the latter two Weibull distributions are the same as that of $\gamma = 1.5$. Similar to the PFM strategy (see Table 5.1), the results show that as γ decreases, the contribution of the first failure decreases whereas the weight of higher number of failures increases. The trend for $\gamma = 1.5$ suggests that the weight of the maintenance cost of four or more failures is less than 1% of the LCC. However, this share is higher as γ decreases, particularly when less than unity. This means that for $\gamma \leq 1$, the error of considering up to three failures in Eqn. (5.31) is greater than 1%. To avoid such an error, higher number of failures should be included in the calculations. However, as pointed out in the previous section, a preventive maintenance decreases the LCC only if $\gamma > 1$. For this range of γ, it is observed that the error of considering up to three failures is bounded to 1%. Hence, in the following examples up to three failures are included in the calculations.

Table 5.10 PrM2 parameters of the element

T (Y)	γ (-)	λ (1/Y)	$s-r$ (1/Y)	c_0 (CAD)	c_{f_0} (CAD)	c_{p_0} (CAD)
10	1.5	0.0639	0.02	3500	30000	3000

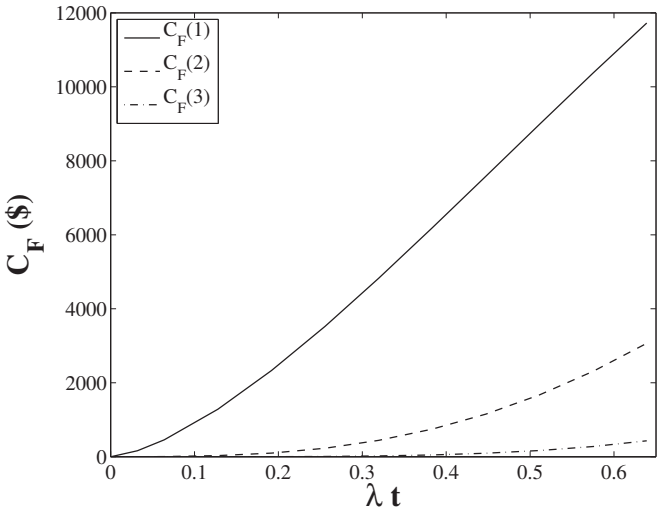

Figure 5.12 First three failure costs of PrM2, $\gamma = 1.5, \lambda = 0.0639$

Comparison of the present PrM2 model and the previous models

The results of the PrM2 model in Blischke and Jardine [42, 43] and the present PrM2 model are compared. The model in Blischke and Jardine [42, 43] gives the expected replacement cost of a cycle per expected cycle length as

$$C(t_p) = \frac{c_p R(t_p) + c_f\big(1 - R(t_p)\big)}{t_p R(t_p) + \int_0^{t_p} t\,p(t)dt} = \frac{\bar{C}_M}{\bar{t}_p}. \tag{5.51}$$

Next, Blischke and Jardine [42, 43] argue that $c_p R(t_p)$ is the expected preventive maintenance cost of a cycle, whereas $c_f\big(1 - R(t_p)\big)$ gives the expected failure cost. Hence, the numerator is the total expected replacement cost of a cycle $\bar{C}_M$. Also, $t_p R(t_p)$ is the expected duration of having

Table 5.11 Convergence study of the PrM2 strategy

γ	$\frac{\bar{C}_P}{\bar{C}_T}(\%)$	$\frac{\bar{C}_{F_1}}{\bar{C}_T}(\%)$	$\frac{\bar{C}_{F_2}}{\bar{C}_T}(\%)$	$\frac{\bar{C}_{F_3}}{\bar{C}_T}(\%)$
1.5	15.7	52.8	13.8	1.9
1.0	14.6	46.3	21.5	5.6
0.5	10.2	38.4	28.1	13.1

no failures, and $\int_0^{t_p} t\,p(t)dt$ gives the expected life of an element. Therefore, the denominator is the expected cycle length $\bar{t}_p$. Consequently, Eqn. (5.51) calculates the expected replacement cost of a cycle per expected cycle length. In Jardine and Tsang [43] this model is used to determine t_p such that $C(t_p)$ on the left-hand side of Eqn. (5.51) is optimum.

Before comparing the results of Eqn. (5.51) and the present model, it is important to raise three points. First, in developing the model, Jardine and Tsang [43] favored the simplicity of the model: the time value of money is not considered and c_p and c_f are assumed time-independent. These assumptions are justified if either the life cycle of the project or the inflation rates are small enough.

Secondly, $1-R(t_p)$ is the probability of having only one failure. It implies that $c_f\big(1-R(t_p)\big)$ ignores the contribution of higher number of failures to the maintenance cost. This assumption may be justified if $R(t_p)$ is close to unity. In any case, the numerator of Eqn. (5.51) provides a lower bound for the expected replacement cost of a cycle. As $R(t_p)$ decreases, its deviation from the correct answer is expected to increase.

Thirdly, if the expected cycle length (denominator) is a divisor of T, Eqn. (5.51) multiplied by T gives the total expected life-cycle maintenance cost. It is important to note that, in general, the expected cycle length is not a divisor of T. As an example, consider a case where $T = 3.7\bar{t}_p$. In this case, the replacement cost during $0.7\bar{t}_p$ is not necessarily equal to $0.7\bar{C}_M$.

In such situation, minimizing the life-cycle replacement cost is not equivalent to minimizing Eqn. (5.51). To resolve this problem, instead of minimizing $\bar{C}_M/\bar{t}_p$ as is the case in Eqn. (5.51), it is best to minimize the maintenance cost over the life cycle, as is the basic idea of the models here.

In comparing the PrM2 model presented in Blischke and Jardine [42, 43] and the present model, in the first step their result is calculated for $t_p = T$. In this scenario, the result of the PrM2 models should converge to the PFM model because no preventive maintenance will be conducted. For the roller bearings and the conditions given in Table 5.12, the results of the analysis are collected in Table 5.13. The bearings are manufacutred by an OEM [77]. The deviation of the previous PrM2 models from the PFM model is 31.0%, 66.1%, and 78.5% for NU322, NU324, and NU326, respectively. Although the PrM2 model presented in Jardine and Tsang [43] follows the same LCC reduction trend with R, it considerably overestimates the LCC. The present model, on the other hand, is in good agreement with the PFM model, having a maximum deviation of 0.3% in NU322. This deviation is caused by the truncation of the PFM and the PrM2 models $\big($see Eqn. (5.10) and Eqn. (5.31)$\big)$. The results of this table indicate that, because of its simplicity, Eqn. (5.51) may lead to considerable errors due to the three aforementioned points.

Table 5.12 PrM2 parameters for NU3xx bearing

Cat. no.	T (Y)	Load (kN)	Cycles (rev./Y)	$s-r$ (1/Y)	c_0 (CAD)	c_{f_0} (CAD)	c_{p_0} (*CAD*)
NU322	1	270.4	12×10^6	0.00	1478.40	30000	3000
NU324	1	270.4	12×10^6	0.00	1902.60	30000	3000
NU326	1	270.4	12×10^6	0.00	2319.80	30000	3000

Table 5.13 Comparison of the PFM and PrM2 models for bearings with $t_p = T$

Cat. no.	Reliability	PFM (CAD)	PrM2 (CAD) [42, 43]	PrM2 (CAD), present
NU322	0.793	8327.88	10913.32	8349.41
NU324	0.928	4227.09	7023.27	4229.48
NU326	0.959	3649.53	6514.88	3650.22

The results of Table 5.13 are for the case of no preventive maintenance. For NU324 undergoing the condition of Table 5.12, the result of different PrM2 models are given in Table 5.14 for different values of n. The deviation of the PrM2 model of Blischke and Jardine [42, 43] from the present model are presented in this table. As n increases, the difference between the two models decreases. Since for large n's the reliability $R(t_p)$ tends to unity, it is expected that the failure maintenance costs, $\bar{C}_{F_k}$'s, are negligible. In such situations, the LCC is mostly composed of the acquisition cost and the preventive maintenance costs, which implies the LCC may be estimated by

$$\bar{C}_T \cong c_0 + n(c_0 + c_p). \tag{5.52}$$

The result of Eqn. (5.52) is equal to $41,123.40$ CAD for $n = 8$, and $46,026.00$ CAD for $n = 9$, which are nearly 1% less than the prediction of the present PrM2 model. This may be a result of excluding $\bar{C}_{F_k}$'s from Eqn. (5.52). On the other hand, the difference of the PrM2 model of Blischke and Jardine [42, 43] is 8.3% and 7.4% for $n = 8$ and $n = 9$, respectively.

The results of Tables 5.13 and 5.14 indicate that for $n = 0$ and for large n's, the present model is much more accurate and coherent than the PrM2 model in Blischke and Jardine [42, 43]. Therefore, in the rest of the model formulation, Eqn. (5.32) will be used in the LCC analysis process.

Table 5.14 LCC of NU324 bearings, different PrM2 models – one year

n	PrM2 (CAD), Jardine	PrM2 (CAD), present	Deviation (%)
1	11083.29	8216.53	34.9
2	15655.99	12756.61	22.7
3	20377.23	17459.51	16.7
4	25163.31	22233.73	13.2
5	29983.94	27046.02	10.9
6	34825.33	31881.22	9.2
7	39680.26	36731.36	8.0
8	44544.54	41591.82	7.1
9	49415.57	46459.75	6.4

The advantage of the Age policy over the Block policy

For the NU2228 and NU2230 bearings of the OEM2 undergoing 270.4 kN for 12 million revolutions per year, the present PrM2 model is used to calculate the LCC after ten years. The saving of the PrM2 over PrM1 is also provided for different values of n. The results are also shown in Fig. 5.13. As n increases, $R(t_p)$ gets closer to unity and the failure probability decreases. Consequently, it is expected that most of the bearings face no failure and operate up to t_p. This implies that as n increases, the LCC of the PrM2 shall approach that of the PrM1. This behavior is observed in Table 5.15 and Fig. 5.13, and is another way of validating the present PrM2 model. For NU2230, this convergence happens at a smaller n because under the same load, the larger bearing has a higher reliability and a lower failure probability.

As a final point, note that for the NU2228 bearing, by switching from n=2 to n=3, the LCC increases 2.4%. Such locally *flat* LCC curves provide a flexibility in selecting n without a considerable increase in the LCC. Such flexibility would be important in large systems where

some savings may be achieved when the preventive maintenance of many elements of the system is conducted at the same time to avoid repetitive system downtimes.

Table 5.15 LCC of NU22xx-M1 bearings – ten years, PrM2

n	NU2228 PrM2	Saving over PrM1 (%)	NU2230 PrM2	Saving over PrM1 (%)
1	55646.06	4.6	44734.82	2.7
2	**53413.46**	4.3	**42677.58**	1.2
3	54688.54	3.1	44975.35	0.7
4	57782.30	2.2	49334.03	0.4
5	61961.62	1.6	54803.85	0.3
6	66842.88	1.2	60933.30	0.1
7	72204.51	1.0	67483.67	0.1
8	77909.52	0.7	74317.94	0.0
9	83868.65	0.5	81352.27	0.0

5.2.4 System-level life-cycle cost of a one-speed gearbox

The goal of this case study is to explore the design space of a conceptual/hypothetical one-speed gearbox. The goal is to improve the reliability and reduce the LCC of the gearbox. The maintenance cost models developed in this chapter as well as the CPR models of the previous chapters are used to this end.

Consider a one-speed gearbox composed of two spur gears, each on a shaft supported by two bearings. On each shaft, the gear is located in the middle of the bearings. Since no axial load is transmitted between the spur gears, deep-groove ball bearings may be selected for the application.

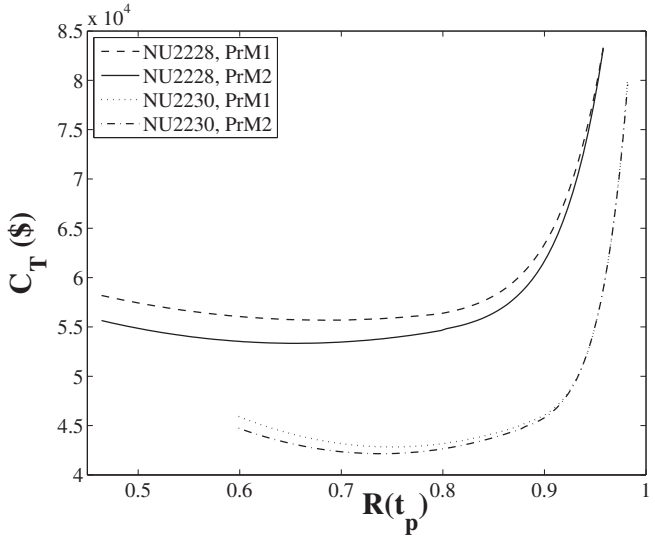

Figure 5.13 LCC of NU22xx bearings for the PrM1 and PrM2 strategies

The desired performance requirements and the working condition of the gearbox, as well as the material type and the geometry of the gears are given in Table 5.16. More details of the gear set and the bearing are listed in Table 5.17. The gears that are bolded in this table are not available in the catalog of the OEM1. To estimate their price, a linear cost-mass correlation Eqn. (3.17) is applied on the price catalog of the gears of NJ and 6HG series of the OEM1 [74].

The component-level reliability target of each gear and bearing is 0.99 at the end of the life cycle. The shaft shall be designed to meet no failure. To reduce the design space of the problem, it is assumed that the four bearings are identical.

According to the AGMA equations [4], the performance and reliability targets for the gears are met by selecting NJ30A (pinion) and 6HG40 (gear) from the catalog of OEM1 [74]. The bearing life equation [6] indicates that the deep groove ball bearing 61905-2Z from the catalog of the OEM2 [77] meets the performance and reliability targets on both shafts.

The price catalogs of the gears OEM [74] and the bearings OEM [78] are consulted to obtain the acquisition cost of the gears and bearings. The price of the gears are corrected

Table 5.16 PrM2 parameters for gears

T (Y)	Cycles (rev./Y)	Torque (Nm)	Gear ratio (-)	$s-r$ (1/Y)	Speed (rpm)
5	9.45×10^6	145	1.33 ± 0.01	0.02	1800

Material –	Hardness (Brinell)	Width (mm)	Module (mm)	Pressure angle (°)
ASTM A576	320	38.1	4.23	14.5

by adding 3.59 CAD to the catalog prices to consider the cost of heat treatment, as quoted by Atlantic Heat Treating [75] for a high production volume. The maintenance cost of the bearings are then calculated using the models presented here. The results are presented in Table 5.18. In the table, (x_1, x_2, x_3) under the second column denotes the number of the pinion teeth number x_1, the gear teeth number x_2, and the bearing catalog number x_3. In the third column, $(y_1, y_2, y_3, y_4, y_5)$ denote the pinion reliability y_1, the gear reliability y_2, the bearing reliability on the input shaft y_3 and on the output shaft y_4, and the system reliability y_5. The system fails if any of the gears or the bearings fail. Hence, these elements operate in series from the reliability perspective, which implies that the system reliability equals the product of the reliability of the two gears and four bearings. It is assumed that the reliability of the shafts is unity.

To estimate the cost of a failure of a gearbox, the empirical data provided by a courier is consulted. The data indicates that the average cost of the downtime plus the labor cost is 2435 CAD [87]. This value may give an estimate for the cost of a failure for the one-speed gearbox. However, two points should be mentioned before making such estimate. First, the transmissions of the courier's trucks are more complicated than the present one-speed gearbox. Second, when a gear fails, the bearings shall be removed to reach the gear, which makes its maintenance generally

Table 5.17 Catalog number and acquisition of the gears and bearings

Pinion no.	NJ27A	**NJ29A**	NJ30A	**NJ31A**	**NJ33A**
Number of teeth	27	**29**	30	**31**	**33**
AC (CAD)	109.92	**115.18**	122.30	**124.93**	**135.34**
Gear no.	6HG36	**6HG39**	6HG40	**6HG41**	**6HG44**
Number of teeth	36	**39**	40	**41**	**44**
AC (CAD)	185.00	**196.09**	201.00	**203.31**	**214.81**
Bearing no.	61903-2Z	61904-2Z	61905-2Z	61906-2Z	61907-2Z
AC (CAD)	35.70	42.77	55.58	71.54	99.82

more time-consuming than the maintenance of a bearing. Hence, in this example it is assumed that for gears $c_{f_0} = 2000$ CAD, and for bearings $c_{f_0} = 1600$ CAD. Moreover, it is assumed that the downtime of a preventive maintenance is much shorter than that of a failure maintenance. Therefore, for both gears and bearings it is assumed that $c_{p_0} = c_{f_0}/4$.

The maintenance cost of each gear and bearing in the PFM strategy is presented in columns seven and eight, respectively, whereas the ninth column presents the maintenance cost of the bearings in the PrM1 strategy with one preventive maintenance (n=1). The continuous annual inflation rate of this example is 0.02. As pointed out in Section 5.2.2 under Eqn. (5.50), for gears the preventive maintenance cost is always higher than that of a PFM. Hence, this example only studies the PFM strategy for gears. Furthermore, as argued for Fig. 5.13, the PrM1 and PrM2 maintenance costs converge as reliability approaches unity. The same behavior is observed for the bearings of this example, such that the deviation of the LCC of the two preventive strategies is less than 0.1%. Hence, for brevity the results of the PrM2 are not reported here.

The last two columns of Table 5.18 compile the LCC of the PFM and PrM1 strategies. The LCC is the sum of the LCC of the bearings and the gears. The LCC of the shaft is excluded from the calculations because, as discussed below, the aim of this example is finding a solution

for the gears and bearings with lowest LCC of the gearbox. For the set of gears presented in Table 5.17, the bore of the gears is 28.6 mm (1.125 in). The bore of the bearings of the table vary from 15 mm to 35 mm. It is assumed that the cost of the filleting process required to fit the bearings to the shaft is minimal compared to other expenses of the system. Therefore, the cost of the shaft is treated as a constant which is dropped from the calculations. In other words, the LCC analysis presented for the gearbox may be viewed as a comparative study between the LCC of different solutions for the gearbox. Considering this point, we may proceed to the LCC analysis.

The solution presented in row 13 of Table 5.18 may be considered as the *baseline* design, where the component-level reliability requirements are met. One reasonable question is: would component-level considerations necessarily lead to an optimum system-level solution? In other words, is it possible to reach a solution that is higher in reliability and lower in the LCC on the system-level by relaxing the component-level reliability requirements?

To answer this question, a set of *neighboring* points of the baseline design is studied. To this end, in addition to the gear set and the bearing of the baseline design, four other gear sets and four other bearings are also examined. In selecting the neighboring gear sets and bearings, two requirements are set. First, the performance requirements (input torque, gear ratio, etc.) shall be met. Second, the dimensions of the new gears and bearing shall be close to those of the baseline design. The latter is quite important when there are space limitations and the final configuration of the gearbox shall not be overly different from that of the baseline design.

By having five gear sets and five bearings, as listed in Table 5.17, twenty five different gearboxes can be achieved, including the baseline design. The reliability and LCC analysis results of each gearbox is reported in Table 5.18. It is observed that the LCC of the PFM strategy is lower than that of PrM1; the cost of a preventive maintenance cannot be covered by the savings on the failure maintenance cost. Hence, PFM is the best strategy.

The results of the PFM strategy is plotted in Fig. 5.14. Design 21 minimizes the LCC (see Table 5.18), which leads to 17.4% LCC reduction compared to the baseline design. The second lowest LCC is the design 22, where a 14.7% saving is achieved over the baseline design. Despite the LCC of the design 22 is only 3.2% higher than that of design 21, the reliability of the former is 0.969, whereas the reliability of the latter is 0.838. Depending on how the design team weights the reliability versus the LCC, the optimum solution may be selected among any of the points on the Pareto front shown in Fig. 5.14. Note that this Pareto front solely identifies the best solutions among the design points studied here. The goal of this case study is to demonstrate the applicability of the developed cost models rather than running a full optimization problem. The latter can be the topic of a future study.

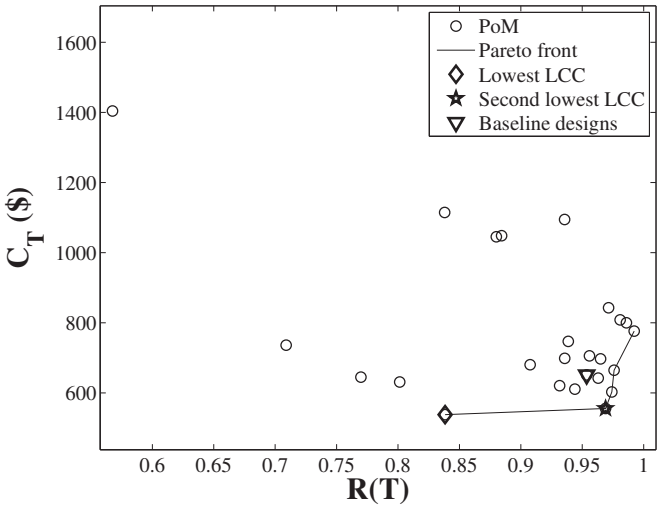

Figure 5.14 LCC of a one-speed gearbox, PFM

Two important conclusion may be drawn from this example. First, $\gamma > 1$ is the necessary condition to reduce the LCC by switching from PFM to PrM1 or PrM2. It is not a sufficient condition to get an LCC reduction. Whether a preventive maintenance strategy reduces the LCC or not depends on all of the inputs of the PrM1 or PrM2 models, as well.

The second conclusion is that if the component-level reliability constraints are relaxed, a solution may be achieved that is higher in reliability and lower in LCC from the system-level perspective. Hence, by changing the design paradigm and considering the component-level reliability as a design variable rather than a design objective, a new window to LCC optimization and system-level reliability improvement may be opened.

Table 5.18 Details of the gearbox

Design no.	Gears & Bearings	Reliability of Gears, Bearings, & System	Gears MC PFM ($)	Bearings MC PFM ($)	Bearings MC PrM1 ($)	LCC, PFM ($)	LCC, PrM1 ($)
1	(27, 36, 61903)	(0.9675, 0.9771, 0.9183, 0.8438, 0.5676)	(138.01, 275.88)	(138.01, 275.88)	(543.89, 641.40)	1404.08	2946.88
2	(27, 36, 61904)	(0.9675, 0.9771, 0.9807, 0.9600, 0.8380)	(35.21, 72.19)	(35.21, 72.19)	(489.23, 515.17)	1114.62	2613.38
3	(27, 36, 61905)	(0.9675, 0.9771, 0.9888, 0.9757, 0.8800)	(20.67, 44.33)	(20.67, 44.33)	(492.64, 509.07)	1045.46	2659.23
4	(27, 36, 61906)	(0.9675, 0.9771, 0.9896, 0.9773, 0.8843)	(19.36, 41.47)	(19.36, 41.47)	(508.51, 523.86)	1048.32	2784.40
5	(27, 36, 61907)	(0.9675, 0.9771, 0.9987, 0.9961, 0.9356)	(2.76, 7.69)	(2.76, 7.69)	(527.04, 530.27)	1094.60	2947.40
6	(29, 39, 61903)	(0.9863, 0.9895, 0.9421, 0.9047, 0.7089)	(94.34, 160.68)	(94.34, 160.68)	(514.06, 559.81)	736.27	2669.20
7	(29, 39, 61904)	(0.9863, 0.9895, 0.9870, 0.9771, 0.9076)	(23.82, 41.48)	(23.82, 41.48)	(481.35, 493.62)	680.35	2499.69
8	(29, 39, 61905)	(0.9863, 0.9895, 0.9926, 0.9865, 0.9357)	(13.73, 24.90)	(13.73, 24.90)	(487.88, 495.56)	698.81	2567.86
9	(29, 39, 61906)	(0.9863, 0.9895, 0.9932, 0.9874, 0.9386)	(12.96, 23.56)	(12.96, 23.56)	(504.12, 511.39)	747.13	2695.86
10	(29, 39, 61907)	(0.9863, 0.9895, 0.9994, 0.9983, 0.9714)	(1.42, 3.60)	(1.42, 3.60)	(526.20, 527.57)	842.97	2885.50
11	(30, 40, 61903)	(0.9907, 0.9925, 0.9510, 0.9304, 0.7698)	(79.07, 115.75)	(79.07, 115.75)	(503.70, 528.61)	645.13	2579.73
12	(30, 40, 61904)	(0.9907, 0.9925, 0.9893, 0.9839, 0.9316)	(19.71, 29.20)	(19.71, 29.20)	(478.51, 485.07)	620.67	2470.57
13	(30, 40),61905)	(0.9907, 0.9925, 0.9940, 0.9907, 0.9536)	(11.26, 17.18)	(11.26, 17.18)	(486.19, 490.23)	651.53	2547.50
14	(30, 40, 61906)	(0.9907, 0.9925, 0.9945, 0.9914, 0.9559)	(10.45, 16.18)	(10.45, 16.18)	(502.42, 506.32)	705.73	2675.98
15	(30, 40, 61907)	(0.9907, 0.9925, 0.9996, 0.9991, 0.9808)	(0.95, 2.04)	(0.95, 2.04)	(525.92, 526.58)	808.37	2876.62
16	(31, 41, 61903)	(0.9931, 0.9943, 0.9585, 0.9399, 0.8014)	(65.39, 98.94)	(65.39, 98.94)	(494.63, 517.10)	631.20	2533.02
17	(31, 41, 61904)	(0.9931, 0.9943, 0.9912, 0.9864, 0.9440)	(16.30, 24.85)	(16.30, 24.85)	(476.17, 482.05)	610.86	2454.27
18	(31, 41, 61905)	(0.9931, 0.9943, 0.9952, 0.9923, 0.9630)	(9.28, 14.34)	(9.28, 14.34)	(484.84, 488.30)	642.32	2535.35
19	(31, 41, 61906)	(0.9931, 0.9943, 0.9956, 0.9929, 0.9649)	(8.59, 13.59)	(8.59, 13.59)	(501.16, 504.55)	697.26	2664.31
20	(31, 41, 61907)	(0.9931, 0.9943, 0.9998, 0.9994, 0.9859)	(0.59, 1.51)	(0.59, 1.51)	(525.72, 526.26)	800.16	2869.98
21	(33, 44, 61903)	(0.9962, 0.9970, 0.9699, 0.9472, 0.8383)	(45.98, 84.93)	(45.98, 84.93)	(481.81, 507.72)	538.11	2496.27
22	(33, 44, 61904)	(0.9962, 0.9970, 0.9994, 0.9883, 0.9690)	(11.23, 21.28)	(11.23, 21.28)	(472.71, 479.60)	555.53	2450.11
23	(33, 44, 61905)	(0.9962, 0.9970, 0.9969, 0.9934, 0.9741)	(6.11, 12.27)	(6.11, 12.27)	(482.72, 486.88)	602.71	2535.95
24	(33, 44, 61906)	(0.9962, 0.9970, 0.9972, 0.9940, 0.9759)	(5.58, 11.49)	(5.58, 11.49)	(499.15, 503.12)	664.77	2665.12
25	(33, 44, 61907)	(0.9962, 0.9970, 1.0000, 0.9995, 0.9923)	(0.11, 1.14)	(0.11, 1.14)	(525.48, 526.03)	776.19	2876.72

5.3 Conclusion

The foundation of the maintenance cost model developed here is deriving the failure distribution function of the element from its reliability function, and then using it as a kernel to calculate the expected cost associated with having failures. This procedure is applied on a post-failure maintenance (PFM) strategy and two preventive maintenance (PrM) strategies. The inputs of the model are the reliability distribution $R(t)$, the price c_0, the cost of a failure c_f, the cost of a preventive maintenance c_p, the inflation rate, the downtime of a failure δ_f, and the downtime of a preventive maintenance δ_p. Having these inputs for any element, the procedure may be applied to calculate the maintenance cost of the product.

In the model formulation, the downtimes appear in the limits of integrals. The model can be simplified by neglecting the downtimes in the integral limits. To assess the level of error associated with such an assumption, a sensitivity analysis of the model to the downtime is conducted. The result suggests that no significant error should be expected upon applying this assumption in a wide range of downtimes. However, any cost associated with loss of productivity because of the downtime shall be lumped into c_f or c_p.

The convergence of the present models is studied. It is observed that for the life cycle considered here and for the range of reliability used in applied engineering practice, the models converge within the error range of 1% by considering the cost of the first four failures. Avoiding calculation of higher number of failures considerably decreases the calculation time without loss of accuracy. Hence, the present models are truncated after the fourth failure.

It is shown that the maintenance cost may be significantly sensitive to the inflation rate. This observation implies the importance of dropping the zero inflation rate assumption of previous models to improve the accuracy of the LCC analysis. To assure the validity of the developed PFM model, in zero inflation rate scenario and for different reliability functions, the

model results are compared with the previous models [42, 43] and a good agreement is observed. In the previous PrM models, in spite of their simple mathematical form, it is observed that the accuracy decreases as the end-of-cycle reliability decreases. The results of the PrM model of [42, 43] and the present PrM model are compared in an example. It is expected that for zero preventive maintenance (i.e. a post-failure maintenance strategy), they shall converge to the result of the PFM strategy. In contrast to the present PrM model, the model of [42, 43] fails to meet this expectation. It is argued that the sources of such deviation for the previous models are probably their simplifying assumptions. The results suggest that although the present model is more complicated in form and more expensive to calculate, it offers a much higher accuracy.

In another set of problems, the maintenance cost and LCC behavior of different Weibull distributions are studied. It is argued that if $\gamma \leq 1$, the LCC of a PFM strategy is always smaller than the PrM. For Weibull distributions with $\gamma > 1$, on the other hand, the LCC of a PrM strategy may be smaller than the PFM strategy depending on the inflation rate, cost of a failure, and cost of a preventive maintenance. These inputs determine whether the investments on conducting a preventive maintenance could be covered by savings on failure cost reduction. This problem is addressed for bearings, as an example of elements with $\gamma > 1$. For deep groove and cylindrical roller bearings under different working conditions, the best maintenance strategy, as well as the savings of the PrM strategy over PFM is studied.

The two preventive maintenance strategies developed here (i.e. PrM1 and PrM2) are compared for ball bearings and roller bearings. The PrM1 strategy is strict in scheduling the preventive maintenance points. The PrM2 strategy, on the other hand, is more flexible to let an element continue operation if no failure occurs. Consequently, it is expected that the maintenance cost of a PrM2 strategy is always lower than a PrM1 strategy. Although the results show this behavior, it is observed that the difference of the LCC of these strategies is insignificant when the end-of-duty reliability is above 0.90. In that case, the maintenance team may prefer to select the PrM1 strategy over PrM2 because it provides the opportunity of scheduling the preventive

maintenance of many different elements of a system at the same time to reduce the total downtime of the system.

For gears and bearings, the maintenance cost models of this chapter are coupled with the acquisition cost models of Chapters 2 and 3 to conduct the LCC analysis of a one-speed gearbox, which is composed of two gears, two shafts, and four bearing (two on each shaft). A baseline design for the gears and bearings is selected such that the component-level performance and reliability requirements are met. Next, the component-level reliability constraints are dropped and the size of the bearings and gears are changed. The aim is studying whether exploring neighboring design points of the baseline design would result in a solution that is lower in LCC and higher in system-level reliability. Interestingly, the answer is positive. The conclusion suggests that the reliability may be considered as a design variable rather than a design objective. Such change of paradigm provides the opportunity to extend the design space and explore new regions in search of increased system-level reliability and lower LCC.

In the formulation of this chapter it is assumed that the reliability function $R(t)$ is deterministic. However, by considering factors such as loading uncertainty, material variability, and assembly accuracy, it is possible to include uncertainties in $R(t)$. In such an approach, in addition to the expected maintenance cost, the resulting model may calculate the standard deviation of the maintenance cost. The standard deviation provides a tool to manage the uncertainty in the maintenance and life-cycle cost of a project. This can be a topic for future work.

Having the CPR model of gearboxes and electric motor, as well as the MC models established, in the following chapter the LCC of the powertrain of a battery electric step van is studied.

Chapter 6

Reliability and Life-Cycle Cost Analysis of Powertrain of Battery Electric Vehicles

At a similar level of performance, when hybrid and electric vehicles are compared with internal combustion engine vehicles, the former has typically a higher acquisition cost mainly due to the high price of their battery pack. On the other hand, HEVs and EVs benefit from lower energy cost. Also, because of having less moving parts compared to ICEVs, a lower maintenance cost is expected for the HEVs and EVs. Therefore, from a life-cycle perspective, the cost of ownership of hybrid and electric vehicles may be comparable with or lower than that of an ICEV. Having a detailed LCC model for electric vehicles may enable the designers to target desired performance and reliability while optimizing the life-cycle cost of the product. As a step towards this, the life-cycle cost and reliability of the powertrain of a battery electric step van is addressed as the sum of the acquisition cost, the maintenance cost, and the energy cost of the powertrain. The salvage value and the disposal costs are outside of the scope of this evaluation. The design space is explored in search of optimum system-level reliability and life-cycle cost while ensuring the specified performance requirements are met.

6.1 Problem definition

For the powertrain of a class-4 battery electric step van (hereafter called the Van), the influence of the design variables on its overall reliability and life-cycle cost (LCC) is studied.

6.1.1 System configuration

Morozov et al. [72] studied the performance of a Van. Here, the cost and reliability analysis is conducted for the powertrain of the single-speed solutions reported by Morozov et al. [72]. The powertrain is composed of a battery pack, an electric motor, and a single-speed gearbox, as shown in Fig. 6.1.

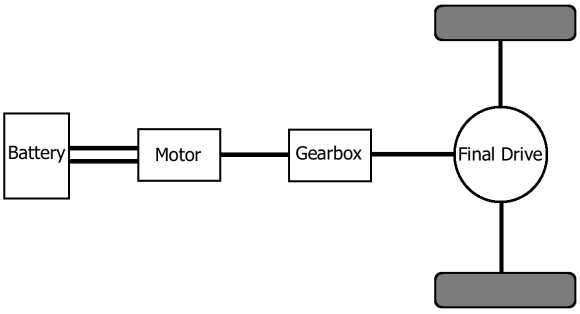

Figure 6.1 Configuration of the powertrain

Gearbox

Three different powertrain layouts are explored by Morozov et al.: a direct drive, a one-speed gearbox, and a two-speed gearbox [72]. In the direct drive option, the electric motor is directly coupled to the final drive differential. In the single/two-speed option, there is a single/two-speed gearbox between the electric motor and the final drive.

As suggested in [88], Morozov et al. select the final drive differential ratio of 5.13 to meet the high pulling performance requirement of the Van [72]. Here, since all of the proposed solutions in [72] have the same final drive ratio, this element is excluded from the cost and reliability analysis, as depicted in Fig. 6.1.

The results of Morozov et al. [72] indicate no significant advantage on the energy consumption for the two-speed gearbox solutions over the single-speed ones. Therefore, the single-speed gearbox options are selected for the powertrain to reduce the acquisition cost compared to the two-speed options.

Electric motor

In Morozov et al. [72], four permanent-magnet synchronous motors (PMSM) were designed to meet power, torque, and efficiency requirements of the Van. The peak power ratings of the four designed motors were 100 kW, 135 kW, 150 kW, and 200 kW. The design details of the motors are provided in [72]. The results imply that the motors smaller than 150 kW cannot provide the specified powertrain performance requirements. Therefore, here, the 150 kW and the 200 kW motors are considered in cost and reliability analysis of the powertrain. Both options have a class H insulation.

Battery pack

A 96 kWh Li-ion battery pack is used in the powertrain, in keeping with Morozov et al. [72].

6.1.2 Design objectives and requirements

In Morozov et al. [72], the performance requirements of the Van are the gradability, the top speed, and the full load acceleration time, as given in Table 6.1. The top speed and the gradibility

requirements impose higher and lower bounds on the transmission ratio [89, 90]. Here, for the operation life given in Table 6.1, the reliability of individual elements must be above 0.98. This reliability constraint is used to select the baseline design.

The acquisition cost (AC) and the maintenance cost (MC) of the Van is outside of the scope of Morozov et al. [72], leaving the overall energy consumption as the objective function of the problem. Here, for the solutions provided in Morozov et al. [72], the LCC is selected as the objective function instead of the energy consumption.

6.1.3 Design variables

In the performance analysis of the Van in Morozov et al. [72], the gear ratio is the design variable. In the cost and reliability analysis here, three design variables are selected. The first design variable is the size of the pinion (or the gear). The second variable is the size of the four bearings of the gearbox. To reduce the size of the design space, it is assumed that the four bearings of the gearbox are identical. It is possible to avoid such an assumption when a more detailed analysis is required. The last design variable is the bearing size of the rotor of the electric motor. As reported in Section 6.3, using these three design variables results in a wide range of solutions in the cost-reliability space of the powertrain. Such degree of exploration is important in finding the design with optimum LCC. Here, the motor size and the battery pack size are considered as performance constraints. They can be added to the design space. However, this larger space does not add to the understanding of the method, merely its complexity.

Table 6.1 System requirements

Gradability (%)	Top speed (km/h)	0-96.6 km/h time (s)	Life (Y)	Operation (day/Y)	Range (km/day)	End of life Reliability
30	105	25	13	250	80	≥ 0.98

6.1.4 Driving cycles

Morozov et al. consider six different driving cycles [72]. Three of the driving cycles have lower maximum and average speeds and more starts and stops, which classifies them as urban cycles. Two of the cycles have characteristics of high speed highways; with high top speeds and few stops. One cycle shares the characteristics of the city and highway cycles. Among the six driving cycles, the analysis here is conducted under the Orange County bus (OCB) cycle [72], as its velocity profile is closer to that of an urban delivery truck.

6.1.5 Assumptions

The cost analysis conducted here is a comparative study, which means that only the costs that vary from one design to the other are considered, neglecting all other expenses which are identical in the different solutions. All of the solutions by Morozov et al. have identical final drives [72]. Therefore, this element is not included in the cost analysis.

Similar to Morozov et al. [72], the energy cost of the powertrain is reported for the case of no regenerative breaking. This effect will be addressed in a future study.

In the cost analysis here, the net present value (NPV) of the LCC is reported. The maintenance cost is discounted continuously assuming a constant discount rate throughout the life cycle of the project.

Lastly, it is assumed that the salvage value of all designs are equal. Therefore, from a comparative cost analysis perspective, the salvage value is excluded from cost analysis.

6.2 Methodology

The LCC here denotes the sum of the AC, the NPV of the MC, and the the NPV of EC throughout the life cycle of the powertrain. For the design points reported in Morozov et al. [72], the three cost categories are calculated to establish the LCC.

6.2.1 Acquisition cost

The acquisition cost is the sum of the price of the gearbox, the electric motor, and the battery pack.

Gearbox

For ten gearboxes of different sizes, the OEM provides the price of the spare parts [91]. The spare parts may be classified into four subsystems: gears, bearing set, casing, and accessories. If the price of the gears and the bearing set are denoted by x_1 and x_2, respectively, the price of the gearbox may be estimated by $2.17x_1 + x_2$, as shown in Table 6.2. The reason is that for the ten gearboxes, the price of the casing and the accessories are 83% and 34% of the gears, respectively. The formula given in the last line of this table predicts the gearbox price within an error range of 0.7%.

Table 6.2 Bill of materials of gearbox

Subsystem	Price
Gears	x_1
Casing	$0.83x_1$
Accessories	$0.34x_1$
Bearing set	x_2
Total	$2.17x_1 + x_2$

It is assumed that the BOM of Table 6.2 may be used for the one-speed gearboxes. Therefore, by knowing the price of the gears and the bearings from the catalog of the OEMs [78, 74], the material cost of the gearbox is calculated. Next, as proposed by Argonne National Laboratory [92], an overhead factor of 2.0 is applied on the material cost to account for the indirect costs and profit margin. The result is the price of the gearbox. If the price of a specific part is not provided in the OEM's catalog, it is estimated using Eqn. (2.36).

Electric motor

For the 150 kW and 200 kW PMSM motors introduced in Morozov et al. [72], the BOM is given in Table 6.3. The second column of this table collects the estimated price of each material suggested by an OEM. The material cost of the motor is the sum of the material cost of its components. Next, an overhead factor of 1.55 and a profit margin of 1.20 is applied on the material cost [29] to estimate the price of the motor, reported in the last line. The influence of the price of the bearings on the acquisition of the motor is analyzed using the approach proposed in Section 4.2.3.

Table 6.3 Bill of materials of the motors

Materia Type	Price (USD/kg)	Mass (kg)	
		150 kW Motor	200 kW Motor
Magnet	112.00	5.9	12.1
Copper	16.00	27.2	51.4
Steel	20.00	38.9	79.9
Material cost (USD)		1874.00	3775.60
Price (USD)		3485.64	7022.62

Battery pack

As proposed in the literature [61], the price of the battery pack is 250 USD/kWh in 2016. Also, it is assumed that its price declines 8% annually [61]. The future price is an input of the maintenance cost model of Chapter 5.

6.2.2 Maintenance cost

Here, the maintenance cost of each component is determined using the method developed in Chapter 5, which is an extension to the method presented in Blischke and Murthy [42] and Jardine and Tsang [43]. In this approach, the failure probability density function (FPDF), which is calculated from the reliability function $R(t)$, is used as kernel to calculate the maintenance cost. Moreover, the time value of money is incorporated in the MC model to calculate the net present value (NPV) of the maintenance cost. The inputs of the maintenance cost model are the reliability function, the time value of money, the price (AC) of the spare part, and the cost of a failure c_f, which accounts for the downtime cost and the shop rate for the maintenance.

Reliability analysis

The reliability analysis of the gears of the gearbox is conducted as instructed in [5]. For the bearings of the gearbox and the electric motor, the reliability is analyzed using the method of [6]. The method presented in Gieras and Wing [17] is used to calculate the reliability of the insulation of the electric motor.

The data sheet of the battery pack is consulted to determine its expected life [93]. Next, as reported in literature [19–21], the reliability of the battery pack is modeled using a Weibull distribution. A Weibull distribution is characterized by two factors, namely the shape parameter and the scaling parameter. Similar to the experimental results of Ran et al., it is assumed that for

the battery pack, the Weibull shape parameter is 10.2 [21]. By knowing the expected life and the Weibull shape parameter, the scale parameter of the Weibull distribution is calculated.

Time value of money

In calculating the NPV of the LCC, as advised by a delivery company [87], it is assumed that the return of investment (ROI) of the project is 4.0% annually. This value is used as an input of the MC model of Chapter 5. For other applications with a different ROI, this input will vary accordingly.

Downtime cost

Here, the downtime cost of the Van is 122.03 USD/hr. The figure is calculated by dividing the daily revenue of a delivery company by the number of vans in its fleet [94], and applying a CAD/USD exchange rate of 0.77, as discussed in Section 6.2.4.

Shop rate

In the United States, the average national-wide hourly shop cost is 80.00 USD/hr [95], and the mean salary of an automobile mechanic is 19.58 USD/hr [96]. Hence, the labor cost is 24.5 % of the shop cost. In Montreal, Canada, the average wage of an automotive technician is 19.00 CAD/hr [97, 98]. Assuming that the ratio of labor cost to shop cost in Canada is the same as US, the shop cost in Montreal is 77.63 CAD/hr. Applying an exchange rate of 0.77, the shop hourly cost of 59.78 USD/hr is reached.

For each element of the powertrain, the average downtime and the average labor time of a maintenance is given in Table 6.4, as advised by a delivery company [87]. The cost of a

failure c_f is calculated based on the downtime and the shop rate, and collected in the last line of Table 6.4.

Table 6.4 Downtime, labor time, and cost of a maintenance

Subsystem	Gearbox	Gearbox	Motor	Motor	Battery
Element	Gears	Bearings	Insulation	Bearings	–
Downtime (hr)	48	48	48	48	48
Labor time (hr)	13	13	16	13	4
Cost of a failure (CAD)	6634.58	6634.58	6813.92	6634.58	6096.56

Maintenance strategy

A post-failure maintenance (PFM) strategy is selected because in the range of reliabilities studied here, the LCC of a PFM is smaller than that of a preventive maintenance (PrM) strategy, as discussed in Chapter 5.

6.2.3 Energy cost

Morozov et al. present the energy consumption for each driving cycle for the different designs reported in [72]. For each of their solutions, the energy consumption per cycle is used in calculating NPV of the energy cost of the Van. It is assumed that the consumption per cycle and the efficiency of the Van does not vary throughout its life.

Present electricity price

It is supposed that the Van operates in Montreal, Quebec, Canada. Each day, the Van leaves the shipping center in the morning, and returns to the shipping center after finishing the delivery tasks. It is recharged during the evening to the full state of charge (SOC) for the next day. It is assumed that the power demand of the shipping center is 100 kW and its monthly consumption is 25000

kWh. For that scenario, Hydro Quebec states that the price of electricity is 0.106 CAD/kWh [99], which is used here as the present price of electricity. As discussed in Section 6.2.4, a CAD/USD exchange rate of 0.77 is applied to get the price of electricity is 0.082 USD/kWh.

Electricity price projection

Annual Energy Outlook 2015 projects the NPV of electricity price in the United States up to 2040 [53]. It is assumed that electricity price in Quebec, Canada follows the same trend as the US. Among the six scenarios discussed in [53], the reference scenario is selected. The projection results are reported in Table 6.5.

Table 6.5 Projection of the electricity price

Year	2015	2016	2017	2018	2019	2020	2021
Price (CAD/kWh)	0.082	0.083	0.084	0.083	0.084	0.086	0.086
Year	2022	2023	2024	2025	2026	2027	2028
Price (CAD/kWh)	0.087	0.087	0.087	0.089	0.089	0.090	0.090

6.2.4 Exchange rates

All of the costs and expenses are reported in 2016 USD. For the bearings, the gears, and the electricity price, where the price is not reported in USD, an exchange rate is applied to convert the currency.

Exchange rate for bearings

In the price catalog of the OEM of the bearings, the prices are in Euros [78]. As the price catalog has not been updated, it is assumed that the prices are still valid. The Euro/USD exchange rate is 1.12 as for September 2016; it is used to obtain the prices in USD [79].

Exchange rate for gears

The price catalog of the gears is published in CAD by the Canadian distributor rather than the American OEM [74]. To get the prices in USD, the CAD/USD exchange rate of 0.80 is used referenced to the publication date of the catalog [79]. The assumption is that the OEM has not significantly changed the prices of their products in USD since the publication date of the catalog.

Exchange rate for motors

The material price of the motors were proposed by an OEM in February 2015 [100]. To convert the material cost from CAD to USD, an exchange rate of 0.80 is used as the average exchange rate in February 2015 [79].

Exchange rate for electricity price and cost of a failure

For the electricity price announced by Hydro Quebec, a CAD/USD exchange rate of 0.77 is used as of September 2016 [79]. The same exchange rate is used for calculating the cost of a failure and the labor cost in USD.

6.3 Results

For the OCB cycle, the output speed and the output torque of the gearbox of the Van is shown in Fig. 6.2. These speed and torque profiles are the inputs to the reliability analysis of the gearbox and the electric motor (See Chapters 2, 3, and 4).

The powertrain is studied in two rated powers, namely 150 kW and 200 kW, corresponding to the rated power of the electric motor. Morozov et al. report that the energy efficiency

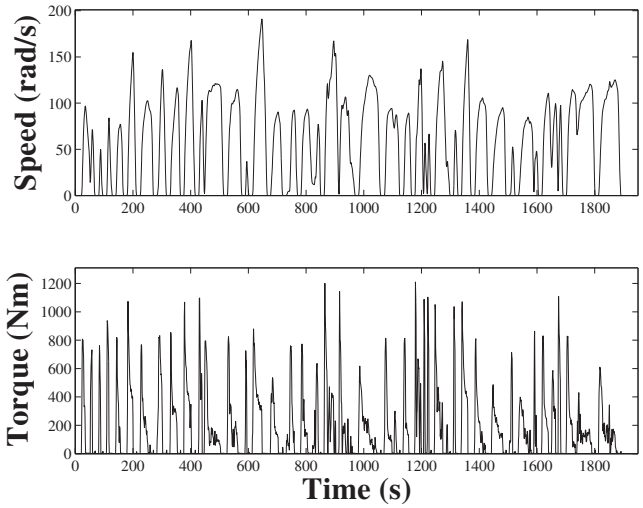

Figure 6.2 The output speed and torque of the gearbox of the Van for the OCB cycle

of the 150 kW Van is optimum at gear ratio of 2.75, and the optimum gear ratio of the 200 kW Van is 1.24 [72]. Here, the gears are chosen within 1% accuracy the gear ratios proposed by Morozov et al. This ensures that the overall design satisfies the performance requirements.

6.3.1 Gearbox

Gear design space

The material type as well as some design details of the gears are given in Table 6.6. The gears are carburized to reach the hardness of 330 Brinell. The catalog number, pitch diameter, and acquisition cost of the gears are listed in Table 6.7 [74].

The catalog number of the gears have the form YJxx, where xx shows the number of the teeth. Hereafter, the gear set (YJxx, YJyy) is denoted by (xx, yy) for brevity.

For the torque and speed profiles of Fig. 6.2, the reliability of the gears are collected in the last line of Table 6.7 following the method of Section 6.2.2. For the 150 kW powertrain, the

reliability of the both pinion and gear are above 0.98 for the gearsets (15, 41), (16, 44), and (17, 47). The gearset (15, 41) is the smallest option that meets the reliability requirement. Therefore, it is selected as the baseline gearset of the 150 kW powertrain. The baseline gearset of the 200 kW powertrain is (24, 30). In Table 6.7, the baseline designs are embolden.

The AC of the gears are also provided in Table 6.7. For the gears that are not provided in the price catalog of the OEM, the AC is estimated using Eqn. (2.35). Since all gears have identical module and face width, the term $\beta_h v_h + \beta_g v_g$ in Eqn. (2.35) is constant and, therefore, can be taken into α_5. This way, Eqn. (2.35) reduces to a linear cost-mass relation. For the gears studied here, this model is characterized by $\alpha_5 = 23.66$ USD and $\beta_5 = 15.30$ USD/kg.

Bearing design space

Table 6.8 pesents the catalog number, dynamic load rating C_r, acquisition cost c_0 of the deep groove ball bearings used in the gearbox [77, 78]. For the baseline gearsets of Table 6.7, the reliabilities of the 6208, 6308, and 6408 bearings on the input shaft and output shaft are reported in Table 6.8. Although the forces on the bearings of the shafts are identical, the bearings on the input shaft have a lower reliability. The reason is that the speed of the input shaft is higher than the output shaft. Therefore, the bearings on the input shaft undergo a higher number of cycles throughout the lifetime of the gearbox, leading to a lower reliability. For both powertrains, the reliability target of 0.98 is met for the bearings 6308 and 6408 on both input and output shafts. Since 6308 is smaller in size, it is selected as the baseline bearing of the gearbox, and is highlighted in Tab 6.8.

Table 6.6 The design details of gears

Material Type	Hardness (Brinell)	Module (mm)	Width (mm)	Pressure angle (^{o})	Safety factor	
					Bending	Pitting
ASTM A576	330	4.23	50.8	20.0	1.50	1.25

Table 6.7 The reliability of pinions and gears

Powertrain	150 kW				
Gear set	(13, 36)	(14, 39)	**(15, 41)**	(16, 44)	(17, 47)
Catalog ID	(YJ13, YJ36)	(YJ14, YJ39)	(YJ15, YJ41)	(YJ16, YJ44)	(YJ17, YJ47)
Diameter (mm)	(55.0, 152.4)	(59.3, 165.1)	(63.5, 173.6)	(67.7, 186.3)	(72.0, 199.0)
c_0 (USD)	(38.08, 134.27)	(40.39, 153.48)	(42.86, 167.13)	(45.51, 188.90)	(48.32, 212.20)
Reliability	(0.913, 0.958)	(0.978, 0.983)	(0.989, 0.992)	(0.994, 0.996)	(0.997, 0.998)
Powertrain	200 kW				
Gear set	(20, 25)	(22, 27)	**(24, 30)**	(27, 33)	(30, 37)
Catalog ID	(YJ20, YJ25)	(YJ22, YJ27)	(YJ24, YJ30)	(YJ27, YJ33)	(YJ30, YJ37)
Diameter (mm)	(84.7, 105.8)	(93.1, 114.3)	(101.6, 127.0)	(114.3, 139.7)	(127.0, 156.6)
c_0 (USD)	(57.80, 77.00)	(64.97, 85.88)	(72.82, 100.47)	(85.88, 116.61)	(100.47, 140.50)
Reliability	(0.886, 0.909)	(0.953, 0.963)	(0.985, 0.989)	(0.995, 0.996)	(0.998, 0.999)

For the 150 kW powertrain, the bearing 6204 is the baseline bearing, whereas the baseline bearing of the 200 kW motor is 6206.

Table 6.8 Reliability of the bearings for the baseline gearset

Powertrain	150 kW					
Subsystem	Gearbox (input shaft, output shaft)			Electric motor		
Bearing no.	6208	**6308**	6408	6004	**6204**	6304
C_r (kN)	31.0	45.5	68.0	10.0	13.6	16.9
c_0 (USD)	40.32	61.71	155.68	13.56	14.68	19.25
Reliability	(0.948, 0.985)	(0.993, 0.999)	(1.000, 1.000)	0.966	0.993	0.999
Powertrain	200 kW					
Subsystem	Gearbox (input shaft, output shaft)			Electric motor		
Bearing no.	6208	**6308**	6408	6006	**6206**	6306
C_r (kN)	31.0	45.5	68.0	13.5	20.7	30.5
c_0 (USD)	40.32	61.71	155.68	19.28	23.13	32.54
Reliability	(0.896, 0.930)	(0.984, 0.990)	(0.999, 1.000)	0.901	0.988	0.999

Gearbox design space

Having the baseline elements identified, the baseline gearbox and motor are configured. For the 150 kW powertrain, the baseline gearbox is composed of the (15, 41) gearset and four 6308 bearings. The 150 kW motor has two 6204 bearings. The baseline gearbox of the 200 kW

powertrain is comprised of the (24, 30) gearset and four 6308 bearings. The 6206 bearing is used in the electric motor.

For each power rating of the powertrain, aside from the baseline gearbox, fourteen other gearbox options are developed using the five gearsets and three bearing options given in Table 6.7. Fig. 6.3 illustrates the LCC of the fifteen 150 kW gearboxes versus their overall reliability. The LCC of the baseline gearbox is 1,603.42 USD at the reliability of 0.965. In this case, the LCC of the baseline is lower than the other fourteen options. The second lowest LCC belongs to the gearbox with the (16, 44) gearset and the 6308 bearings, where reliability is 0.980 with LCC of 1,622.18 USD; 1.2% higher than the LCC of the baseline. Depending on how the designer weights LCC versus reliability, the baseline or the second lowest LCC option may be selected.

The LCC versus the reliability of the fifteen 200 kW gearboxes are plotted in Fig. 6.4. For the baseline gearbox, the LCC is 1,661.53 USD and the reliability is 0.924. The best gearbox consists of the (27, 33) gearset and the 6308 bearing, whose reliability is 0.961 at LCC of 1,574.49 USD. In this power rating, the investment on the AC and increase in the gear size is advantageous since there are savings on the MC, such that a lower LCC is achieved.

6.3.2 Motor

For the 150 kW and 200 kW motors coupled to the corresponding baseline gearboxes, the LCC is given in Table 6.9 for different bearing sizes. In both cases, the results suggest that the best motor is different from the baseline design; the LCC is the lowest at the largest bearing size.

Table 6.9 Life-cycle cost of the motors coupled to the baseline gearset

	150 kW motor			200 kW motor		
Bearing no.	6004	6204	**6304**	6006	6206	**6306**
LCC (USD)	3824.04	3558.56	3525.89	8018.23	7148.59	7073.02

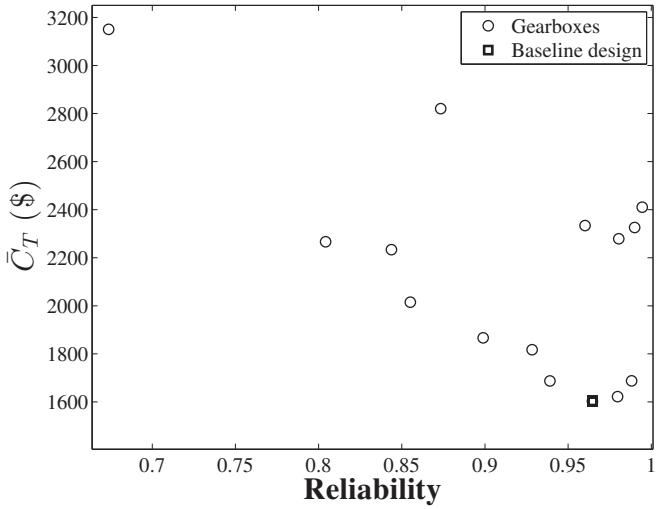

Figure 6.3 LCC of the 150 kW gearboxes

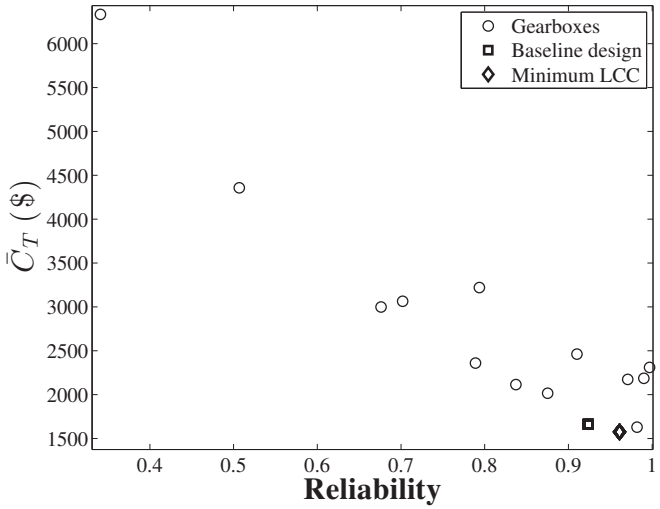

Figure 6.4 LCC of the 200 kW gearboxes

6.3.3 Powertrain

The combination of five gearsets, three bearing options for the gearbox, and three bearing options for the motor leads to a total of forty five powertrain options for each of the 150 kW and 200 kW ratings. For the 150 kW powertrain, the LCC-reliability results are illustrated in Fig. 6.5. The baseline is made of the (15, 41) gearset, the 6308 bearings for the gearbox, and the 6204 bearings for the motor. The reliability and LCC of this configuration are 0.949 and 41,704.87 USD, respectively. The best powertrain is comprised of the same gearbox, but the 6304 bearings for the electric motor. The corresponding reliability is 0.959 with the LCC of 41,672.20 USD; 0.1% lower than the baseline. Although the best solution does not achieve a significant saving over the baseline design, it benefits from a higher overall reliability.

The LCC-reliability data of the 200 kW powertrains is plotted in Fig. 6.6. The baseline has the (24, 30) gearset, the 6308 bearings for the gearbox, and the 6206 bearings for the electric motor, where reliability is 0.899 and LCC equals 45,117.67 USD. The best gearbox is composed of the (27, 33) gearset, the 6308 bearings for the gearbox, and the 6306 bearings for the motor. Compared to the baseline powertrain, a higher reliability of 0.957 is reached while the LCC is 44,954.78 USD; 0.4% lower than the baseline.

For the 150 kW and 200 kW optimum designs, the contribution of each cost category in the LCC is illustrated in Fig. 6.7. For both power ratings, the maintenance cost is less than 0.6% of the LCC. The AC of the 200 kW powertrain is 3519.40 USD higher than the 150 kW option mainly because a more expensive motor is used. This investment is not sound because the EC of the 200 kW system is only 232.77 USD lower than the 150 kW option. Therefore, the best solution is the optimum 150 kW design.

As seen in Fig. 6.7, for both power ratings, the AC is the major expense. AC of the optimum 150 kW solution comprises 69.4% of its LCC. The figure is 72.1% for the 200 kW optimum design. Moreover, the MC and the EC of the two optimum solutions are not

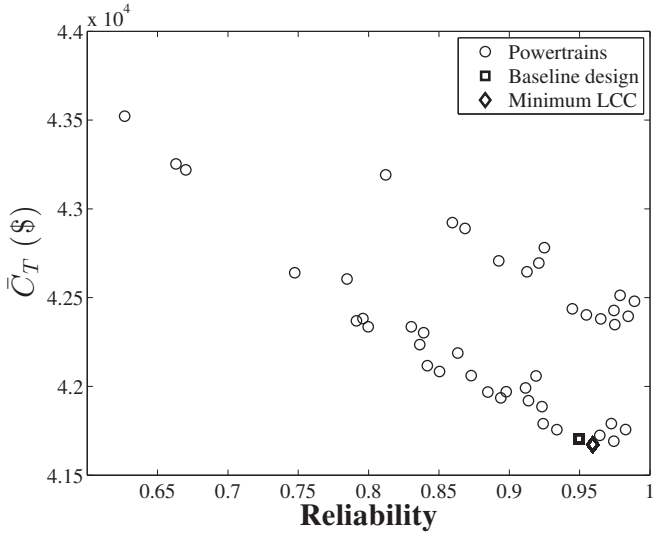

Figure 6.5 LCC of powertrains for the 150 kW motor

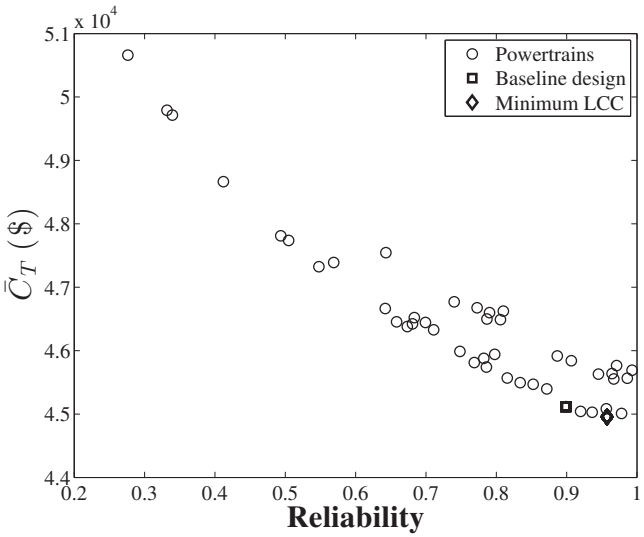

Figure 6.6 LCC of powertrains for the 200 kW motor

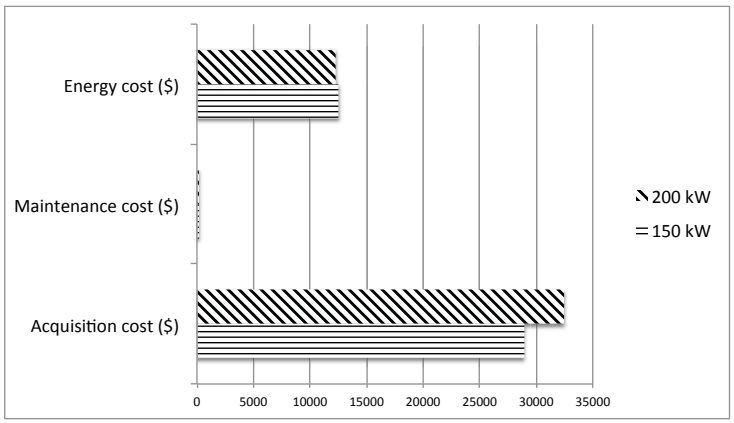

Figure 6.7 Contribution of each cost category on the LCC

significantly different. Therefore, in minimizing the LCC, lowering the AC plays an important role. The details of the AC for the individual subsystem are found in Tab. 6.10. The battery cost is 83.0% of the AC of the 150 kW best solution. This figure is 74.0% for the 200 kW best powertrain.

Moreover, as given in Tab. 6.10, the reliability of the battery pack is higher than the other subsystems, which implies that the 96 kWh battery pack is over-designed for this application. This battery pack is employed because it is the only option available to the authors which meets the performance requirement and has necessary data for reliability analysis. Using a smaller battery pack in this application decreases its AC and increase its MC. This implies the importance of considering the battery size as a design variable to further reduce LCC. This problem will be addressed in future research.

Table 6.10 AC and reliability of the subsystems

	Acquisition cost ($)			Reliability		
	Gearbox	Motor	Battery	Gearbox	Motor	Battery
150 kW	1405.06	3503.17	24000.00	0.965	0.995	0.999
200 kW	1372.47	7055.16	24000.00	0.961	0.997	0.999

6.4 Conclusions

For the powertrain of a class-4 step van, Morozov et al. select the gear ratio to optimize its energy consumption [72]. As an extension to that research, life-cycle cost (LCC) of the powertrain of the van is studied here. The powertrain is composed of a battery pack, an electric motor, and a single-speed gearbox. Two power ratings of 150 kW and 200 kW are considered for the powertrain. The performance requirements are the top speed, the gradability, and the full load acceleration time from 0 to 96.6 km/hr for the Orange County bus (OCB) cycle [72]. To minimize the energy consumption of the van, the gear ratio proposed by Morozov et al. [72] is selected as a design constraint. The objective function is the LCC and the design variables are the gear size, the bearing size of the gearbox, and the bearing size of the electric motor. The LCC is composed of the acquisition cost (AC) and the maintenance cost (MC) of the components, as well as the energy cost (EC) of the powertrain over thirteen years of operation. The gear CPR model of Chapter 2, bearing CPR model of Chapter 3, electric motor CPR model of Chapter 4, and the MC model of Chapter 5 are used. These four models establish the influence of the material type and the size of each element on its reliability and cost. The resulting models establish the interplay between the cost, the reliability, and the performance of the elements.

For each power rating, first the baseline design is determined by selecting the size of the gears and bearings such that the reliability of each individual element is at least 0.98 after thirteen years of operation. Next, the reliability constraint is relaxed and the gears and bearings are resized to explore the design space for reducing the LCC. Employing five gear sizes, three bearing sizes for the gearbox, and three bearing sizes for the electric motor, 45 powertrain solutions are achieved, including the baseline design.

By switching from the baseline to the best solution, a higher reliability is achieved with a slightly lower LCC. For the 150 kW power rating, the LCC of the best solution is 0.1% less than the baseline, while the reliability increases from 0.949 to 0.959. The LCC of the best 200

kW solution is 0.4% reduced with respect to the baseline, and its reliability is 0.957 compared to 0.899 for the baseline.

Three points should be considered to understand why the LCC reduction is not significant. Firstly, all of the powertrain options have the same battery pack; battery size is not a design variable. Secondly, the AC of the battery pack contributes to more than 50% of the LCC in both power ratings. Lastly, the reliability of the battery pack is higher than the other components; the battery pack is over-designed and its MC is negligible. These three points imply that for all powertrain options, the LCC of the battery pack is a large, constant portion of the powertrain LCC and, therefore, diminishes the role of element resizing on LCC reduction. In a comparative cost analysis where the constant battery cost is excluded, the LCC advantage of the best design increases; 0.3% LCC improvement for the best 150 kW solution over the baseline, and 0.8% reduction for the best 200 kW option in comparison with the baseline.

The investment on deploying a 200 kW electric motor leads to savings on the EC, but the savings do not justify the investment. Therefore, for the present application, the best 150 kW option has a lower LCC compared to the best 200 kW powertrain.

The size of gears and bearings are considered as the design variables to enhance the exploration of the design space compared to Morozov et al. [72]. For a future study, the constraint on the gear ratio can be dropped to add the size of the pinion to the design space. Also, as discussed in Chapter 4, changing the insulation class of electric motor may reduce the LCC of this component and, consequently, the LCC of the powertrain. This parameter can be added to the design space in future research. Furthermore, modelling the cost-performance-reliability of battery packs provide the necessary tool for considering the battery size as a design variable in future LCC analysis of BEVs. A significant LCC reduction is expected by resizing the battery pack. The salvage value of the powertrain is neglected in the present study. Having a better understanding of this cost category may improve the accuracy of the present cost analysis.

Chapter 7

Conclusions and Recommendations for Future Work

7.1 Conclusions

The present research aims to establish a reliability-based life-cycle cost (LCC) model for engineering elements and systems. To this end, the following objectives are addressed:

1. Proposing a procedure for correlating the acquisition cost of a product to its reliability and performance.
2. Acquisition cost-performance-reliability (CPR) modelling of gears.
3. Developing the CPR model of rolling bearings.
4. CPR modelling of gearboxes.
5. Establishing the CPR model of electrical insulations.
6. Building the CPR model of electric motors.

7. Deriving reliability-based cost models for post-failure and preventive maintenance strategies.

8. Analyzing the LCC of a system of components for reliability improvement and cost reduction.

These objectives are addressed in separate chapters as specified below.

In Chapter 2, Objective 1 is achieved by generating a procedure for CPR modelling of engineering elements. This includes studying the influence of design variables, such as size and material properties, on the acquisition cost and the reliability at a specified performance. The procedure is used to develop the CPR model of spur and helical gears, as specified in Objective 2. The reliability analysis is conducted using the AGMA stress and strength formula. A simple cost-size relation is considered. The resulting CPR model quantifies the marginal cost of reliability improvement for different throughput torques. The model results are compared with the catalog prices of a manufacturer for a wide range of gear sizes and different modules. The difference of the model and the catalog price is bounded to 5%. It is found out that the reliability is more sensitive to the gear size at higher torques. Under a specified torque profile, the cost is a typically convex function of reliability, which approaches infinity as reliability tends to unity.

In Chapter 3, the CPR modelling procedure of Chapter 2 as well as the ABMA bearing life equation and a linear cost-mass relation are used to derive the CPR model of rolling bearings, as Objective 3 states. The price catalog of a manufacturer is consulted to validate the bearings CPR model. To meet the requirement of Objective 4, the gears and bearings models are coupled to build the gearbox CPR model, which is used in cost and reliability analysis of a one-speed gearbox. It is shown that by changing the gear and bearing sizes, a wide region of the cost-reliability plane is explored. Among the bearings considered for building the gearbox, the smallest one should be selected to minimize the gearbox acquisition cost if the gearbox reliability

target is below 0.985. If the gearbox reliability must be above 0.990, the largest bearing gives the lowest acquisition cost.

In Chapter 4, Objective 5 is addressed by combining the price and the reliability models of electrical insulations to develop the CPR model of insulations. Next, to address the Objective 6, by coupling the CPR model of bearings and electrical insulations, the electric motor CPR model is derived. The bearings size and insulation class are varied while the overall motor features and characteristics are kept unchanged. The result is a set of motors with similar characteristics but different reliability and acquisition cost. The results suggest that depending on the duty cycle and the reliability target, it is possible to find designs with a lower acquisition cost and a higher reliability compared to the baseline design.

The post-failure maintenance and preventive maintenance cost models are derived in Chapter 5 to comply with Objective 7. The foundation of the models is using the failure probability distribution function as the kernel in determining the maintenance cost (MC). The inputs of the models are the reliability function of the element, the failure downtime, the preventive maintenance downtime, the cost of a failure, the cost of a preventive maintenance, the inflation rate, and the price of the spare part. Having these seven inputs for any arbitrary element, its MC model can be established. The models in the literature assume that the element has a high reliability and that the inflation rate is zero. These assumptions are dropped here. The results show that the MC models may be highly sensitive to the inflation rate, which emphasizes the importance of including this factor in the model. The numerical examples suggest that the developed models benefit from a higher accuracy compared to the models in the literature. The present models converge when the cost of the first four maintenances are considered. For selecting a preventive maintenance over a post-failure maintenance, it is necessary that the Weibull shape parameter of the element's reliability is greater than unity, which is the case for bearings. Otherwise, the cost of a preventive maintenance will be higher than that of a post-failure maintenance, which holds for gears. The MC models along with the gears and

bearings CPR models of Chapters 2 and 3 are used in the LCC analysis of a one-speed gearbox. The results show that by dropping the component-level reliability targets, it is possible to find solutions which are higher in reliability and lower in cost compared to the baseline design.

Compared to Chapter 5, Chapter 6 includes the energy cost into the definition of the LCC. In a case study, the life-cycle cost (LCC) of the powertrain of a battery electric step van is studied to meet Objective 8. The baseline design is determined to meet the performance and component-level reliability requirements. Next, keeping the performance fixed, the reliability constraint is relaxed and the gear and bearing sizes are varied. It is found out that by exploring the previously excluded regions of the design space, it is possible to find solutions which are lower in LCC and higher in reliability compared to the baseline designs. The battery pack of the powertrain is over-designed for this application. As a result, it has a significant contribution to the LCC. To add the battery size as a design variable in the LCC analysis, it is important to develop the CPR model of the batteries. This will be an important step towards LCC reduction and market diffusion of battery electric vehicles.

The main conclusions of this research are:

1. By increasing the size of gears and bearings, the acquisition cost is a typically convex function of reliability and tends to infinity as the reliability approaches unity. This cost-reliability behavior is formulated for gears, bearings, and electrical insulations in separate chapters. A good agreement is observed between the models and the catalog prices of OEMs, whenever such data was available.

2. When the CPR model of a system is built by combining the CPR models of its sub-systems, the best component sizing for cost and reliability improvement highly depends on the inputs of the CPR model and the system configuration.

3. The developed maintenance cost models extend the models in the literature to the case where the inflation rate is not zero and the reliability of the component is not close to unity.

The results show that the maintenance cost can be highly sensitive to the inflation rate. In such a case, the developed models have a higher accuracy than the models in the literature.

4. For gears, where the Weibull shape parameter of the reliability function is smaller than unity, the post-failure maintenance is the best maintenance strategy. On the other hand, the Weibull shape parameter of the reliability function of bearings is greater than unity. Therefore, depending on the downtime and the cost of a failure, either a preventive maintenance or a post-failure maintenance could be the best strategy for cost minimization.

5. If the component-level reliability constraints are avoided, it is possible to reach a solution which increases the overall reliability and reduces the life-cycle cost of the system.

6. The battery pack used in the case study of Chapter 6 is over-designed for that application. To further reduce the LCC of the powertrain, it is important to develop the CPR model of batteries, which will be used to down-size the battery pack.

7.2 Discussion

The procedure generated in Chapter 2 seems to be applicable to other engineering elements and systems such as shafts, bolts/nuts, welding, pressure vessels, mills, heat exchangers, compressors, turbines, civil engineering systems (beams, bridges, etc), batteries, electrical components, and electronic components. Having the CPR models of different engineering elements, engineers/designers may optimize the reliability and life-cycle cost of their products. As an example, since after the bearings and gears failure, the damage of shafts and lubrication systems are the major failure modes of gearboxes [8, 9], by having the CPR models of the shafts and the lubrication systems a more accurate gearbox CPR model can be achieved.

The findings of the gearbox case study of Chapter 5 and the powertrain case study of Chapter 6 show that the component-level reliability constraints may exclude the design points

with optimum overall reliability and LCC. This finding suggests a paradigm shift: *From a life-cycle cost and reliability optimization perspective, reliability should be viewed as a design variable rather than a design objective.*

The modelling of this thesis is design and manufacturing-oriented. In the context of this thesis, the material properties or the size of components can be considered as the design resources– this research deals with the quality of the resources assuming no limitation on the quantity of the resources. It is possible to ask about the influence of the quantity of resources on the models developed here. Factors such as the lack of spare parts, shortage of raw materials, or the production volume have not been explicitly incorporated into the models. Including them into the analysis extends the scope of this work.

7.3 Future Work

The present research can be extended to other applications as specified below.

1. The CPR model of other engineering elements and systems such as shafts, pressure vessels, mills, compressors, turbines, batteries, bridges, bolts, nuts, welding, electric components, and power electronics can be derived following the procedure introduced in Chapter 2. Having a rich library of the CPR model of engineering elements enables engineers of different disciplines and industries to optimize the reliability and life-cycle cost of systems of elements.

2. By taking into account the standard deviation of the reliability distribution, the CPR model may be extended to calculate the standard deviation of the acquisition cost and the maintenance cost. Other factors that can influence the standard deviation of the cost categories are the material variability, assembly accuracy, and loading uncertainty. The study of these factors may be a subject of future research.

3. Although this thesis is focused on engineering elements, the procedure proposed in Chapter 2 and the maintenance cost models of Chapter 5 can be used in other fields, too. Health science is an interesting application where the human body can be thought as a system of components. A similar approach can be used to answer a question like: *How the failure rate of body organs such as heart, kidney, liver, and bones, are influenced by parameters such as person's diet, lifestyle, age, wealth, genetics, etc?* In the context of this research, parameters such as diet and lifestyle can be considered as the body performance, the failure rate is exactly the failure probability distribution of different organs, and the health care expenses translate to the maintenance cost. Such a model may provide a good macro-level cost estimation tool which can be of high practical interest to governments (for health care budgeting), or insurance companies (for announcing better service rates in a competitive market, while keeping a safe profit margin).

4. The scope of this thesis can be extended by incorporating the distribution aspects of the product to answer: *How may the supply chain parameters such as procurement and resource management influence the cost models presented here?*

Bibliography

[1] N. Humphrey, *Growing Points in Ethology*, Cambridge University Press: Cambridge, 1976, ch. 9, 303–317.

[2] R. A. Laird, T. N. Sherratt, “The economics of evolution: Henry Ford and the Model T", *Oikos*, pp. 3–9, vol. 119, 2010.

[3] J. Pukite, P. Pukite, *Modeling for Reliability Analysis*, IEEE Press, New York, NY, 1998.

[4] R. G. Budynas, J. K. Nisbett, *Shigley’s Mechanical Engineering Design*, 8th ed., McGraw-Hill, Boston, MA, 2008, ch. 14.

[5] R. G. Budynas, J. K. Nisbett, *Shigley’s Mechanical Engineering Design*, 8th ed., McGraw-Hill, Boston, MA, 2008, ch. 15.

[6] R. G. Budynas, J. K. Nisbett, *Shigley’s Mechanical Engineering Design*, 8th ed., McGraw-Hill, Boston, MA, 2008, ch. 11.

[7] International Organization for Standardization, *ISO 281: Rolling Bearings–Dynamic Load Ratings and Rating Life*, 2010.

[8] S. Sheng, *Report on Wind Turbine Subsystem Reliability– A Survey of Various Databases*, NREL/PR-5000-59111, June, 2013.

[9] J. Ribrant, *Reliability Performance and Maintenance - A Survey of Failures in Wind Power Systems*, Masters Thesis, KTH School of Electrical Engineering, 2006.

[10] P. F. Albrecht, J. C. Appiarius, R. M. McCoy, E. L. Owen, D. K. Sharma, “Assessment of the reliability of motors in utility applications– Updated", *IEEE Transactions on Energy Conversion*, pp. 39–46, vol. EC-1, No. 1, 1986.

[11] P. F. Albrecht, J. C. Appiarius, E. P. Cornell, D. W. Houghtaling, R. M. McCoy, E. L. Owen, D. K. Sharma, “Assessment of the reliability of motors in utility applications", *IEEE Transactions on Energy Conversion*, pp. 396–406, vol. EC-2, No. 3, 1987.

[12] A. H. Bonnett, “Root cause failure analysis for AC induction motors in the petroleum and chemical industry", *57th Annual Petroleum and Chemical Industry Conference*, pp. 1–13, 2010.

[13] O. V. Thorson, M. Dalva, “A survey of faults on induction motors in offshore oil industry, petrochemical industry, gas terminals, and oil refineries", *IEEE Transactions on Industry Applications*, pp. 1186–1196, vol. 31, No. 5, 1995.

[14] Motor Reliability Working Group, “Report of Large Motor Reliability Survey of Industrial and Commercial Installations, Part I", *IEEE Transactions on Industry Applications*, pp. 853–864, vol. IA-21, No. 4, 1985.

[15] Motor Reliability Working Group, “Report of Large Motor Reliability Survey of Industrial and Commercial Installations, Part II", *IEEE Transactions on Industry Applications*, pp. 865–872, vol. IA-21, No. 4, 1985.

[16] Motor Reliability Working Group, “Report of Large Motor Reliability Survey of Industrial and Commercial Installations, Part 3", *IEEE Transactions on Industry Applications*, pp. 153–158, vol. IA-23, No. 1, 1987.

[17] J. F. Gieras, M. Wing, *Permanent Magnet Motor Technology: Design and Applications*, 2nd ed, Marcel Dekker Inc., New York, NY, 2002, ch. 12.

[18] G. C. Stone, E. A. Boulter, I. Culbert, H. Dhirani, *Electrical Insulation for Rotating Machines, Design, Evaluation, Aging, and Repair*, John Wiley & Sons, 2004, ch. 2.

[19] S. W. Eom, M. K. Kim, I. J. Kim, S. I. Moon, Y. K. Sun, H. S. Kim, “Life prediction and reliability assessment of lithium secondary batteries", *Journal of Power Sources*, vol. 174, 954–958, 2007.

[20] C. M. Herman, J. Lim, “Cycle life measurement of a sealed lead/acid battery", *Journal of Power Sources*, vol. 34, 25–29, 1991.

[21] L. Ran, W. Jun-feng, W. Hai-ying, G. Jian-ying, L. Ge-chen, “Reliability assessment and failure analysis of lithium iron phosphate batteries", *Information Sciences*, vol. 259, 359–368, 2014.

[22] W. R. Blischke, D. N. P. Murthy, *Reliability Modeling, Prediction, and Optimization*, John Wiley & Sons, New York, NY, 2000, ch. 4.

[23] T. A. Cruse, *Reliability-Based Mechanical Design*, Marcel Dekker, New York, NY, 1997, ch. 5.

[24] K. K. Aggarwal, *Reliability Engineering*, Springer Science+Business Media: Dordrecht, 1993, ch. 12.

[25] K. H. Chang, *e-Design, Computer-Aided Engineering Design*, Academic Press, Amsterdam, 2015, ch. 15.

[26] R. D. Stewart, *Cost Estimation*, 2nd ed., John Wiley & Sons, New York, NY, 1991.

[27] D. Ullman, *The Mechanical Design Process*, 3rd ed., McGraw-Hill, Boston, MA, 2003, ch. 12.

[28] C. S. Park, *Contemporary Engineering Economics*, 5th ed., Pearson, Essex, UK, 2014.

[29] R.M. Cuenca, L.L. Gaines, and A.D. Vyas, *Evaluation of Electric Vehicle Production and Operating Costs*, Argonne National Laboratory, November 1999.

[30] N. Murgovski, L. Johannesson, J. Sjoberg, B. Egardt, “Component sizing of a plug-in hybrid electric powertrain via convex optimization", *Mechatronics*, vol. 22, 103–120, 2012.

[31] R. Graham, *Comparing the Benefits and Impacts of Hybrid Electric Vehicle Options*, EPRI, 2001.

[32] K. Okabe, K. Shoda, Y. Tozaki, M. Nabekura, T. Ohira, T. Yoshimi, A. Umeda, “A design guide for very small power transmission gears considering tooth surface strength andmanufacturing cost", *Proceedings of International Gear Conference*, 858–868, September, 2014.

[33] R. Lotfalian, S. Martins, P. Radziszewski, B. Boulet “Acquisition cost-performance-reliability modelling of Gears", Submitted to *Journal of Mechanical Design*.

[34] M. A. Delucci, T. E. Lipman, “An analysis of the retail and lifecycle cost of battery-powered electric vehicles", *Transportation Research Part D*, vol. 6, 371–404, 2001.

[35] M. A. Delucci, A. Burke, T. Lipman, M. Miller, “An analysis of the retail and lifecycle cost of battery-powered electric vehicles", *Electric and Gasoline Vehicle Lifecycle Cost and Energy-Use Model– Report for the California Air Resources Board*, April 2000.

[36] R. Graham, *Comparing the Benefirst and Impacts of Hybrid Electric Vehicle Options– Final Report*, July 2001.

[37] A. Simpson, “Cost-Benefit Analysis of Plug-In Hybrid Electric Vehicle Technology", *22nd International Battery, Hybrid and Fuel Cell Electric Vehicle Symposium and Exhibition*, Yokohama, Japan, October 2006.

[38] A. Mettas, “Reliability Allocation and Optimization for Complex Systems", *Proceedings of Annual Reliability and Maintainability Symposium*, Los Angeles, CA, 216–221, 2000.

[39] K. B. Misra, M. D. Ljubojevic,“Optimal Reliability Design of a System: A New Look", *IEEE Transactions on Reliability*, 255–258, vol. R-22, no. 5, 1973.

[40] S. Twum, E. Aspinwall, J. Fliege, “A multicriteria optimisation model for reliability design of series-parallel systems: part 1", *International Journal of Quality and Reliability Management*, 1038–1055, vol. 29, no. 9, 2012.

[41] S. Twum, E. Aspinwall,“Complex System Reliability Optimization: A Multi-Criteria Approach", *International Journal of Engineering Research in Africa*, pp. 13-21, vol. 9, 2013.

[42] W. R. Blischke, D. N. P. Murthy, *Reliability Modeling, Prediction, and Optimization*, John Wiley & Sons, New York, NY, 2000, ch. 16.

[43] A. K. S. Jardine, A. H. C. Tsang, *Maintenance, Replacement, and Reliability Theory and Application*, 2nd ed., CRC Press, Boca Raton, FL, 2013, ch. 2.

[44] W. L. Smith, “Regenerative Stochastic Processes", *Proceedings of the Royal Society of London, Series A. Mathematical and Physical Sciences*, 8–31, vol. 232, 1955.

[45] D. Lin, M. J. Zuo, R. C. M. Yam, “Sequential imperfect preventive maintenance models with two categories of failure modes", *Naval Research Logistics*, 172–183, vol. 48, no. 2, 2001.

[46] A. Grall, C. Berenguer, L. Dieulle, “A condition-based maintenance policy for stochastically deteriorating systems", *Reliability Engineering and System Safety*, 167–180, vol. 76, no. 2, 2002.

[47] B. Lhorente, D. Lugtigheid, P. F. Knights, A. Santana, “A model for optimal armature maintenance in electric haul truck wheel motors: a case study", *Reliability Engineering and System Safety*, 209–218, vol. 84, no. 2, 2004.

[48] R. I. Zequeira, C. Berenguer, “Periodic imperfect preventive maintenance with two categories of competing failure modes", *Reliability Engineering and System Safety*, 460–468, vol. 91, no. 4, 2006.

[49] M. Bartholomew-Biggs, M. J. Zuo, X. Li, “Modelling and optimizing sequential imperfect preventive maintenance", *Reliability Engineering and System Safety*, 53–62, vol. 94, no. 1, 2009.

[50] J. H. Lim, J. Qu, M. J. Zuo, “Age replacement policy based on imperfect repair with random probability", *Reliability Engineering and System Safety*, 24–33, vol. 149, 2016.

[51] C. A. V. Cavalcante, “A preventive maintenance decision model based on multicriteria method PROMETHEE II integrated with Bayesian approach", *IMA Journal of Management Mathematics*, 333-–348, vol. 21, no. 4, 2010.

[52] A. A. Tabriz, B.z Khorshidvand, A. Ayough, “Modelling age based replacement decisions considering shocks and failure rate", *International Journal of Quality and Reliability Management*, 107–119, vol. 33, no. 1, 2016.

[53] Department of Energy, U.S. Energy Information Administration, *Annual Energy Outlook 2015 with Projections to 2040*, April 2015.

[54] S. Eaves, J. Eaves “A cost comparision of fuel-cell and battery electric vehicles", *Journal of Power Sources*, vol. 130, 208–212, 2004.

[55] Y. Ito, S. Managi, “The potential of alternative fuel vehicles: A cost-benefit analysis", *Research in Transportation Economics*, vol. 50, 39–50 , 2015.

[56] R. A. Barnitt, A. D. Broker, L. Ramroth, “Model-based analysis of electric drive options for medium-duty parcel delivery vehicles", 25^{th} *World Battery, Hybrid and Fuecl Cell Electric Vehicle Symposium & Exhibition*, Shenzhen, China, November 2010.

[57] A. Brooker, M. Thornton, J. Rugh, “Technology improvement pathways to cost-effective vehicle electrification", *SAE 2010 World Congress*, Detroit, MI, United States, February 2010.

[58] United States Government Accountability Office, *Plug-in Vehicles Offer Potential Benefits, but High Costs and Limited Information Could Hinder Integration into the FederalFleet– Report to Congressional Requesters*, June 2009.

[59] C. Lin, T. Wu, X. Ou, Q. Zhang, X. Zhang, “Life-cycle private costs of hybrid electric vehicles in the current Chinese market", *Energy Policy*, vol. 55, 501–510, 2013.

[60] G. J. Offer, D. Howey, M. Contestabile, R. Clague, N. P. Brandon, “Comparative analysis of battery electric, hydrogen fuel cell and hybrid vehicles in a future sustainable road transport system", *Energy Policy*, vol. 38, 24–29, 2010.

[61] B. Nykvist, M. Nilsson, “Rapidly falling costs of battery packs for electric vehicles", *Nature Climate Change*, vol. 5, 329–332, 2015.

[62] J. Cobb, “GM says Li-ion battery cells down to $145/kWh and still falling", *http://hybridcars.com/gm-ev-battery-cells-down-to-145kwh-and-still-falling/*, October 2015.

[63] J. Cobb, “Tesla projects battery costs could drop to $100/kWh by 2020", *http://hybridcars.com/tesla-projects-battery-costs-could-drop-to-100kwh-by-2020*, June 2015.

[64] A. J. Seixax, S. Simoes, L. Dias, A. Kanudia, P. Fortes, M. Gargiulo, “Assessing the cost-effectiveness of electric vehicles in European countries using integrated modeling", *Energy Policy*, vol. 80, 165–176, 2015.

[65] T. E. Lipman, M. A. Delucchi, *Hybrid-Electric Vehicle Design Retail and Lifecycle Cost Analysis– Analysis and Report Prepared for The Energy Foundation*, April 2003.

[66] T. E. Lipman, M. A. Delucchi, “A retail and lifecycle cost analysis of hybrid electric vehicles", *Transportation Research Part D*, vol. 11, 115–132, 2006.

[67] R. A. Barnitt, *FedEx Express Gasoline Hybrid Electric Delivery Truck Evaluation: 12-Month Report– Technical Report NREL/TP-5400-48896*, January 2011.

[68] K. Funk, A. Rabl, “Electric versus conventional vehicles: social costs and benefits in France", *Transportation Research Part D*, vol. 4, 397–411, 1999.

[69] M. Granovskii, I. Dincer, M. A. Rosen, “Economic and environmental comparison of conventional, hybrid, electric and hydrogen fuel cell vehicles", *Journal of Power Sources*, vol. 159, 1186–1193, 2006.

[70] S. Bubeck, J. Tomashek, U. Fahl, “Perspectives of electric mobility: Total cost of ownership of electric vehicles in Germany", *Transport Policy*, vol. 50, 63–77, 2016.

[71] B. S. M. Fan, *Multidisciplinary Optimization of Hybrid Electric Vehicles: Component Sizing and Power Management Logic*, PhD Thesis, University of Waterloo, 2011.

[72] A. Morozov, K. Humphries, T. Rahman, T. Zou, J. Angeles, “Analysis and optimization of a drive- train for two-speed class-4 electric delivery truck", Technical Report TR-CIM-2017-25-01-01, Department of Mechanical Engineering and Centre for Intelligent Machines, McGill University, Montreal, January 2017.

[73] American Gear Manufacturers Association, “AGMA 908-B89: Geometry Factors for Determining the Pitting Resistant and Bending Strength of Spur, Helical, and Herringbone Gear Teeth", 1989.

[74] Toronto Gear, *Stock Production Catalogue*, vol. 8, 2014.

[75] Atlantic Heat Treating, *http://atlanticheattreat.ca*.

[76] Timken, *Timken Engineering Manual–Metals Industry Edition*, 2013.

[77] FAG online catalog, *http://medias.schaeffler.de*.

[78] FAG, *Price List*, 2014.

[79] Bank of Canada, *http://bankofcanada.ca/rates/exchange*.

[80] SKF, *Rolling Bearings Catalog*, 2013.

[81] TM4 inc., *http://tm4.com*.

[82] Techo-Westinghouse inc., *Motors and Drives Price Book*, 2015.

[83] Siemens, *SIMOTICS Low-Voltage Motors–Catalog D 81.1*, 2013.

[84] Siemens, *Price List–Catalog D 81.1 P*, 2015.

[85] WEG, *WEG Motor Catalog*, 2014.

[86] T. A. Cruse, *Reliability-Based Mechanical Design*, Marcel Dekker, New York, NY, 1997, ch. 3.

[87] Purolator, *Private Communication*, February 2016.

[88] B. Dahl, *http://4-wheeling-in-western-australia.com/differential-gear-ratio.html*, 2015.

[89] H. Naunheimer, *Automotive Transmissions: Fundamentals, Selection, Design, and Application*, 2nd ed., Springer-Verlag, Berlin, 2011.

[90] P. D. Walker, S. A. Rahman, B. Zhu, N. Zhang, “Modelling, simulations, and optimisation of electric vehicles for analysis of transmission ratio selection", *Advances in Mechanical Engineering*, vol. 2013, 1–13, 2013.

[91] Rotomotive Powerdrives India, *Price List of Worm Gear Boxes (Box Series) and Variators (VARIO) and Heliworm Gearboxes*, 2011.

[92] A. Vyas, D. Santini, R. Cuenca, *Comparison of Indirect Cost Multipliers for Vehicle Manufacturing– Technical Memorandum in support of Electric and Hybrid Electric Vehicle Cost Estimation Studies*, 2000.

[93] EnerDel Inc, *http://enerdel.com*.

[94] Purolator, *https://purolator.com/en/resources-and-support/about-us/corporate- information/facts.page*, May 2016.

[95] S. Porter "What's a reasonable hourly labor rate for an auto mechanic?", *https://quora.com/Whats-a-reasonable-hourly-labor-rate-for-an-auto-mechanic*, September 2011.

[96] Bureau of Labor Statistics, "Occupational employment statistics", *http://bls.gov/oes/current/oes493023.htm*, May 2015.

[97] PayScale, "Automotive Service Technician/Mechanic in Montréal, Québec Salary (Canada)", *http://payscale.com/research/CA/Job=Automotive_Service_Technician_%2f_Mechanic/Hourly_Rate/76bae0e6/Montreal-QC*.

[98] Statistics Canada, "Average hourly wages of employees by selected characteristics and occupation, unadjusted data, by province (Quebec)", *http://statcan.gc.ca/tables-tableaux/sum-som/l01/cst01/labr69f-eng.htm*, September 2016.

[99] Hydro Quebec, *Comparison of Electricity Prices in Major North American Cities. Rates in Effect April 1, 2015*, 2015.

[100] TM4 inc., *Private Communication*, February 2016.